CHEMICAL REVIEWS

Review

Cite This: Chem. Rev. 2017, 117, 7190-7239

pubs.acs.org/CR

Application of Ionic Liquids to Energy Storage and Conversion Materials and Devices

Masayoshi Watanabe,*[,†] Morgan L. Thomas,[†] Shiguo Zhang,[†] Kazuhide Ueno,[‡] Tomohiro Yasuda,[§] and Kaoru Dokko[†,∥]

[†]Department of Chemistry and Biotechnology, Yokohama National University, 79-5 Tokiwadai, Hodogaya-ku, Yokohama 240-8501, Japan

[‡]Department of Applied Chemistry, Graduate School of Sciences and Technology for Innovation, Yamaguchi University, 2-16-1 Tokiwadai, Ube 755-8611, Japan

[§]Institute of Catalysis, Hokkaido University, Kita 21. Nishi 10, Kita-ku, Sapporo 001-0021, Japan

[∥]Unit of Elements Strategy Initiative for Catalysts & Batteries (ESICB), Kyoto University, Kyoto 615-8510, Japan

ABSTRACT: Ionic liquids (ILs) are liquids consisting entirely of ions and can be further defined as molten salts having melting points lower than 100 °C. One of the most important research areas for IL utilization is undoubtedly their energy application, especially for energy storage and conversion materials and devices, because there is a continuously increasing demand for clean and sustainable energy. In this article, various application of ILs are reviewed by focusing on their use as electrolyte materials for Li/Na ion batteries, Li-sulfur batteries, Li-oxygen batteries, and nonhumidified fuel cells and as carbon precursors for electrode catalysts of fuel cells and electrode materials for batteries and supercapacitors. Due to their characteristic properties such as nonvolatility, high thermal stability, and high ionic conductivity, ILs appear to meet the rigorous demands/criteria of these various applications. However, for further development, specific applications for which these characteristic properties become unique (i.e., not easily achieved by other materials) must be explored. Thus, through strong demands for research and consideration of ILs unique properties, we will be able to identify indispensable applications for ILs.

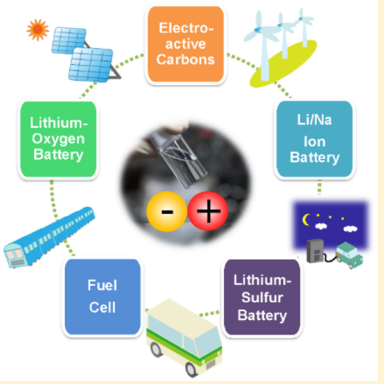

CONTENTS

Special Issue: Ionic Liquids

Received: July 30, 2016
Published: January 13, 2017

DOI: 10.1021/acs.chemrev.6b00504
Chem. Rev. 2017, 117, 7190–7239

Table 1. Abbreviations of Typical Cations and Anions Comprising ILs

Cation		
[$C_n$mim]	[$C_n$mpyr]	[$C_n$mpip]
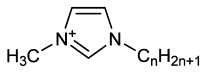	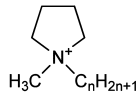	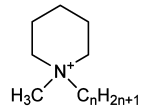
[DEME]	[Nabcd]	[Pabcd]
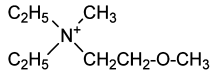	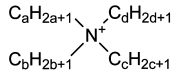	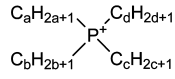
[$C_n$dmim]	[dema]	[DBU]
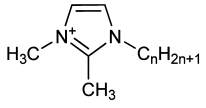	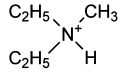	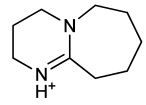
Anion		
[TFSA]	[FSA]	[FTA]
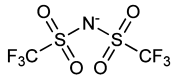	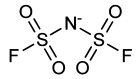	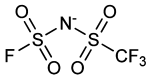
[BETA]	[TSAC]	[FAP]
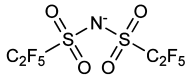	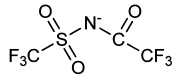	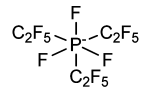
[TfO]	[MS]	[DFOB]
$CF_3SO_3^-$	$CH_3SO_3^-$	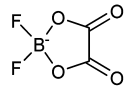
[DCA]		
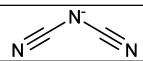		

DOI: 10.1021/acs.chemrev.6b00504
Chem. Rev. 2017, 117, 7190−7239

1. INTRODUCTION

Ionic liquids (ILs) are defined as molten salts having melting points lower than 100 °C, and most of them are organic salts having a large variety of designability. They are recognized as a third group of solvents (and electrolytes), following water and organic solvents, and are typically characterized by unique properties such as nonvolatility, high thermal stability, and high ionic conductivity. These properties are, however, much affected by Lewis acidity/basicity of cations/anions (i.e., Coulombic interactions), the directionality of interactions between cations and anions, and van der Waals interactions between ions. In other words, regarding the properties of ILs, it should be understood with the greatest care that the characteristic properties as mentioned above are not always afforded by all ILs, which in turn provides the scope to design new task-specific ILs.

One of the most important application research areas for IL utilization is undoubtedly their energy application. There is increasing demand for clean and sustainable energy, especially for energy storage and conversion materials and devices. Typical examples are lithium batteries and fuel cells, for which commercial application in hybrid, electric, and fuel cell vehicles as well as for stationary use in homes, buildings, and up to large power grid-scale has already commenced. Active and thorough research has supported the development of innovational materials utilized in these devices. For instance, carbonate-based electrolytes have been used in Li-ion batteries, which ensured the highest energy density secondary batteries ever developed. However, at the same time, such flammable organic carbonates still have a safety issue especially when Li-ion batteries are used on a large scale such as in electric vehicles and power grids. Furthermore, in so-called "beyond Li-ion batteries" such as Li-sulfur batteries and Li-oxygen batteries, conventional carbonate-based electrolytes cannot be used due to side reactions, dissolution of electroactive materials, and evaporation of the solvents. In the case of the fuel cells, water-assisted proton conductivity of proton conducting membranes, typically Nafion, hampers their elevated temperature use at higher than 100 °C due to rapid evaporation of water and concomitant decrease of the proton conductivity. These issues are prompting research on new electrolytes materials based on ILs. Meanwhile, nonvolatility and high thermal stability of ILs have enabled certain ILs to be precursors of carbon materials. This new methodology has unveiled highly functional and task-specific carbon materials for energy applications.

In this article, energy applications of ILs are reviewed. In the following three chapters, the electrolyte applications of ILs to Li/Na ion batteries, Li-sulfur batteries, and Li-oxygen batteries are critiqued. In the following chapter, the application of protic ILs as proton conductors for fuel cells is reviewed, where composite membrane fabrication consisting of protic liquids and polymers is essential and crucial for practical application. Finally, carbon materials derived from ILs are demonstrated, which indicates that ILs can be new building blocks of new functional materials for energy applications, especially for catalysts and electrodes. Abbreviations of typical cations and anions comprising ILs appearing in this review are shown in Table 1.

2. LI/NA ION BATTERY ELECTROLYTES

Li-ion batteries have high energy density and high power density and have been widely used as power sources for portable devices. Li-ion batteries are typically comprised of a carbon negative electrode, a Li-containing transition metal oxide ($LiMO_2$, M: transition metal) positive electrode, and an organic electrolyte.[1−3] Li^+ is intercalated into the carbon negative electrode and Li^+ deintercalation from the $LiMO_2$ positive-electrode occurs during the charging of a Li-ion cell, and the reverse reactions proceed during the discharge. The potential of $LiMO_2$ positive electrodes are typically in the range of 3.5−4.2 V versus Li/Li^+ (0.36−1.16 V vs SHE). On the other hand, the potential of carbonaceous negative electrodes is as low as 0−0.3 V versus Li/Li^+ (−3.04 ∼ −2.74 V vs SHE), therefore, aprotic electrolytes are used to avoid significant side reactions at the negative electrode. Nowadays, Li salts dissolved in aprotic molecular solvents such as ethylene carbonate (EC) and diethyl carbonate (DEC) are used as electrolytes in practical Li-ion batteries.[4,5] The organic molecular solvents exhibit flammability and volatility. Improvement of electrolyte safety for Li-ion batteries is strongly desired, especially for large-scale energy storage systems, such as batteries for electric vehicles and power grids. Room temperature Na-ion batteries using aprotic electrolytes have also been investigated as alternative power sources.[6] Thermally stable electrolytes have been extensively investigated to improve the thermal stability of these batteries.[1−5]

ILs are thermally stable and exhibit low-volatility and fire-retardant ability, and many researchers are attempting to use ILs as electrolytes for the batteries.[7−17] In pioneering studies of ILs for battery application, chloroaluminate ($AlCl_4^-$) based ILs were investigated.[18−23] However, the chloroaluminate anion is quite water-sensitive and corrosive, therefore chloroaluminate-based ILs have not been so common in recent Li and Na battery research. The electrolytes for Li and Na ion batteries should have Li^+ and Na^+ ion conducting ability, respectively. In addition, the electrolytes should also have sufficient electrochemical stability. If irreversible reductive decomposition at the negative electrode and oxidative decomposition at the positive electrode occur in batteries, the discharge/charge becomes less efficient. The negative and positive electrodes are highly reducing and oxidizing agents, respectively, when the battery is in the fully charged state. Therefore, a wide electrochemical window is desirable for Li/Na ion battery electrolytes. In this section, IL electrolytes for Li/Na ion batteries are reviewed. ILs for Li/Na ion battery electrolytes can be categorized into 3 types: (i) Li/Na salts having melting points lower than 100 °C, (ii) Li/Na salts dissolved in room temperature ILs, and (iii) solvate ILs composed of complex $[A(solvent)_x]^+$ (A: Li or Na) cations and counteranions. The characteristics of each type of IL will be highlighted in this section.

2.1. Low Melting Alkaline Salts

2.1.1. Low Melting Li Salts. The melting points of conventional Li salts are typically above 200 °C, for example, 236 °C for $LiClO_4$, 296.5 °C for $LiBF_4$, and 200 °C for $LiPF_6$. This is mainly because of the strong electrostatic attraction between the Li^+ ion and anion. The charge density of Li^+ ion is high, because of its small ionic radius, resulting in a strong electrostatic attraction between the Li^+ ion and the anion. Therefore, a high temperature is generally needed for melting. It should be noted here that some inorganic Li salts have relatively low melting temperatures. For example, the melting point of $LiClO_3$ is 128 °C, and the quaternary system of $NaNO_3$−$LiNO_3$−$LiClO_3$−$NaClO_3$ melts at temperatures lower than 100 °C.[24] $LiAlCl_3SCN$ melts at 110 °C and can maintain a

DOI: 10.1021/acs.chemrev.6b00504
Chem. Rev. 2017, 117, 7190−7239

liquid state at room temperature as a supercooled liquid, while the melting point of $LiAlCl_4$ is 143 °C.[25] In the $LiAlCl_3SCN$ melt, the anion is a mixed ligand compound of $AlCl_3SCN^-$ with an asymmetric structure, while the $AlCl_4^-$ anion has a symmetric structure. It is difficult to predict the melting temperatures of Li salts because fusion is affected by many factors, such as the electrostatic interaction between Li^+ and anion, size of anion, anion symmetry, conformations of anion, and so on. The effects of the cation mixing and the asymmetric structure of anion in the mixtures of alkaline amide salts on the fusion of the salts will be reviewed in section 2.1.2.

Here we introduce an effective way to lower the melting point of a Li salt down to room temperature. Li^+ is a relatively strong Lewis acid. According to the HSAB theory, weaker Lewis-basic anions interact with Li^+ weakly. However, even the Li salt of a large aluminate anion with very low Lewis basicity has a melting point much higher than room temperature.[26,27] Fujinami et al. reported that the introduction of ether groups into the aluminate structure gave liquid-like Li salts.[28,29] The ether groups act as Li^+ coordinating ligands, dissociating the Li^+ cations from the central atom of the anions centers. Watanabe and co-workers prepared lithium ILs consisting of Li^+ and borates having electron-withdrawing groups, to reduce the anionic basicity, as well as Li^+ coordinating ether ligands, to dissociate the lithium cations from the central atom of the anions.[30−32] Similarly, other alkali metal (Li^+, Na^+, and K^+) ILs can also be prepared with anions having ether groups and bulky structures. For example, alkali metal oligoether carboxylate maintains a liquid state at ambient temperature.[33,34] Figure 1

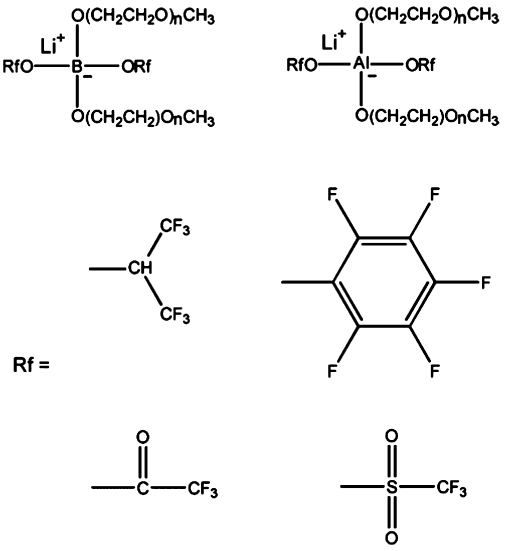

Figure 1. Structures of Li ILs.

shows the examples of low melting Li salts with weaker Lewis-basic anions. Although the melting points of these salts are low, the ionic conductivity of the molten salts is as low as 10^{-5}−10^{-4} S cm^{-1} at room temperature.[30,31] This is because of their very high viscosity and the long lifetime of ion pairs (i.e., coordination between anion and cation remains). The bulky structure of the anions infers high viscosity for these melts. In addition, the strong Lewis-acidic nature of the Li^+ ion favors ion pairing even in the molten state. However, by elevating the temperature, the ionic conductivity can be enhanced, and it is possible to use such Li ILs as electrolytes for Li batteries. Figure 2 shows galvanostatic charge and discharge curves of a [Li | Li

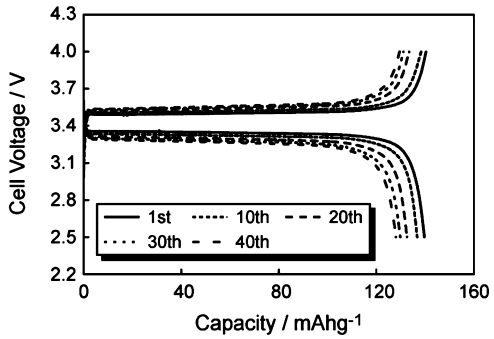

Figure 2. Charge and discharge curves of [Li | $Li[B(OCOCF_3)_2(O(CH_2CH_2O)_{7.2}CH_3)_2]$ | $LiFePO_4$] cell measured at 1/10 C rate at 60 °C. Reprinted with permission from ref 32. Copyright 2008 The Committee of Battery Technology, The Electrochemical Society of Japan.

ionic liquid | $LiFePO_4$] cell measured at 60 °C.[32] During the charging of the cell, Li^+ is extracted from the $LiFePO_4$ positive electrode ($LiFePO_4 \rightarrow Li_{1-x}FePO_4 + xLi^+ + xe^-$)[35] and Li metal is deposited on the negative electrode ($Li^+ + e^- \rightarrow Li$), and the reverse reactions take place during discharging. The cell could be operated stably for more than 40 cycles, suggesting that severe side reactions do not occur in the cell.

2.1.2. Mixtures of Alkaline Amide Salts. The melting point of A[TFSA] (A: alkali metal, TFSA: bis(trifluoromethanesulfonyl)amide = $[(CF_3SO_2)_2N]^-$) is relatively high (Table 2); for example, the melting point of

Table 2. Melting points (T_m) and Decomposition Temperatures (T_d) of A[TFSA] and A[FSA] salts (A: Li, Na, K, Rb, and Cs). Data for A[TFSA] and A[FSA] are from refs 36 and 40, respectively.

salt	T_m (°C)	T_d (°C)
Li[TFSA]	233	384
Na[TFSA]	257	441
K[TFSA]	199	460
Rb[TFSA]	177	467
Cs[TFSA]	122	472
Li[FSA]	130[a]	70[a]
Na[FSA]	106	140
K[FSA]	102	150
Rb[FSA]	95	162
Cs[FSA]	92	170

[a]The decomposition rate of Li[FSA] was slow enough to measure its melting point by DSC at 10 K min^{-1}.

Li[TFSA] is 233 °C. Molten A[TFSA] salts have negligibly low vapor pressure, nonflammability, and high thermal stability.[36] In addition, the $[TFSA]^-$ is electrochemically stable, and the molten A[TFSA] salts show wide electrochemical windows. The binary and ternary mixtures of A[TFSA] salts (A: Li, Na, K, Rb, and Cs) were investigated systematically by Hagiwara and co-workers.[37,38] It has been found that the cation mixing of the salts lowers the melting points (typically 120−150 °C). They also reported the application of mixtures of A[TFSA] salts as electrolytes in Li batteries operating at medium temperature range.[39] The melting point of $Li_{0.2}K_{0.1}Cs_{0.7}$[TFSA] is 146 °C, which is much lower than that of Li[TFSA], and the ionic conductivity at 150 °C is high, 14 mS cm^{-1}. The electrochemical deposition/dissolution of Li metal occurs

DOI: 10.1021/acs.chemrev.6b00504
Chem. Rev. 2017, 117, 7190−7239

reversibly in the melt. In addition, the anodic limit (oxidative stability) of the melt is as high as 5.0 V vs Li. Watarai et al. demonstrated the stable operation of a Li battery with Li metal negative electrode and $LiFePO_4$ positive electrode at 150 °C using molten $Li_{0.2}K_{0.1}Cs_{0.7}$[TFSA] as electrolyte.[39]

The structure of anions also has a significant effect on the melting point. Interestingly, the binary or ternary mixtures of [FSA] (FSA: bis(fluorosulfonyl)amide = $[(FSO_2)_2N]^-$)-based alkaline metal salts have melting points lower than 100 °C.[40−42] Figure 3 shows the phase diagram of the Na[FSA]−K[FSA] system; the phase diagram is a simple eutectic type.[40] The eutectic temperature is much lower than the melting temperatures of the constituent salts. The eutectic point is found at $(x_{Na[FSA]}, x_{K[FSA]}) = (0.45, 0.55)$ with a eutectic temperature of 61 °C. This eutectic melt can be used as an electrolyte for Na batteries.[43,44] Figure 4 shows the galvanostatic charge and discharge curves of a Na/NaFSA-KFSA/$NaCrO_2$ cell measured at 80 °C.[43] During the charging of the cell, Na^+ is extracted from the $NaCrO_2$ positive electrode ($NaCrO_2 \rightarrow Na_{1-x}CrO_2 + xNa^+ + xe^-$),[45] and Na metal is deposited on the negative electrode ($Na^+ + e^- \rightarrow Na$). The reverse reactions take place during discharge. The cell could be operated stably for more than 100 cycles using the melt as electrolyte. The Coulombic efficiencies of discharge/charge of the cell were higher than 99.9% for 100 cycles. However, it should be noted that the decomposition temperate of A[FSA] salts are relatively low compared with the A[TFSA] salts, as shown in Table 2. Therefore, the batteries using the [FSA]-based melts as electrolytes should be operated in a limited temperature range. The ionic conductivity of the melt at around the melting point is relatively low, and the temperature should be elevated but lower than the decomposition temperature.

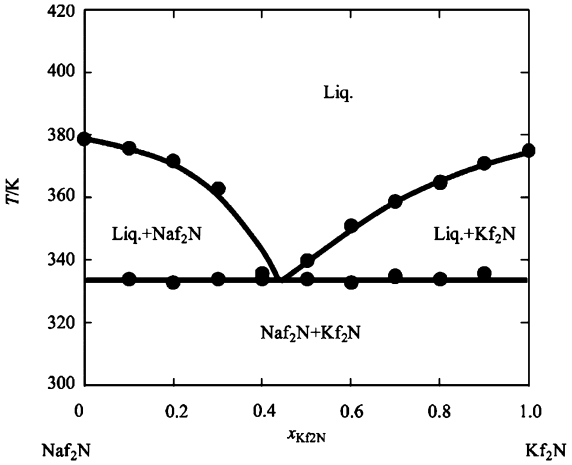

Figure 3. Phase diagram of the Na[f_2N] and K[f_2N] system. [f_2N] = [FSA]. Reprinted from ref 40. Copyright 2010 American Chemical Society.

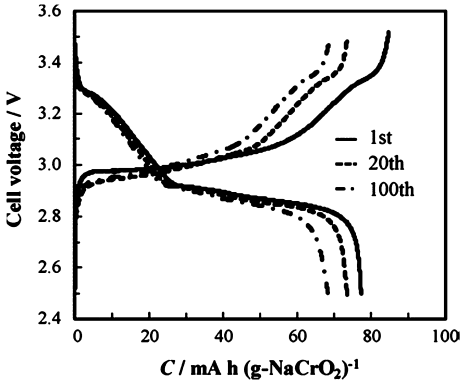

Figure 4. Charge−discharge curves for a Na/Na[FSA]-K[FSA]/$NaCrO_2$ cell at 353 K. Charge−discharge rate: 15 mA g^{-1}. Cut-off voltage: 2.5−3.5 V. Cycle number: 1, 20, and 100. Reprinted with permission from ref 43. Copyright 2012 Elsevier.

Recently, Kubota et al. reported that introducing an asymmetric structure into the amide-type anion can further reduce the melting point.[46−49] They synthesized (fluorosulfonyl) (trifluoromethylsulfonyl)amide anion ($[(FSO_2)(CF_3SO_2)N]^-$ denoted as $[FTA]^-$). The melting point of Li[FTA] is as low as 100 °C. In addition, the thermal stabilities of [FTA] salts are relatively high compared with [FSA] salts. By mixing Li[FTA] with Cs[FTA], the melting point can be further reduced. The melting point of $Li_{0.4}Cs_{0.6}$[FTA] is 33 °C, and Li-ion batteries can be successfully operated using the melt as electrolyte in the temperature range 45−100 °C.[49]

2.2. Alkaline Salts Dissolved in Organic Ionic Liquids

There are numerous aprotic ILs composed of organic cations and counteranions, having melting points lower than room temperature.[7] However, these organic ILs do not contain Li^+/Na^+ ions, therefore, Li or Na salts should be mixed with the organic ILs to use them as electrolytes for Li/Na ion batteries. In other words, the ILs are used as electrolyte solvents for the Li or Na salts. The physicochemical properties of Li salt/IL binary mixtures are significantly affected by the structures of cations and anions of the organic IL. Herein, we highlight the characteristics of Li salt/IL binary mixtures.

2.2.1. Effects of Cation Structure. The reductive stability of the organic ILs is strongly affected by the chemical nature of the cations. It is widely known that aliphatic quaternary ammonium (AQA) cations, including pyrrolidinium ($[C_n mpyr]^+$) and piperidinuim ($[C_n mpip]^+$) cations,[50−55] and aliphatic quaternary phosphonium (AQP) cations have good reductive stability.[56,57] Reversible Li deposition and stripping are possible in the mixture of a Li salt and AQA- and AQP-based ILs.[51,57] Hence, many researchers have investigated AQA- and AQP-based ILs as electrolyte solvents for Li/Na ion batteries. Figure 5 shows linear sweep voltammograms of [TFSA]-based ILs.[50] The cathodic (reductive) decomposition of $[C_2mim]^+$ and pyridinium cations irreversibly occur at electrode potentials of −2.3 V and −1.3 V versus I^-/I_3^-, respectively (0 V vs I^-/I_3^- corresponds to +2.9 V vs Li/Li^+). These potentials are more positive than those for AQA and AQP cations.[51,57] However, $[C_2mim]^+$ based ILs can be used in a Li ion cell with a negative electrode material $Li_4Ti_5O_{12}$ working at 1.5 V versus Li^+.[58,59] Also, modification of the imidazolium cation is effective in enhancing the reductive stability.[60−63] For example, the reductive stability of the 1,2-dimethyl-3-propylimidazolium cation is better than that of 1-ethyl-3-methylimidazolium.[60−63] However, the electrochemical reactions of negative electrode materials are affected by not only the cation species but also the anion species. It has been reported that $[C_n mim][FSA]$ can be employed in Li-ion batteries with graphite negative electrode, whose operating potential is as low as 0.1 V versus Li/Li^+ (vide infra). Therefore, the combination of cation and anion of an IL and the Li salt should be selected carefully for battery applications.

DOI: 10.1021/acs.chemrev.6b00504
Chem. Rev. 2017, 117, 7190−7239

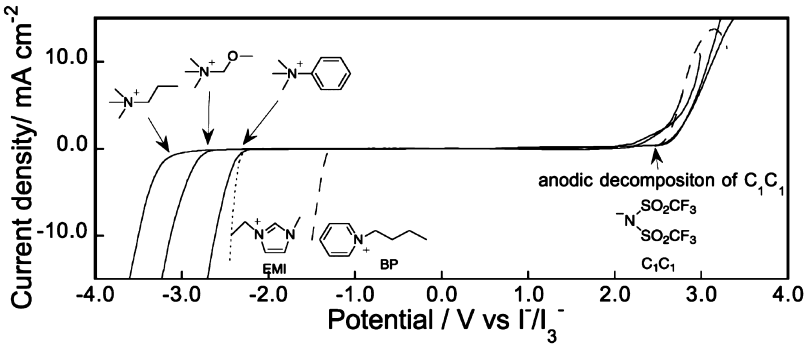

Figure 5. Linear sweep voltammograms of [TFSA]-based ILs measured at a scan rate of 50 mV s^{-1} at 30 °C. Working and counter electrodes were glassy carbon and Pt, respectively. Reference electrode was Pt wire immersed in [C_2mim][TFSA] containing 15 mM I_2 and 60 mM tetrapropylammonium iodide. Reprinted with permission from ref 50. Copyright 2000 The Electrochemical Society.

The transport properties of Li salt/IL binary mixtures are significantly affected by the organic cations. In general, with increasing ionic radius of the organic cation, the viscosity increases and ionic conductivity decreases.[64] Of course, not only the cation size but also the anion size, the conformational freedom (flexibility) of cation and anion, and the interactions between ions affect the viscosity and ionic conductivity of ILs (vide infra). Functional groups contained in the cation structure also affect the viscosity and ionic conductivity of the ILs. For example, organic cations containing ether groups tend to result in lower viscosities for the Li salt/IL binary mixtures owing to the interaction between the Li^+ and ether group.[65−72]

2.2.2. Effects of Anion Structure. The oxidative stability of anions mainly determines the anodic limit of the ILs. Fluorinated anions such as BF_4^-, PF_6^-, and amide type anions, such as $[TFSA]^-$ and $[FSA]^-$, are frequently used in the electrolytes owing to their good anodic stability. The Lewis basicity of these fluorinated anions is rather weak, resulting in weak interactions with the weakly Lewis-acidic organic cations in the liquids.[73]

When a Li salt is dissolved in molecular solvents (e.g., propylene carbonate), the Li^+ ion is stabilized by solvation and the salt dissociates into a solvated cation $[Li(solvent)_x]^+$ and counteranion. In the case of a binary mixture of Li salt and IL, the Li^+ is solvated by anions and forms complexes $[Li(X)_x]^{(x-1)-}$ (X: anion). For example, as shown in Figure 6, Li^+ and $[TFSA]^-$ may form complexes of $[Li(TFSA)_2]^-$ in certain binary mixtures.[74] The hydrodynamic radius of Li^+ is increased due to the complex formation, and the viscosity of the mixture is increased with increasing Li salt concentration, resulting in a decrease in ionic conductivity. Seki et al. reported the transference number of Li^+ (t_{Li}) in 0.32 mol/kg Li[TFSA]/[DEME][TFSA] to be as low as 0.13.[70] This value is much smaller than that of Li^+ in molecular solvents. The t_{Li} in $LiPF_6$/propylene carbonate solution can be evaluated from the self-diffusion coefficients of Li^+ (D_{Li}) and PF_6 (D_{PF6}) as follows: $t_{Li} = D_{Li}/(D_{Li} + D_{PF6})$. In accordance with the literature, t_{Li} in solutions of $LiPF_6$ dissolved in molecular solvents is in the range of 0.3−0.5.[75] In the binary mixture of Li salt/IL, in addition to Li^+, the organic cation and anions are mobile. Besides, the Li forms complexes with anions, resulting in the relatively low t_{Li}. The low mobility of Li^+ results in low limiting current density in the Li-ion cells.[76]

To increase the mobility of Li^+ ion, the design of the anion structure is critical. The viscosity of ILs is significantly affected by the anion structure. Matsumoto et al. reported the correlation between size of anion and viscosity of the ILs.[65] As can be seen in Figure 7, not only the anion size but also the structure significantly affects the viscosity. For example, the viscosity of $[DEME]C_2F_5BF_3$ is much lower than that of $[DEME]BF_4$, despite the larger size of $C_2F_5BF_3^-$. The introduction of asymmetric structure in the anion is effective in decreasing the viscosity,[77,78] possibly resulting from a

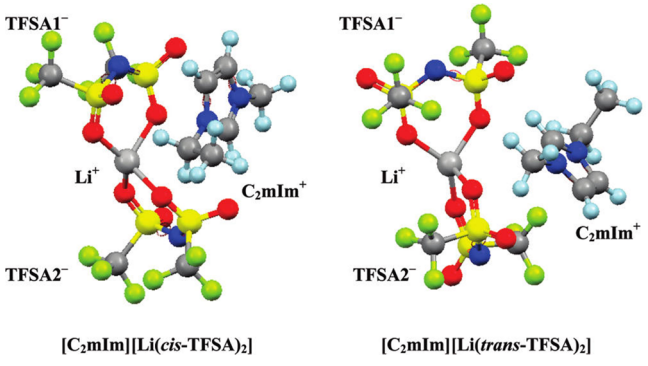

Figure 6. Respective most stable configuration for $[C_2mim][Li(cis\text{-}TFSA)_2]$ and $[C_2mim][Li(trans\text{-}TFSA)_2]$. Reprinted from ref 74. Copyright 2010 American Chemical Society.

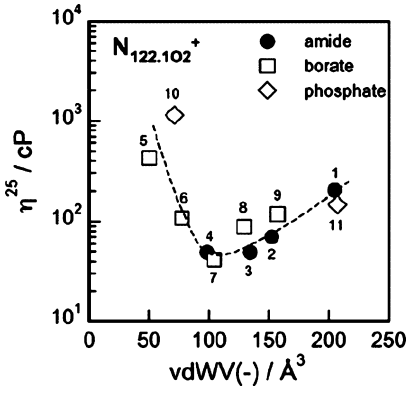

Figure 7. Relationship between viscosity of $[DEME]^+$-based ILs at 25 °C (η^{25}) and van der Waals volume of perfluoroanion (vdWV(−)) obtained by 6-311++G** level ab initio calculation. Cation: [DEME] = $N_{122.102}^+$ = diethylmethylmethoxyethylammonium. Anions: (1) [BETA], (2) [TFSA], (3) [TSAC], (4) [FSA], (5) BF_4^-, (6) $CF_3BF_3^-$, (7) $C_2F_5BF_3^-$, (8) n-$C_3F_7BF_3^-$, (9) n-$C_4F_9BF_3^-$, (10) PF_6^-, and (11) [FAP]. Reprinted with permission from ref 65. Copyright 2008 The Electrochemical Society.

DOI: 10.1021/acs.chemrev.6b00504
Chem. Rev. 2017, 117, 7190−7239

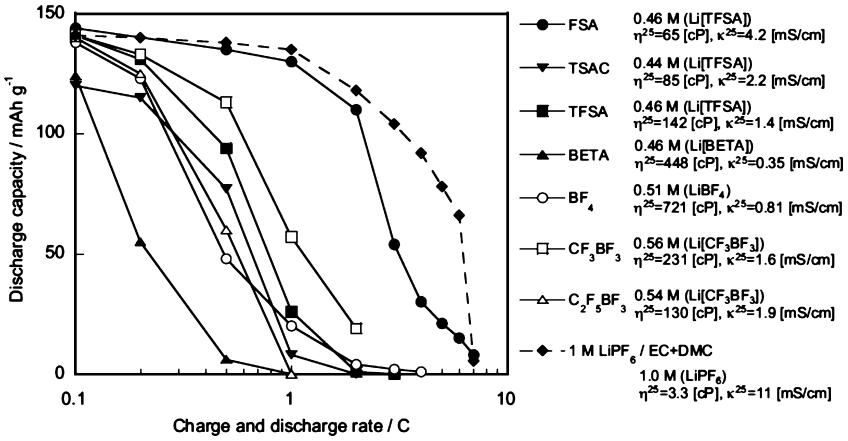

Figure 8. Charge−discharge rate property of Li/$LiCoO_2$ cell using $[DEME]^+$-based ILs measured at 25 °C. 1C rate corresponds to 0.2 mA cm^{-2}. The physical properties of lithium electrolytes at 25 °C used were also indicated. Reprinted with permission from ref 65. Copyright 2008 The Electrochemical Society.

decrease in melting points. Among the ILs with a common cation $[DEME]^+$, [DEME][FSA] possesses the lowest viscosity. Low viscosity is favorable as it enhances the Li^+ mobility in the electrolyte. Li salts were dissolved in various [DEME]X ILs, and the prepared electrolytes were used for Li/$LiCoO_2$ cells (Figure 8). In the cells, Li^+ extraction from the $LiCoO_2$ positive electrode ($LiCoO_2 \rightarrow Li_{1-x}CoO_2 + xLi^+ + xe^-$)[79] and Li metal deposition occur at the negative electrode during charge, and the reverse reactions occur during discharge. Figure 8 shows the discharge capacities of Li/$LiCoO_2$ cells measured at various current densities. Li[TFSA]/[DEME][FSA] has the lowest viscosity and highest ionic conductivity among the IL-based electrolytes in Figure 8, leading to the high rate capability of the corresponding Li/$LiCoO_2$ cell. The advantages of [FSA]-based ILs as electrolytes for Li batteries have been reported by many researchers.[80−89]

The electrode/electrolyte interfacial charge transfer process is also greatly affected by the anion structure of the IL. At the interface, the decomplexation (desolvation) of $[Li(X)_x]^{(x-1)-}$ occurs and anions are liberated. Therefore, the interaction between Li^+ and anions has a significant effect on the interfacial charge transfer process.[90−93] Figure 9 shows the charge transfer resistances (R_{ct}) for the electrode/electrolyte interfaces in Li/$LiCoO_2$ cells with Li salt/[DEME][X] electrolytes evaluated by AC impedance method.[65] Apparently, the charge transfer resistances at both the Li metal electrode and $LiCoO_2$ electrode change depending on the anion species of IL. The R_{ct} values of Li metal and $LiCoO_2$ are lower in the [FSA]-based IL compared with those in other IL-based electrolytes, and this attractive feature is favorable to the development of high power Li batteries.

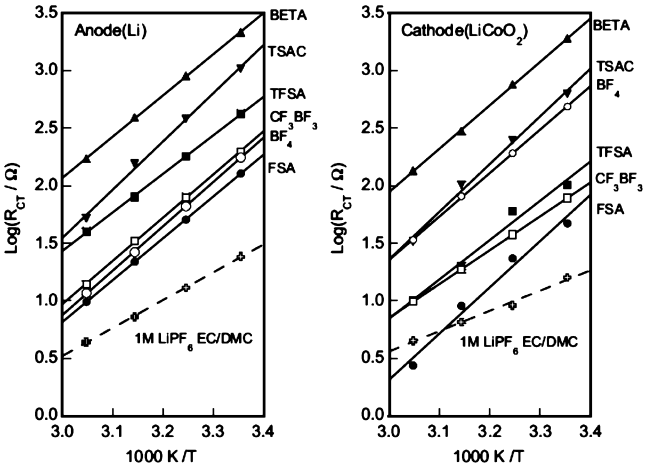

Figure 9. Arrhenius plot of apparent charge transfer resistance of $LiCoO_2$ cathode and Li anode observed in various $[DEME]^+$-based ILs. Cell voltage was kept to be 4.2 V. Reprinted with permission from ref 65. Copyright 2008 The Electrochemical Society.

Graphite is a representative commonly employed negative electrode material for Li ion batteries.[4] During the charging of a Li-ion cell, the reduction reaction of graphite occurs and Li^+ intercalates into the layered graphite structure to maintain electrical neutrality ($6C + Li^+ + e^- \rightarrow LiC_6$).[94] In the case of Li salt/IL electrolytes (except for [FSA]-based ILs), it is known that the organic cation is inserted into the graphite instead of Li^+, and destruction of the layered structure of graphite takes place.[95,96] However, in the [FSA]-based ILs, the intercalation of organic cation into graphite is suppressed and reversible Li^+ intercalation occurs.[81] Figure 10 shows cyclic voltammograms of graphite electrodes in binary mixtures of Li[TFSA]/ILs. In the case of Li[TFSA]/$[C_2mim][TFSA]$, the $[C_2mim]^+$ cation is intercalated into the graphite at an electrode potential of ca. 1 V versus Li/Li^+ during the first cathodic scan, and this intercalation is irreversible. On the other hand, in the case of [FSA]-based ILs, the Li^+ intercalation reaction takes place reversibly in the potential range of 0.2−0 V. In addition, in the case [FSA]-based ILs, the reductive decomposition of $[C_2mim]^+$ cation at the negative electrode is also prohibited. At present, it is not clear why the intercalation of organic cation and decomposition of $[C_2mim]^+$ cation are prevented in the [FSA]-based ILs. It has been reported that a small amount of $[FSA]^-$ anion is decomposed during the initial charging, and the decomposition products form a stable passivation layer on the graphite electrode,[97] which may prohibit the intercalation and decomposition of organic cation. However, another mechanism was also proposed recently,[98] and further research is needed for elucidating the electrode process in the [FSA]-based ILs. In any case, it is worth mentioning that owing to the favorable nature of [FSA]-based ILs, a Li-ion cell with a [FSA]-based IL electrolyte was adopted as a power source for an artificial satellite in 2014.[99]

DOI: 10.1021/acs.chemrev.6b00504
Chem. Rev. 2017, 117, 7190−7239

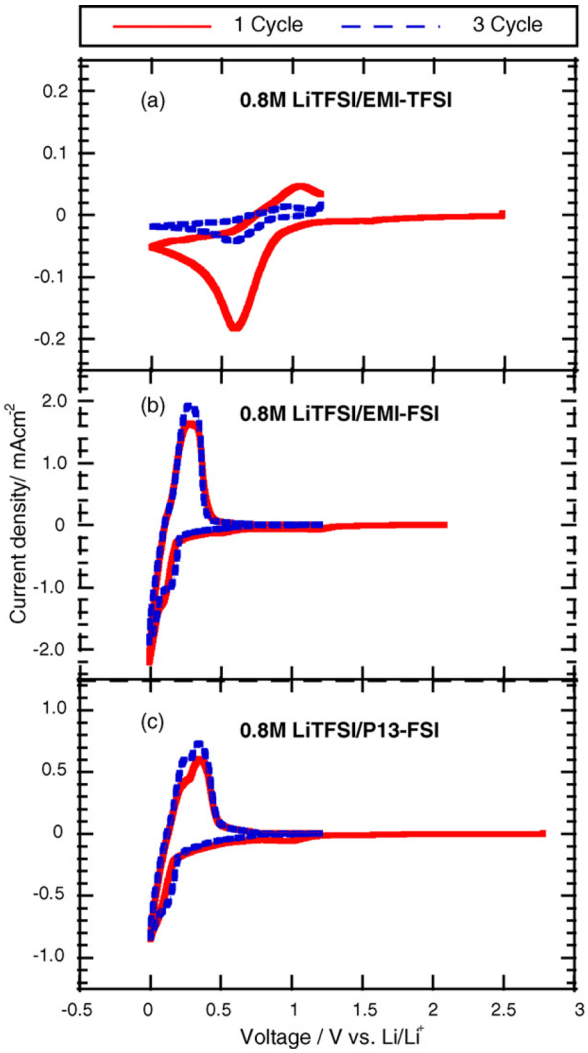

Figure 10. Cyclic voltammograms of natural graphite in various ionic liquid electrolytes between 0 and 1.2 V at a scan rate 0.1 mV s^{-1}: (a) 0.8 M Li[TFSA]/[C_2mim][TFSA], (b) 0.8 M Li[TFSA]/[C_2mim]-[FSA], and (c) 0.8 M Li[TFSA]/ [C_3mpyr][FSA]. Reprinted with permission from ref 81. Copyright 2006 Elsevier.

As well as Li salt/organic IL binary systems, the Na salt/organic ILs can also be used as the electrolytes for Na and Na-ion batteries.[100−114] Hagiwara et al. demonstrated the operation of Na batteries using Na[FSA]/[C_3mpyr][FSA] as the electrolyte in the wide temperature range of −20−90 °C.[100]

2.2.3. Organic Ionic Plastic Crystals. Organic ionic plastic crystals have been investigated as solid electrolytes for Li batteries. The organic ionic plastic crystals are solids at room temperature; however, their constituent ions are very similar to those of Li salt/organic ILs.[115−119] Of course, upon elevating the temperature, the ionic plastic crystals melt and become ILs. Herein, we briefly highlight the Li^+ ion conducting organic ionic crystals. In organic ionic plastic crystal phases, ions have conformational and rotational motion in the crystalline lattice.[116] Although the ionic conductivity of neat ionic plastic crystals such as [C_2mpyr][TFSA] is not so high (10^{-6} S cm^{-1} at 60 °C), the doping of a small amount of Li[TFSA] (4.8 mol %) dramatically enhances the conductivity to 10^{-4} S cm^{-1}. The ion conduction mechanism in the plastic crystal is still unclear but has been thought to be related in part to rotatory and vacancy motions.[116] The doping of organic ionic plastic crystals with Li salts is expected to increase the number of defects (vacancies and/or dislocations), and this probably facilitates the ion transport. However, a different ion conduction mechanism was proposed recently,[120,121] and further research may be needed. In any case, many Li-salt-doped organic ionic plastic crystals possess Li^+ conductivity, and several groups have demonstrated the operation of all-solid-state Li batteries using the plastic crystals as solid electrolytes.[122−125]

2.3. Li/Na Solvate Ionic Liquids and Solvent-in-Salt Electrolytes

2.3.1. Solvate Ionic Liquids. Li salts and glymes form complexes in certain molar ratios, and the complexes are low melting.[126,127] Among the complexes, the equimolar complexes of Li amide salts and triglyme (G3) or tetraglyme (G4) can be regarded as ILs (Figure 11). The melting point of the

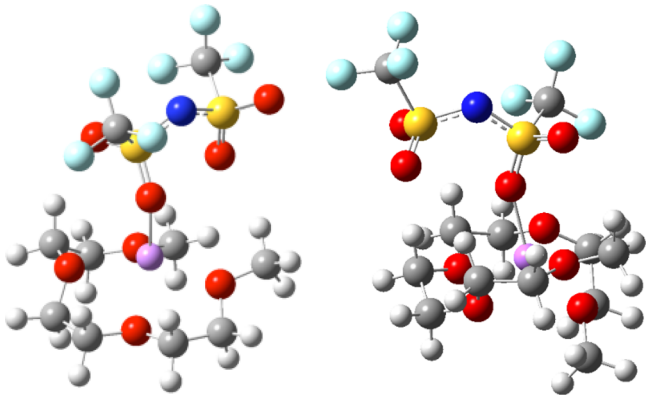

Figure 11. Optimized structures of [Li(G3)][TFSA] (left) and [Li(G4)][TFSA] (right). Purple, Li; red, O; silver, C; blue, N; yellow, S; light blue, F; and white, H. Reprinted from ref 130. Copyright 2011 American Chemical Society.

equimolar complex of Li[TFSA] and G3, [Li(G3)][TFSA], is 23 °C and the complex maintains a liquid state in a wide temperature range as a supercooled liquid. The complex of Li[TFSA] and G4, [Li(G4)][TFSA], is also liquid at room temperature and is a glass forming liquid with a glass transition temperature of −54 °C. Smyrl et al. pointed out for the first time that the molten [Li(G4)][TFSA] and [Li(G4)][BETA] complexes can be regarded as ILs;[128] however, no actual evidence was demonstrated. In the molten complex of [Li(G3 or G4)][TFSA], the Li^+ and glyme (G3 or G4) form a long-lived complex cation in 1:1 ratio, $[Li(G3 \text{ or } G4)]^+$, owing to the chelate effect, and the molten complex can be regarded as an IL consisting of a solvate cation $[Li(G3 \text{ or } G4)]^+$ and $[TFSA]^-$ anion.[129−134] [Li(glyme)][TFSA] is nonflammable and shows negligible vapor pressure at a temperature under 100 °C.[134] We have to mention here that, historically, Angell was the first who noticed in 1965 that the "hydrate melts", such as $Mg(NO_3)_2 \cdot nH_2O$ and $Ca(NO_3)_2 \cdot 4H_2O$, behave as molten salts composed of a solvated (hydrated) $[M(H_2O)_n]^{2+}$ (M = Mg and Ca) cation and NO_3^- anion,[135,136] and he named such ILs comprised of solvated ions "solvate (chelate) ILs".[137]

The [Li(glyme)][TFSA] dissociates into $[Li(glyme)]^+$ and $[TFSA]^-$ anion at room temperature and exhibits ionic conductivity. The ionic conductivities of [Li(G3)][TFSA] and [Li(G4)][TFSA] are 1.1 and 1.6 mS cm^{-1}, respectively, at 30 °C.[129,130] [Li(glyme)][TFSA] possesses a high concentration of Li^+ of ca. 3 mol dm^{-3}, and the transference number of

DOI: 10.1021/acs.chemrev.6b00504
Chem. Rev. 2017, 117, 7190−7239

Li^+ is higher than 0.5. The ether-based electrolytes have not been used in Li-ion cells because the oxidation of the ethers occurs at an electrode potential close to 4 V versus Li/Li^+. The oxidative stability of glyme can be enhanced by complexation with Li^+.[130] Figure 12 shows the linear sweep voltammograms

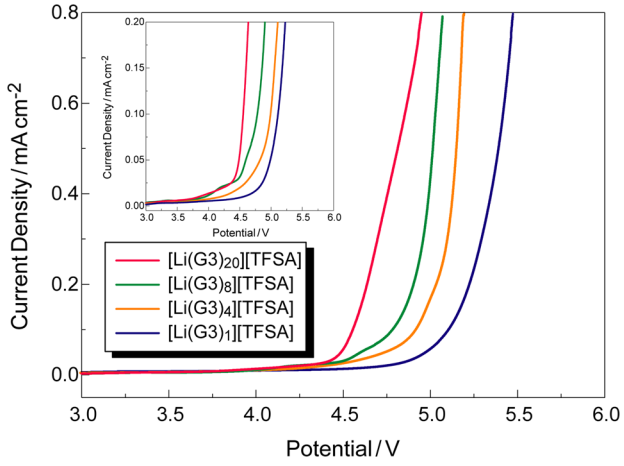

Figure 12. Linear sweep voltammograms of $[Li(G3)_x][TFSA]$ (x = 1, 4, 8, and 20) at a scan rate of 1 mV s^{-1} at 30 °C. Reprinted from ref 130. Copyright 2011 American Chemical Society.

of mixtures of G3 and Li[TFSA]. When the molar ratio of G3/Li[TFSA] is higher than 1, the onset of anodic current can be seen at around 4 V versus Li/Li^+. The anodic current originates from the irreversible oxidation of G3. Upon decreasing the amount of G3 in the mixtures, the anodic limit shifts toward a more positive potential, and the 1:1 complex [Li(glyme)][TFSA] is stable up to 4.5 V versus Li/Li^+. The oxidation of G3 is caused by the extraction of electrons from the lone pairs of ether oxygen atoms. The lone pairs are attracted to Li^+, and the HOMO energy level of glyme is lowered by complexation with Li^+. According to ab initio molecular orbital calculations, the HOMO levels of neat G3 and G4 are −11.45 and −11.46 eV, respectively, and these are lowered to −12.10 and −11.80 eV, respectively, upon complexation with Li[TFSA].[130] The lowering of the HOMO level results in the enhancement of oxidative stability of the glyme molecules. In the molten [Li(glyme)][TFSA] complex, almost all the glyme molecules participate in the complexation and free glyme scarcely exists in the [Li(glyme)][TFSA] solvate ILs,[132] resulting in the suppression of oxidative decomposition of glyme. With the use of the solvate IL of [Li(G3 or G4)][TFSA] as an electrolyte, a 4 V-class Li ion cell of $Li/LiCoO_2$ can be charged and discharged stably for more than 200 cycles as shown in Figure 13. Moreover, in the Li-glyme solvate ILs, the reversible Li^+ intercalation into graphite becomes possible.[138,139] Therefore, we can construct Li-ion cells using the [Li(glyme)][TFSA] electrolyte with a graphite negative-electrode and 4 V-class positive-electrode.

As well as the [Li(glyme)][TFSA] for Li cells, the corresponding complexes for the Na system, [Na(glyme)][TFSA], can also be used as electrolytes for Na cells. The physicochemical properties and battery applications of [Na(glyme)][TFSA] have been reported recently.[140−142]

The ionic conductivities of [Li(G3)][TFSA] and [Li(G4)][TFSA] are relatively low (~10^{-3} S cm^{-1}) compared with those of conventional organic electrolytes [e.g., ~10^{-2} S cm^{-1} for 1 mol dm^{-3} $LiPF_6$ dissolved in ethylene carbonate and diethyl

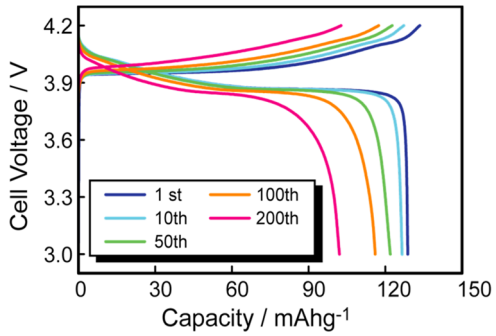

Figure 13. Charge and discharge curves of the [Li metal anode | [Li(G3)][TFSA] | $LiCoO_2$ cathode] cells measured with a current density of 50 μA cm^{-2} (1/8 C-rate) at 30 °C. Reprinted from ref 130. Copyright 2011 American Chemical Society.

carbonate (1:1 in volume)].[4] Therefore, Li-ion cells with [Li(glyme)][TFSA] electrolyte cannot be charged and discharged at high current densities.[76] The addition of another solvent to the solvate ILs is a facile and effective way to lower viscosity and enhance ionic conductivity. [Li(glyme)][TFSA] is miscible with a wide variety of solvents. Ueno et al. reported the physicochemical properties of mixtures of [Li(glyme)][TFSA] and a hydrofluoroether (HFE) having the chemical structure $CF_2H-CF_2-O-CH_2-CF_2-CF_2H$.[143,144] This HFE is chemically stable and nonflammable.[145] By the dilution of [Li(glyme)][TFSA] with the HFE, the viscosity and ionic conductivity are decreased and increased, respectively. In [Li(glyme)][TFSA]/HFE mixtures, the HFE molecule hardly participates in the solvation of Li^+ owing to the low electron-pair donating ability. The complex $[Li(glyme)]^+$ structure is maintained in the [Li(glyme)][TFSA]/HFE solutions and free glyme hardly exists.[143,144] Hence, the oxidative stability of the electrolyte does not change after the addition of HFE. Furthermore, the graphite/$LiCoO_2$ cell can be stably operated using a [Li(G3)][TFSA]/HFE electrolyte.[146]

2.3.2. Solvent-in-Salt Electrolytes. As mentioned before, the concentration of Li salt in the solvate ILs of [Li(glyme)]X (X: amide-type anion) is as high as ca. 3 mol dm^{-3}. We can also prepare highly concentrated electrolytes of over 3 mol dm^{-3} using various solvents other than glymes.[147−161] In these highly concentrated electrolytes, the Li^+ and solvent form a solvate $[Li(solvent)_x]^+$ cation. The coordination number of Li^+ in liquids is typically 4 or 5.[4] Therefore, in extremely concentrated electrolytes with a molar ratio of solvent/Li salt less than the coordination number of 4, all of the solvent molecules can be assumed to be in the first solvation shell of Li^+, and free (uncoordinated) solvents thus scarcely exist in the solution. This situation is very similar to that of solvate ILs of [Li(glyme)]X. However, when a monodentate (e.g., tetrahydrofuran) or bidentate ligand (e.g., 1,2-dimethoxyethane) is used as the solvent, the lifetime of the solvent in the first solvation shell of $[Li(solvent)_x]^+$ is much shorter than that of $[Li(G3 \text{ or } G4)]^+$ of the [Li(G3 or G4)]X solvate ILs.[133] This is because the ligand exchange between the $[Li(solvent)_x]^+$ cations (solvent: monodentate or bidentate ligand) occurs at a high frequency, while the $[Li(G3 \text{ or } G4)]^+$ has a relatively long lifetime owing to the chelate effect. Therefore, the extremely concentrated $[Li(solvent)_x]X$ solutions cannot be regarded as ILs. However, the extremely concentrated electrolytes possess unique properties, some of them very similar to those of solvate ILs, but different from those of common

DOI: 10.1021/acs.chemrev.6b00504
Chem. Rev. 2017, 117, 7190−7239

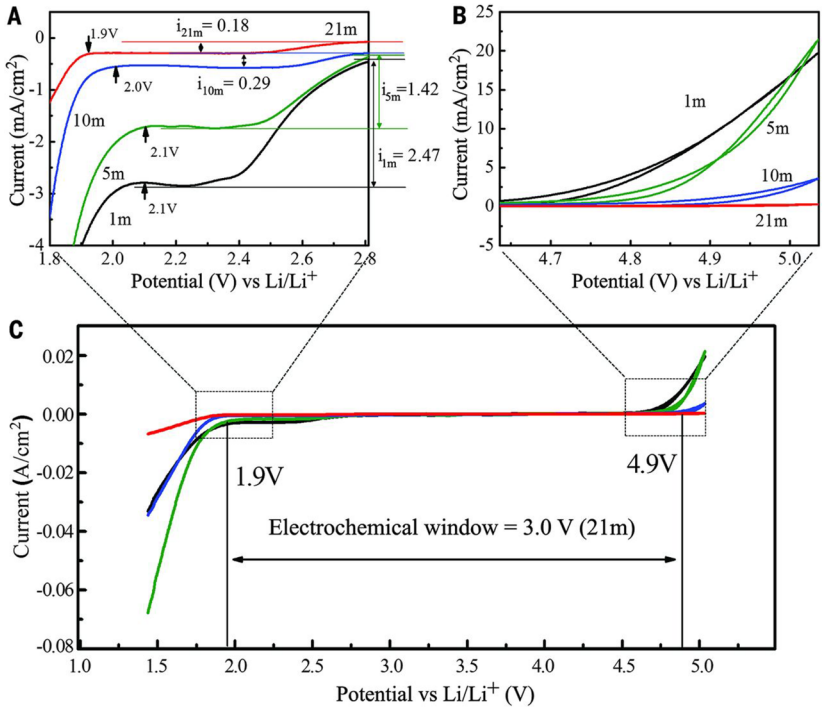

Figure 14. Electrochemical stability window of Li[TFSA]-H_2O electrolytes on nonactive electrodes. Reprinted with permission from ref 163. Copyright 2015 AAAS.

electrolyte solutions with salt concentrations less than 2 mol dm^{-3}.[162] The extremely concentrated electrolytes are recently termed "solvent-in-salt"[155] or "superconcentrated"[160] electrolytes. With regard to the organic solvent-in-salt electrolytes for Li batteries in a review article by Yamada et al., the advantages of the electrolytes, such as the wide electrochemical windows, suppression of volatility, suppression of Al corrosion, and highly reversible reactions of Li metal and graphite electrodes were well-highlighted.[162]

Recently, the solvent-in-salt concept was extended to the aqueous electrolytes[163−167] (i.e., a revival of "hydrate melts")[135,136] for Li-ion cells. Figure 14 shows the electrochemical stability window of Li[TFSA]−H_2O system. Suo et al. found that the electrochemical window of water is clearly expanded with increasing Li[TFSA] concentration.[163] A solution of 21 mol/kg Li[TFSA]−H_2O (molar ratio of Li[TFSA]: H_2O = 1:2.64) possesses a 3 V window, much wider than the thermodynamic limit for pure H_2O (1.23 V). The anodic limit expansion can be attributed to the decrease of free water in solution (i.e., water that is not coordinated to Li^+). Suo et al. suggested that a decrease in the number of adsorbed water molecules on the electrode surface and the exclusion of water from the inner-Helmholtz layer at the electrode surface enhances the oxidative stability of the electrolyte. The cathodic limit expansion is attributed to the formation of a LiF-based passivation layer, which is a decomposition product of the $[TFSA]^-$ anion. The layer passivates the electrode surface and suppresses the further reductive decomposition of electrolyte (water). A 2.3 V Li-ion cell using the water-in-salt electrolyte could be operated stably for more than 1000 cycles. Further research on water-in-salt electrolytes may open up the development of high-voltage aqueous Li-ion cells.

2.4. Li^+-Conducting Polymer Electrolytes Containing Ionic Liquids

ILs can be gelated by mixing with polymers.[168−171] The resultant gels, hereafter termed as "ion-gels", can be used as electrolytes for batteries. In ion-gels, ILs are confined in the polymer matrix, and this is advantageous to avoid the leakage of electrolytes and realize high safety of batteries. Ion-gels are polymer electrolytes; however, they are clearly different from conventional polymer electrolytes. In the case of Li^+-conducting conventional polymer electrolytes, Li salts are dissolved in polymers such as poly(ethylene oxide) (PEO), and the ionic conduction is coupled with the segmental motion of the polymer chains.[172] Therefore, the ionic conductivities of conventional polymer electrolytes (i.e., "salt-in-polymer" type electrolytes)[168] are as low as 10^{-6}−10^{-4} S cm^{-1} at room temperature. On the other hand, in the case of ion gels, the liquid state salts such as Li salt/organic ILs are mixed with polymers and the ILs behave as both charge carriers and plasticizers in the gels. By utilizing ILs, we can prepare "polymer-in-salt"[168] type electrolytes having relatively high ionic conductivity of ca. 10^{-4}−10^{-3} S cm^{-1} at room temperature. Applications of ion gels in Li batteries have been reported by many groups.[173−186] For example, Passerini and co-workers prepared ion gels consisting of PEO, Li[TFSA], and a room temperature IL (Figure 15) and demonstrated the operation of Li/$LiFePO_4$ cell at 40 °C.[174]

There are several methods to prepare ion gels such as hot-pressing,[174] solvent casting,[170] and in situ polymerization.[171] To confine the ILs in the polymer matrix, the polymer should be compatible with the liquids. The polyethers (such as PEO),[174] poly(methyl methacrylate) (PMMA),[171] and copolymer of poly(vinylidene fluoride-*co*-hexafluoropropylene) (PVDF-HFP) have been reported to be compatible with ILs.[170] It is known that the PVDF-HFP has relatively good mechanical strength due to the partially crystalline nature even if some plasticizer is

DOI: 10.1021/acs.chemrev.6b00504
Chem. Rev. 2017, 117, 7190−7239

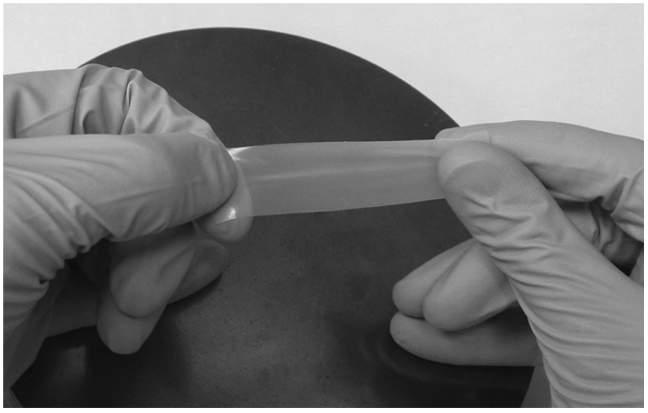

Figure 15. $P(EO)_{20}Li[TFSA]$ + 80 wt % $[C_3mpyr][TFSA]$ (wt % relative to PEO) solid polymer electrolyte. Reprinted with permission from ref 174. Copyright 2005 The Electrochemical Society.

included in the matrix.[187] However, the mechanical properties of PEO and PMMA are affected by the amount of plasticizer. With increasing content of IL in an ion-gel, the ionic conductivity is enhanced; however, the gel also becomes mechanically weaker. To achieve both high ionic conductivity and sufficient mechanical strength, the polymer cross-linking is effective. For example, ion gels can be easily prepared by in situ polymerization of MMA in an IL, and the PMMA matrix can be cross-linked using ethylene glycol dimethacrylate (EGDMA) as a cross-linker.[171] Another way is the use of physical cross-linking. An ion-gel consisting of the block copolymer of P(MMA-*b*-St) (St: styrene) and an IL possesses a microphase separated structure because the PSt block is incompatible with the IL, and the PSt blocks aggregate in the gel and act as physical cross-linking points.[188] The addition of a ceramic filler such as γ-$LiAlO_2$ to the polymer matrix may also be effective in enhancing the mechanical strength of the ion gel.[189,190]

3. LITHIUM–SULFUR (LI–S) BATTERY ELECTROLYTES

3.1. Li–S Batteries

Elemental sulfur has an extremely high theoretical capacity of 1672 mA h g^{-1}, which is an order of magnitude higher than capacities of transition metal-based cathode materials in lithium-ion batteries. When combined with a lithium metal anode, the specific energy of the Li–S cell is projected to be 400–600 Wh kg^{-1} and is approximately three times higher than that of state-of-the-art lithium-ion batteries.[191] Therefore, elemental sulfur has attracted much attention as a cathode material that has the potential to meet the demand for efficient, clean, and high density electric energy storage and conversion in the contemporary world. Furthermore, sulfur is naturally abundant, environmentally benign, and thereby the Li–S battery is expected to be a promising future energy storage for achieving a sustainable society.

Typical Li–S batteries consist of sulfur/carbon composites as the positive electrode, lithium metal as the negative electrode, and a Li-ion conducting electrolyte, commonly an ether-based organic electrolyte (Figure 16).[192] The overall reaction in a Li–S cell can be simply written as $S_8 + 16Li \rightarrow 8Li_2S$, where octacyclo sulfur (S_8) is converted to Li_2S upon discharge, and average cell voltage is about ~2.1 V based on the above reaction. However, the conversion reaction involves a multistep reduction process, forming lithium polysulfide intermediates (Li_2S_m, generally m = 2–8), and the polysulfide anions are

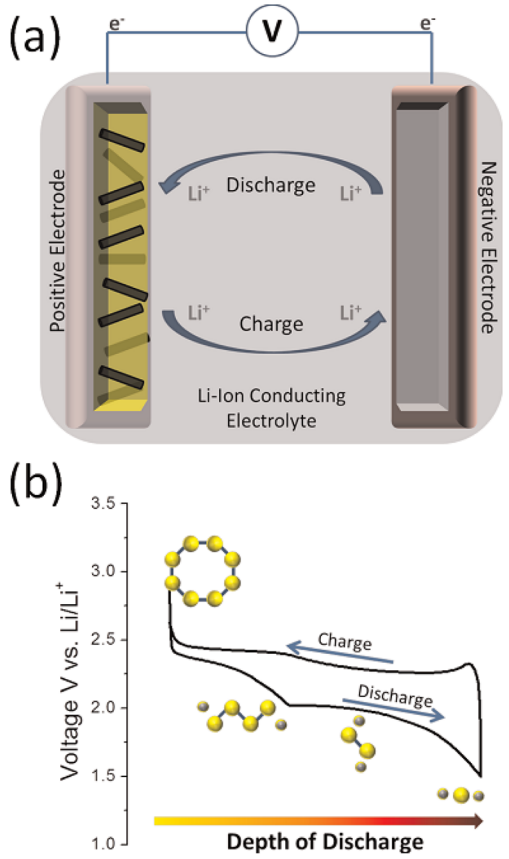

Figure 16. (a) Schematic illustration of a typical Li–S cell. (b) A typical voltage vs capacity profile for a Li–S cell. During discharge, S_8 is opened and shortened until the final discharge product Li_2S is formed. Reprinted from ref 192. Copyright 2013 American Chemical Society.

known to undergo disproportionation reactions between S_8 and Li_2S_m (e.g, $2S_m^{2-} \rightarrow S_n^{2-} + (m-n)S_8/8$, $2S_n^{2-} \rightarrow S_{m+n}^{2-} + S_{m-n}^{2-}$, and $S_m^{2-} \rightarrow 2S_{m/2}^{\bullet-}$).[193] As shown in Figure 16b, there are two voltage plateaus of approximately 2.4 and 2.0 V in the discharge curves. The first discharge plateau region at ~2.4 V is assigned to the reduction of S_8 via a 4-electron process: $S_8 + 4Li^+ + 4e^- \rightarrow 2Li_2S_4$. The second plateau at ~2.0 V provides a large part of the discharge capacity and is assigned to the further reduction of longer polysulfides to yield shorter sulfides such as Li_2S. In the charge curves, Li_2S is oxidized to longer polysulfides at ~2.3 V, and the subsequent potential rise at the end of the charge plateau corresponds to the oxidation of longer polysulfides (solution) to S_8 (solid).

Since the Li–S battery concept was first proposed in 1962,[194] much effort has been devoted to both understanding the complicated chemistry of the sulfur redox reactions and developing battery component materials to improve the charge–discharge performance (including carbon current collector as host of sulfur, electrolyte, and binder).[195–197] However, the reported charge–discharge performance of Li–S batteries has yet to satisfy requirements for their practical application although some companies have developed prototype Li–S cells. Major obstacles facing Li–S batteries are the inherent insulating property of the active species and dissolution of high-order lithium polysulfides (Li_2S_m, generally m = 4–8) into the electrolyte. These act to diminish the electrochemical contact of the active species to the conductive

DOI: 10.1021/acs.chemrev.6b00504
Chem. Rev. 2017, 117, 7190–7239

host during charge−discharge cycles, leading to low utilization of the active material (i.e., low discharge capacity) and sluggish electrochemical reactions. The latter dissolution also causes a rapid capacity fade (i.e., short cycle life) and low Coulombic efficiency, whereby the dissolved Li_2S_m undergoes unfavorable side reactions, namely repeated shuttling of polysulfides through reduction at the lithium metal anode and reoxidation at the sulfur cathode (so-called, redox shuttle mechanism). The shorter reduction products, Li_2S_2 and Li_2S, are believed to be insoluble in organic electrolytes. If these shorter Li_2S_m precipitate elsewhere in the cell (i.e., not in contact with the carbon current collector), they then also become electrochemically inactive and the capacity fades. Therefore, developing electrolyte solutions that control the solubility of Li_2S_m and S_8 has been the one of the subjects of intense research on Li−S batteries.

In a typical Li−S cell, an organic electrolyte solution composed of 1 mol dm^{-3} Li[TFSA] in a binary mixture of 1,2-dimethoxyethane (DME) and 1,3-dioxolane (DOL) at 1:1 by volume is used as a standard electrolyte.[198] Instead of the highly volatile DME and DOL, longer oligoether solvents such as G3 and G4 were also used as solvents. Dissolution of high-order Li_2S_m is not impeded in these organic electrolytes, and the redox reactions of the positive electrode take place through solution-mediated dissolution/precipitation processes (from solid S_8 to dissolved high-order Li_2S_m and then to solid low-order Li_2S_m). Hence, the Li_2S_m solubilizing electrolyte functions as a liquid catholyte in the Li−S cells (Figure 17 left).[199] The

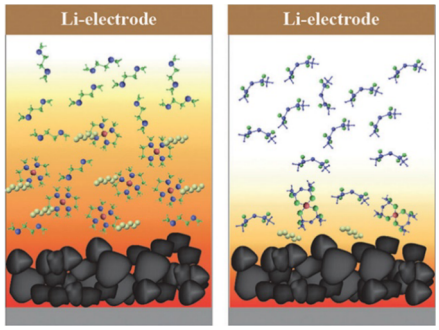

Figure 17. Concept of two different strategies of electrolytes for Li−S batteries. (Left) Li−S cell separated by a typical organic electrolyte, for example, 1 mol dm^{-3} Li[TFSA] in a binary mixture DME and DOL. (Right) Li−S cell separated by a Li_2S_m sparingly soluble electrolyte; for example, consisting of an IL [C_3mpyr][TFSA] as the solvent. The region of solubilized Li_2S_m in the electrolyte was indicated as orange. Reprinted with permission from ref 199. Copyright 2016 Royal Society of Chemistry.

solvated Li_2S_m can easily access the carbon current collector, so that the sulfur active materials are effectively utilized, leading to high capacity. Their faster mass transport and higher ionic conduction allow higher-rate charge−discharge of the cell. The solution-mediated dissolution/precipitation redox reaction, without the large volume changes observed for the solid-phase process, can mitigate the breakdown of the electrical contact within the composite cathode. An effective passivation layer is further required on the Li metal anode to inhibit the direct reduction of soluble S_m^{2-} at the Li metal (i.e., redox shuttling). $LiNO_3$ has been commonly used as additive or cosalt to form an effective protective layer by sacrificial decomposition of the nitrate anion on the Li metal surface.[200] However, such additives are consumed during repeated charge−discharge cycles, which is problematic for realizing a long-life cell. Moreover, a Li−S cell with a Li_2S_m dissolving electrolyte requires a larger solvent content for effective charge−discharge with high utilization, which would result in a lowering of the specific energy density of the package cell due to the increased weight of the solvent.[201]

To realize high energy density Li−S cells, an alternative strategy aiming at low solubility of all the active species in the electrolyte has also been proposed (Figure 17 right).[199] Without dissolution of Li_2S_m, the redox reactions of the positive electrode can occur as solid-to-solid reactions, and so in this type of electrolyte, the parasitic redox shuttle is no matter of concern. However, the solid-state redox reaction may lead to slower electrochemical kinetics. Polymer and inorganic solid electrolytes can physically (or kinetically) block the dissolution of Li_2S_m, but they suffer from slower Li^+ conduction and difficulty in forming good electrolyte/electrode interfaces. For liquid electrolytes, a solvent that only sparingly dissolves the active species (S_8 and Li_2S_m) but sufficiently dissolves supporting Li salt is required. This is a somewhat demanding requirement because the hydrophobic S_8 is soluble only in nonpolar solvents, whereas Li_2S_m and the supporting Li salt are highly soluble in polar solvents. Recent studies have shown that ILs can play an important role as electrolyte in addressing the requirement of the latter strategy following the first report by Yang et al., who first used an IL, [C_4mpip][TFSA], containing 1 mol dm^{-3} Li[TFSA] as the electrolyte for the Li−S battery.[202] Certain neat IL-based liquid electrolytes were found to show very low solubility of all the redox-active species (S_8 and Li_2S_m).[203] These results are associated with the unique solvation properties for solutes in ILs, which can differ from molecular solvents as already revealed by fundamental studies on solute−solvent interaction in ILs. The Li_2S_m dissolution can also be suppressed by highly concentrated electrolytes having similar ionic concentration to ILs, such as Li-glyme solvate ILs,[134] or so-called "solvent-in-salt" electrolytes.[155] More recently, hybrid liquid electrolytes that contain organic solvents and ILs have been proposed to control the solubility of the active sulfur materials more precisely in electrolyte as well as to improve upon the lower ionic conductivity of highly viscous IL-based electrolytes.[203]

In the recent review papers on electrolytes for Li−S batteries, the detailed experimental battery test data using IL-based electrolytes have already been summarized and compared to those using organic electrolytes.[204,205] However, it is not easy to compare the battery data (capacity, efficiency, and cycle ability) from different reports using IL-based electrolytes because the battery performance is governed by many factors such as temperature, current collector, carbon materials, amount of electrolyte in the cell, sulfur loading in the cathode, and charge−discharge current density. Therefore, in this section, we will provide an overview on the effects of ILs on Li−S battery chemistry, especially for chemical stability of ions in the Li−S cell, the solubility of Li_2S_m, and their correlations with the battery performance.

3.2. Stability of Ions in the Presence of Li_2S_m

When ILs are considered as alternative electrolytes, one may be first interested in the stability of the constituent ions in the Li−S cell. Indeed, relatively high nucleophilicity of S_m^{2-} anions has a potential to cause side reaction with electrolyte components. Abruña et al. reported that carbonate solvents commonly used in lithium-ion batteries such as ethylenecarbonate and

DOI: 10.1021/acs.chemrev.6b00504
Chem. Rev. 2017, 117, 7190−7239

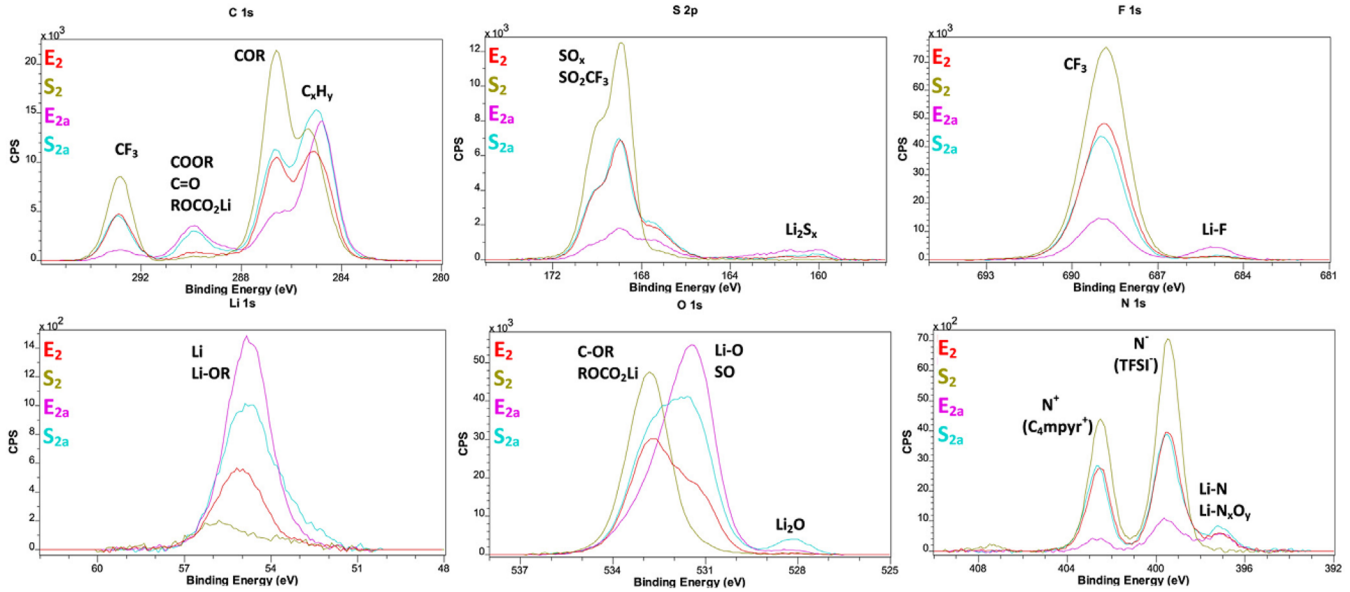

Figure 18. XPS spectra of Li surfaces prepared using (El_2) [C_3mpyr][TFSA]/G4 mixture (1:1, v/v) containing 1 mol kg^{-1} Li[TFSA] and 0.1 mol kg^{-1} $LiNO_3$ and (El_{2a}) [C_4mpyr][TFSA]/G4 mixture (1:1, v/v) containing 1 mol kg^{-1} Li[TFSA]. Legends E_2 and E_{2a} indicate XPS spectra of the anode of the cycled cell for 10 cycles at C/10 in El_2 and El_{2a}, respectively. Legends S_2 and S_2a indicate XPS spectra of fresh lithium disk soaked and stored in El_2 and El_{2a} respectively. Reprinted with permission from ref 214. Copyright 2015 Elsevier.

diethylcarbonate decomposed in Li−S batteries by the nucleophilic attack of S_m^{2-} to produce thioether and sulfonium functionalities.[206] This is one of the reasons that ether-based DME/DOL organic electrolytes have replaced the common carbonate-based electrolyte for Li−S cells. Because the number of studies on the stability of ILs in the presence of Li_2S_m has been rather limited, the stability of ions studied in organic electrolytes are also reviewed here.

BF_4^- is a weakly coordinating anion and has often been chosen to yield room temperature ILs. However, Park et al. in the Watanabe group reported that the irreversible decomposition of BF_4^- in [DEME]BF_4 occurs in the presence of S_m^{2-}.[207] Nucleophilic attack to the borate center of BF_4^- generates byproducts such as LiF and adducts of BF_3 and S_m^{2-} such as $[BF_3(LiS_m)]^-$, $[BF_2(LiS_m)_2]^-$, and $[(BF_3)_2(S_m)]^{2-}$ as suggested by ^{11}B and ^{19}F NMR spectra of the polysulfide solution in the electrolyte. The inherently high ionic strength in the IL electrolytes would allow the side reactions between the otherwise mutually repulsive negatively charged BF_4^- and S_m^{2-}. The decomposition of BF_4^- in the presence of Li_2S_m was also reported in an organic electrolyte[198] and a solvate IL [Li(G4)]BF_4.[208]

Zhang suggested that PF_6^- undergoes a similar side reaction with Li_2S_m in ether-based organic electrolytes.[198] This side reaction was not apparent in Li−S cells using 0.5 mol kg^{-1} $LiPF_6$ in [DEME][TFSA] IL-based electrolyte in Park's work.[207] Probably, the decomposition of PF_6^- was mitigated in the IL-based electrolyte where the solubility of Li_2S_m was greatly suppressed.

[FSA]-based ILs offer high ionic conductivity compared to other ILs having related fluorinated sulfonylamide anions such as $[TFSA]^-$ and $[BETA]^-$. However, Watanabe et al.[207] and Aurbach et al.[209] observed poor charge−discharge performance for Li−S cells with [FSA]-based IL electrolyte due to the decomposition of $[FSA]^-$ through the nucleophilic attack of S_m^{2-} at the $-SO_2F$ group. XRD spectra of the cathode after charge−discharge cycles indicated that solid byproducts including Li_2SO_4 and Li_2S were formed, and the surface-insulating layer drastically increased the charge-transfer resistance during charge−discharge. However, these side reactions can be prevented by combining $[FSA]^-$ based electrolytes with well-designed sulfur/carbon composite cathodes. Aurbach et al.[209] and Ishikawa et al.[210] observed stable charge−discharge cycling for Li−S cells even in IL-based electrolytes with $[FSA]^-$, using microporous activated carbon having a pore size of less than 2 nm as the carbon host for sulfur. It appears that small micropores that confine sulfur at the molecular level can protect against diffusion of solvents or the anion of the electrolyte to inside the pores. Although a number of other anions and cations have been employed as IL-based electrolytes or components of supporting Li salts for Li−S batteries, other than the aforementioned cases (BF_4 and PF_6), chemical stability of the ions to nucleophilic attack by S_m^{2-} has not been reported.

3.3. Stability of Ions and Protective Film Formation on Lithium Metal Anode

Stability of electrolyte components toward the lithium metal anode is also an important factor for designing the electrolyte solution for Li−S batteries. A common homologous series of IL cations, 1-alkyl-3-methyl imidazolium ($[C_n mim]^+$), is known to be unstable in contact with the lithium metal anode because the hydrogen atom at the C2-position of the imidazolium cation is readily reduced around 1.0 V versus Li/Li^+.[61] Wan et al. compared the battery performance of Li−S cells using 1 mol dm^{-3} Li[TFSA] in [C_3mim][TFSA] and in [C_3mpyr]-[TFSA].[211] The capacity of the cell with [C_3mim][TFSA] decreased rapidly down to 70 $mAhg^{-1}$ after 50 cycles, whereas the cell with [C_3mpyr][TFSA] showed stable charge−discharge cycles with a higher capacity (450 $mAhg^{-1}$ after 50 cycles). Although the fast capacity fade for the cell with [C_3mim]-[TFSA] was interpreted as higher solubility of Li_2S_m in this IL, it may also be attributed to the reductive decomposition of $[C_3mim]^+$ at the lithium metal anode. Watanabe and co-workers examined [C_4dmim][TFSA] where the proton at the

DOI: 10.1021/acs.chemrev.6b00504
Chem. Rev. 2017, 117, 7190−7239

C2-position of the imidazolium is replaced by a methyl group as electrolyte for the Li−S battery and found that $[C_4dmim]^+$ is stable in the Li−S cell operation.[207] Park et al. observed the opposite behavior in their study on the cationic effect on cycle life performance in Li−S cells using DME/DOL electrolytes containing ILs as supporting salt.[212] Li−S cells with $[C_2mim]$-[TFSA] or $[C_4mim]$[TFSA] showed much larger capacities and longer cycle life performance compared to the cell with $[C_3dmim]$[TFSA]. They claimed that this phenomenon is due mainly to the deactivation of the carbon cathode caused by a coating of insulating and insoluble materials, which might result from side reactions between $[C_3dmim]^+$ and Li_2S_m. However, further characterization of the cycled carbon cathode was not performed in their early paper.

The reductive decomposition of certain ions or solvents has often been exploited to form a good solid electrolyte interphase (SEI), which not only inhibits the direct reaction of dissolved Li_2S_m with the lithium metal anode and resultant parasitic shuttle effect but also mitigates dendritic growth of lithium metal during the Li plating reaction (charging). In Li−S battery chemistry, $LiNO_3$ is predominantly used as a sacrificial additive to form an effective protective layer on the lithium metal anode. NO_3^- is reduced at lithium metal anode to form Li_xNO_y.[213] However, Zhang pointed out that NO_3^- is also reduced at the carbon host of the positive electrolyte at 1.5 V versus Li/Li^+, which adversely affected the battery performance, and thus the cutoff voltage should be higher than 1.5 V.[200] Despite the fact that $LiNO_3$ was supposed to be an effective additive, considerable decomposition of NO_3^- during the discharge process and rapid failure of Li−S cells were also observed in a $[Li(G3)]NO_3$ electrolyte containing only NO_3^- as the anionic species.[208]

Hollenkamp et al. studied the effect of a $LiNO_3$ additive on the protective film on the lithium metal anode in an IL-based electrolyte, namely a 1 mol kg^{-1} Li[TFSA] in $[C_4mpyr]$-[TFSA]/G4 mixture.[214] Although $LiNO_3$ improved the battery performance (better capacity retention and higher Coulombic efficiency of above 99% over 100 cycles) with the IL-based electrolyte when compared to that with $LiNO_3$-free electrolyte, it was not as effective as in typical DME/DOL organic electrolytes. XPS data on the protective film suggested that the decomposition products of $[C_4mpyr]$[TFSA] such as CF_3, SO_2CF_3, $-N^+$, and $-N^-$ also participated in forming the protective layer (Figure 18). This observation is consistent with Matic et al., who analyzed the SEI film on a lithium electrode cycled in 0.4 mol kg^{-1} Li[TFSA] in $[C_4mpyr]$[TFSA] without the $LiNO_3$ additive.[215] A stable SEI film was formed in the IL-based electrolytes, and the film mainly consists of the decomposition fragments of $[TFSA]^-$. Matic et al. also compared the resistance for lithium ion transfer across the SEI film (R_{SEI}) formed in the IL-based electrolyte in the presence/absence of Li_2S_m and found that R_{SEI} for the cell cycled with Li_2S_m was higher. This was because the chemical composition of the SEI film contained more sulfide-related species in the top layer in the presence of Li_2S_m. These works suggest that $[TFSA]^-$ originating from both the Li salt and IL solvents partially decomposed at the lithium metal anode, and the decomposition byproducts serve as a good protective layer for the lithium negative electrode of Li−S batteries.

The stability and the film forming ability of $[TFSA]^-$ derivatives on the lithium metal anode were also investigated. In the report by Zhang et al.,[216] Li−S cells containing 3 mol dm^{-3} Li[FSA] in DME/DOL exhibited rapid capacity decay and failed after only about 30 cycles, whereas Li−S cell containing 3 mol dm^{-3} Li[TFSA] in DME/DOL delivered relatively stable cycling with good capacity retention even after 200 cycles. Poor cycle ability of the Li−S cells containing Li[FSA] was rationalized by the rapid growth of a passivation layer made up of insulating $LiSO_x$ on the metallic lithium anode. DFT calculation suggested that the N−S bond strength in the $[FSA]^-$ (192.7 kJ mol^{-1}) is much weaker than that in $[TFSA]^-$ (581 kJ mol^{-1}), and the scission of this bond in $[FSA]^-$ is responsible for the formation of insulating $LiSO_x$ in the presence of Li_2S_m. Gao et al. examined a Li[FSA]−Li[TFSA] (total concentration of 1.5 mol dm^{-3}) binary-salt electrolyte in DME/DOL as a low-viscosity and highly conductive electrolyte for the Li−S battery.[217] Compared to Li−S cells with either Li[FSA] or Li[TFSA], the Li−S cell using the binary-salt electrolyte showed a high capacity and stable cycle performance accompanied by smooth lithium deposition on the lithium anode. Very recently, an asymmetric fluorinated sulfonylamide lithium salt, $Li[(CF_3SO_2)(n\text{-}C_4F_9SO_2)N]$, (Li[TNFSA]) in DME/DOL was reported to form a more stable SEI film on lithium metal anode than those formed in the Li[TFSA]-based electrolyte.[218] The Li−S cell with Li[TNFSA] salt exhibited a more stable cycle performance than that with Li[TFSA] salt. The binary salt or the asymmetric sulfonylamide anion likely give rise to a synergistic effect on the formation of a suitable SEI on the lithium metal anode.

Chen et al. tested lithium difluoro(oxalate)borate (Li-[DFOB]), for which the anion incorporates structural features of both Li[BOB] (lithium bis(oxalate)borate) and $LiBF_4$, as a supporting lithium salt in IL-based electrolytes for Li−S battery.[219] Undesired charge−discharge performance of the cell with Li[DFOB] salt was explained as a result of continuously reductive decomposition of Li[DFOB] in the electrolyte during discharge process. The resulting byproducts were deposited as an excessive passivation film on the electrode surface, which increased charge transfer resistance of the cell. Chen et al. also examined Li[DFOB]/Li[TFSA] binary lithium salts, and the Li−S cell showed superior battery performance compared to those using either of the component lithium salts. In the electrolyte with the binary mixture of lithium salts, formation of a compact and uniform film was confirmed as the smooth surface morphology on the cycled lithium anode surface. The parent Li[BOB] was also tested as an additive in an organic electrolyte solution by Xiong et al. and contributed to formation of a smooth morphology on the lithium surface in Li−S batteries.[220] As another lithium salt additive, $LiClO_4$ is also effective in forming a suitable protective layer on lithium metal anode.[221]

Many ions in IL solvents and Li salts, predominantly the anion, have been found to decompose when in contact with lithium metal anode in Li−S cells, and their decomposition products participate in the SEI formation. It seems that either positive or negative effects on the battery performance occur, depending on the composition and thickness of the film in relation to Li^+ conductivity, which vary according to the electrolyte species (or their combination) and Li salt concentration. For further understanding of this complicated surface chemistry of the SEI formation in the presence of Li_2S_m and its correlation with Li−S battery performance, systematic studies using a series of ions and concentrations should be carried out under the same experimental conditions.

DOI: 10.1021/acs.chemrev.6b00504
Chem. Rev. 2017, 117, 7190−7239

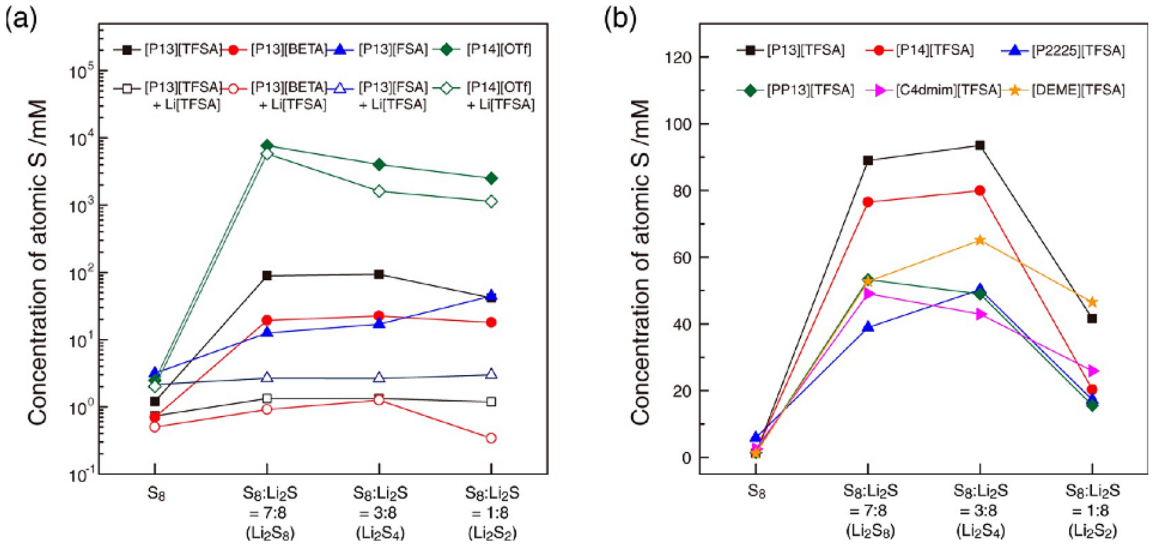

Figure 19. Saturation concentrations of S_8 and mixtures of S_8 and LiS_2 (Li_2S_m), represented in units of total atomic−S concentration (a) in pyrrolidinium ILs with different anions in the absence and presence of 0.5 mol kg^{-1} Li[TFSA] (on semilogarithmic scale), and (b) in [TFSA]-based ILs with different cations without LiTFSA. [P13] = [C_3mpyr], [P14] = [C_4mpyr], and [PP13] = [C_3mpip]. Reprinted from ref 207. Copyright 2013 American Chemical Society.

3.4. Solubility of Li_2S_m and S_8 in Ionic Liquids

Ai et al. reported a greatly improved discharge ability and cycle ability of Li−S cells with 1 mol dm^{-3} Li[TFSA] in [PP14][TFSA], and they interpreted that the improved performance was due to the suppression of polysulfide dissolution into electrolyte.[202] Wang et al. also suggested the reduced dissolution of Li_2S_m into 1 mol dm^{-3} in [C_2mim]-[TFSA] for their Li−S cell tests by comparing the battery performances between the IL-based electrolyte and ether-based organic electrolyte.[222] Although the above studies did not reveal any solubility data for Li_2S_m, the saturated solubility of Li_2S_m in an IL-based electrolyte, 0.64 mol dm^{-3} Li[TFSA] in [DEME][TFSA], has been determined by electrochemical titration of Li_2S_m followed by quantification using UV−vis spectroscopy of S_8 that was converted from the dissolved Li_2S_m.[223] The solubility of a series of polysulfides, with the nominal formulas Li_2S_8, Li_2S_4, and Li_2S_2 was higher for higher-order Li_2S_m, and the solubility of Li_2S_8 was 7 mmol dm^{-3} (atomic S basis), which is 3 orders of magnitude lower than that in an organic electrolyte, 0.98 mol dm^{-3} Li[TFSA] in G4. It was claimed that the significant difference in the solubility between these two electrolytes is attributed to the difference in the solvent affinity for Li^+ and Li_2S_m. This was based on the hypothesis that the dissolution of ionic Li_2S_m takes place through the solvation of Li^+ with the electrolyte molecules (i.e., $[TFSA]^-$ or G4). The Gutmann's donor number (DN) for [DEME][TFSA] was estimated to be ca. 10 kcal mol^{-1}, whereas the DN for G4 was reported to be 16.6 kcal mol^{-1}. Thus, Li_2S_m was expected to have lower solubility in the IL. Park et al. also showed that the Li_2S_m solubility further decreased in this IL in the presence of Li[TFSA] because some $[TFSA]^-$ anions in the IL were used to form a $Li[TFSA]_2^-$ complex anion.[223]

The dependence of Li salt concentration on the solubility of Li_2S_m was also studied in organic electrolytes. Oh et al.[224] and Hu et al.[155] reported that the dissolution of Li_2S_m was greatly suppressed in extremely concentrated electrolytes containing Li in DME/DOL. Oh et al. simply explained the lower solubility of Li_2S_m in the concentrated electrolyte in terms of the common ion effect. On the basis of dissociation equilibrium in the electrolyte, $Li_2S_m \rightleftarrows 2Li^+ + S_m^{2-}$, the solubility product constant (K_{sp}) of Li_2S_m is given as $K_{sp} = [Li^+]^2[S_m^{2-}]$. Hence, the dissolution of Li_2S_m can be mitigated when the electrolyte has a high concentration of the supporting Li salt. The nearly saturated electrolyte of Li[TFSA] (~7 mol dm^{-3}) in DME/DOL, termed a "solvent-in-salt" electrolyte by Hu et al., showed reversible plating/dissolution reaction of lithium metal anode as well as almost no solubility of Li_2S_m. An initial capacity exceeded 1000 mAh g^{-1}, with nearly 100% efficiency achieved for the Li−S cell using the "solvent-in-salt" electrolyte.

Interestingly, [TFSA]-based ILs or concentrated electrolytes with Li[TFSA] dominate most studies of the Li_2S_m-sparingly-soluble electrolytes for Li−S batteries (as depicted in Figure 17 right), even though many other ions and Li salts are available. Lower melting point, higher conductivity, and compatibility with the lithium metal anode of [TFSA]-based electrolytes are probably the principal reason for selecting this anionic species. However, the weak coordinating property is also another key factor for choosing $[TFSA]^-$ to inhibit the dissolution of Li_2S_m into the electrolytes.

The superiority of [TFSA]-based electrolytes with respect to the solubility of Li_2S_m was highlighted by a systematic study of the ionic effect on the Li_2S_m solubility and the Li−S battery performance in IL-based electrolytes. The saturated solubility of Li_2S_m in various ILs with different anionic and cationic species was determined in the same way as their previous investigation (Figure 19).[207] Among pyrrolidinium ILs ([C_4mpyr][TfO], [C_3mpyr][TFSA], [C_3mpyr][FSA], and [C_3mpyr][BETA]), [C_4mpyr][TfO] showed significantly higher solubility of Li_2S_m exceeding 2500 mM (atomic S basis) for all compositions of Li_2S_m, which is nearly 2 orders of magnitude higher than the solubility in other ILs. The strong donor ability of [C_4mpyr]-[TfO], estimated as $DN \sim 20$ kcal mol^{-1}, was the cause of the higher solubility than the other ILs with fluorinated sulfonylamide anions ($DN \sim 10$ kcal mol^{-1} or even less). The difference in the solubility of Li_2S_m in the other ILs was small. These results indicate that IL-based electrolytes do not necessarily suppress the dissolution of Li_2S_m into the electro-

DOI: 10.1021/acs.chemrev.6b00504
Chem. Rev. 2017, 117, 7190−7239

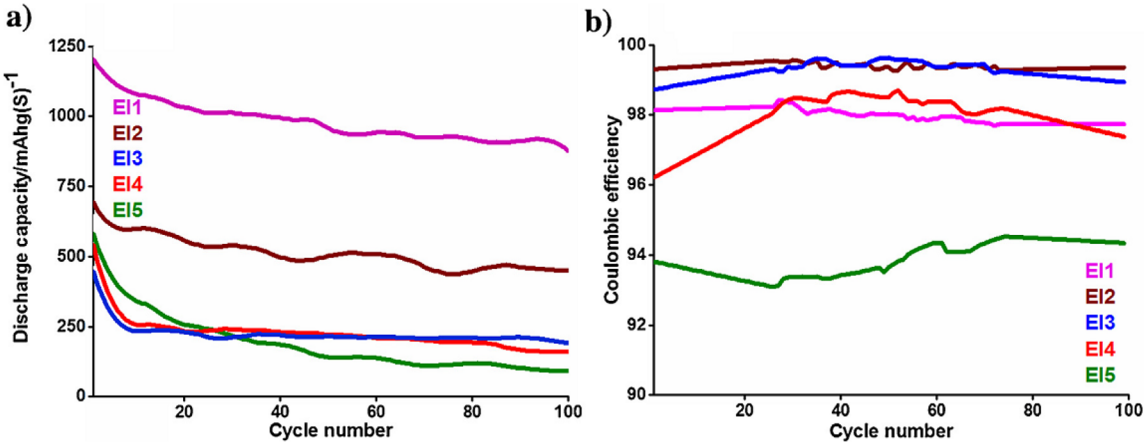

Figure 20. (a) Discharge capacity of batteries assembled with different electrolytes. Ell, DME/DOL (1:1, v/v) containing 1 mol kg^{-1} Li[TFSA] and 0.1 mol kg^{-1} $LiNO_3$. El2-El5: pyrrolidinium IL/G4 mixture electrolytes (1:1, v/v) containing 1 mol kg^{-1} Li[TFSA] and 0.1 mol kg^{-1} $LiNO_3$; El2, [C_4mpyr][TFSA]; El3, [C_4mpyr][FAP]; El4, [C_4mpyr][OTf]; El5, [C_4mpyr][$C(CN)_3$] and (b) their Coulombic efficiency. Reprinted with permission from ref 226. Copyright 2015 Elsevier.

lyte, and ILs with weakly coordinating fluorinated sulfonylamide anions result in low solubility of Li_2S_m. Moreover, Park in the Watanabe group further investigated the effect of counteranions of Li salts on the solubility of Li_2S_m in [DEME][TFSA] containing 0.5 mol kg^{-1} Li salt: the solubility was higher in the order [TFSA] > [BETA] > PF_6, which is consistent with the donor ability of the anions in the reported literature. In terms of higher conductivity and low solubility of Li_2S_m, 0.5 mol kg^{-1} Li[TFSA] in [C_3mpyr][TFSA] showed the best battery performance with stable cycle ability under the same charge−discharge conditions in Park's study: an initial capacity of ca. 800 mAh g^{-1} and Coulombic efficiency of ∼98%.[207]

Anionic dependency of the solubility of Li_2S_m in Li salt-glyme 1:1 molar molten complexes (solvate ILs: [Li(G3)]X or [Li(G4)]X, see also section 2.3.1) was also studied.[208] Similar to aprotic ILs, [Li(G3)][TfO] and [Li(G3)]NO_3, having strongly Lewis basic anions, dissolved a large amount of Li_2S_m, similar to that in an organic electrolyte (0.98 mol dm^{-3} Li[TFSA] in G4). In these molten complexes, the solvate cation [Li(G3)]$^+$ was unstable with regard to ligand exchange, and there are uncoordinated glyme solvents to some extent as indicated by Raman spectroscopic analysis and diffusivity measurements of the glyme and Li^+; thus these molten complexes were deemed as poor solvate ILs or concentrated solutions.[132] They suggested that the high solubility of Li_2S_m was primarily due to the presence of uncoordinated glymes that enable the solvation of Li_2S_m. The strongly Lewis basic NO_3^- and $[TfO]^-$ can also contribute to the solvation of Li_2S_m in a similar way as for aprotic ILs, leading to the high solubility of Li_2S_m. In contrast, uncoordinated glymes were found to hardly exist in the molten complexes [Li(G3)][TFSA], [Li(G4)][TFSA], and [Li(G4)][BETI], which thus are considered good solvate ILs. In addition to the weakly coordinating properties of $[TFSA]^-$ and $[BETA]^-$, lack of free glyme solvents that are capable of solvating Li_2S_m likely account for the lower solubility of Li_2S_m in these good solvate ILs. Among the solvate IL electrolytes, the Li−S cell with [Li(G4)][TFSA] delivered the best initial discharge capacity of ca. 1100 mAh g^{-1} with high Coulombic efficiency (>97%).[225]

With consideration of the Li salt concentration in the Li salt-glyme 1:1 molten complexes, [Li(G3)][TfO] (3.90 mol dm^{-3}) and [Li(G3)]NO_3 (4.77 mol dm^{-3}) had higher salt concentration than [Li(G3)][TFSA] (3.06 mol dm^{-3}), [Li(G4)][TFSA] (2.75 mol dm^{-3}) and [Li(G4)][BETI] (2.39 mol dm^{-3}).[208] This implies that Li salt concentration is not always a determining factor for the solubility of Li_2S_m. Instead, activity of Li^+ (based strictly on common ion effects) and uncoordinated solvent dominate the solubility of Li_2S_m. High activity of Li^+ and low activity of uncoordinated solvents can be realized with highly dissociable and weakly coordinating anions such as $[TFSA]^-$. Therefore, this can be another incentive for selecting [TFSA]-based ILs or concentrated electrolyte with LiTFSA as the Li_2S_m sparingly soluble electrolyte for Li−S batteries.

Hollenkamp et al. investigated the effect of anions in pyrrolidinium IL/G4 mixture electrolytes on Li−S battery performance (Figure 20).[226] They compared the solubility of Li_2S_m and the resulting capacity and efficiency of Li−S cells assembled with electrolytes containing [C_4mpyr][FAP], [C_4mpyr][TfO], [C_4mpyr][$C(CN)_3$], and [C_4mpyr][TFSA]. They observed higher solubility of Li_2S_m in the electrolytes containing Lewis basic $[TfO]^-$ and $[C(CN)_3]^-$ than in the electrolytes containing weakly coordinating $[TFSA]^-$ and $[FAP]^-$. These results validated the Watanabe group's work that solubility of Li_2S_m is strongly correlated with the donor ability of anions and not all ILs decrease the solubility of Li_2S_m. As shown in Figure 20, the low solubility of Li_2S_m resulted in high Coulombic efficiency of Li−S cells with electrolytes containing [C_4mpyr][FAP] and [C_4mpyr][TFSA] due to suppression of parasitic redox shuttle reactions, whereas the higher solubility of Li_2S_m caused rapid capacity decay and low efficiency for Li−S cells with electrolytes containing [C_4mpyr][TfO] and [C_4mpyr][$C(CN)_3$]. The low capacity and capacity fading in Li−S cells with electrolytes containing [C_4mpyr][FAP] was attributed to low conductivity, probably arising from the high viscosity of [C_4mpyr][FAP]. [C_4mpyr][TFSA] with higher ionic conductivity and lower solubility of Li_2S_m showed the best performance for Li−S batteries in this study.

In addition to studies on the anionic dependency of Li_2S_m solubility, cationic dependency of the Li_2S_m solubility in [TFSA]-based ILs has also been determined for six different cations, including pyrrolidinium, ammonium, piperidinium, imidazolium, and phosphonium types (Figure 19).[207] The

DOI: 10.1021/acs.chemrev.6b00504
Chem. Rev. 2017, 117, 7190−7239

difference in Li_2S_m solubility was much smaller than was observed when varying the anions. The ILs with larger cations are prone to exhibit lower solubility for Li_2S_8: [C_3mpyr] > [C_4mpyr] > [DEME] > [C_3mpip] > [C_4dmim] > [P2225]. The solubility of Li_2S_m in Li salt glyme solvate ILs containing $[TFSA]^-$ was comparable to that for aprotic ILs in the absence of supporting Li salt, which were less than 100 mmol dm^{-3} (atomic S basis).

Nonionic S_8 is generally less soluble than higher-order Li_2S_m in electrolytes. The saturation concentration of S_8 was comparable among various pyrrolidinium ILs and less than 32 mmol dm^{-3} (atomic S basis).[207] On the other hand, Hardacre et al. reported a significantly higher solubility of S_8 in [C_4mim][DCA] than in [C_4mim][TFSA] and [C_4mim]-[TfO].[227] Earle et al. observed color changes from transparent to blue or carmine red in ILs having carboxylates and phosphates depending on the concentration of S_8.[228] This indicated the occurrence of a ring-opening reaction of S_8 with the anions to yield polysulfide anions and anion radicals. Although the basicity of $[TfO]^-$ appears to be insufficient to react with S_8, ILs having highly basic anions such as carboxylates and phosphates can dissolve S_8 in the form of polysulfides. As a result, the solubility of S_8 and high-order polysulfides was predominantly dictated by the donor ability of the ILs.

3.5. Ionic Liquids-Organic Solvent Mixtures

IL-based electrolytes, despite mitigating the serious dissolution of Li_2S_m, suffer from low ionic conductivity and slower mass transport. For this reason, high capacity in charge−discharge of Li−S cells can only be achieved at a slow rate with limited current density; high-rate charge−discharge results in a large polarization of the cell and low capacity. Mixing the IL with a low viscosity molecular solvent is a reasonable approach to improve the conductivity and mass transport of IL-based electrolytes. In addition, ILs appear to play several important roles in Li−S batteries with IL-molecular solvent mixture electrolytes.

When ILs are present as only a minor part of the electrolyte, the ILs are expected to serve as a supporting salt for enhancing the ionic conductivity of an organic electrolyte. A greater discharge capacity and more stable cycle performance over 100 cycles is reported in the presence of 5−10 vol % of imidazolium-based ILs in DOL/DME electrolyte due to improved conductivity.[212] Zhang claimed that organic cations of ILs in the mixed electrolytes can stabilize the polysulfide in the electrolyte according to the hard and soft acids and bases (HSAB) theory. High-order S_m^{2-} can be more stabilized in the electrolyte solution when combined with soft counter cations.[229] This stabilization of S_m^{2-} in the electrolyte solutions is likely important for a Li−S cell with the Li_2S_m highly soluble electrolytes (Figure 17 left) because it can mitigate the disproportionation to form lower-order precipitates, namely Li_2S_2 and Li_2S. Cairns et al. employed a cetyltrimethylammonium bromide (CTAB)-modified sulfur-graphene oxide nanocomposite as the cathode and the mixture of [C_4mpyr][TFSA] and DME/DOL (2:1:1 in volume) containing 0.5 mol dm^{-3} $LiNO_3$ and 1 mol dm^{-3} Li[TFSA] as the electrolyte.[230] CTAB layer stabilized the sulfur active species within the cathode, whereas [C_4mpyr][TFSA] in the electrolyte inhibited the dissolution of Li_2S_m into the electrolyte. The Li−S cell achieved significantly improved rate capability (at 6C and 3C for discharge and charge, respectively) and a long cycle life exceeding 1500 cycles.

Addition of a large amount of ether-based molecular solvents into [TFSA]-based ILs can improve the conductivity and Li^+ transport property but simultaneously increases the solubility of Li_2S_m. Cairns et al. studied the effect of PEGDME content in a mixture of [C_4mpyr][TFSA] and PEGDME containing 0.5 mol dm^{-3} Li[TFSA] on the Li−S battery performance.[231] Higher capacity and more stable charge−discharge cycles were demonstrated in the mixed electrolyte containing a 2:1 volume excess of PEGDME. Xiao et al. also explored the effect of IL in the mixed electrolyte of [C_4mpyr][TFSA] and DME/DOL on the Li−S battery performance (Figure 21). A stable SEI film

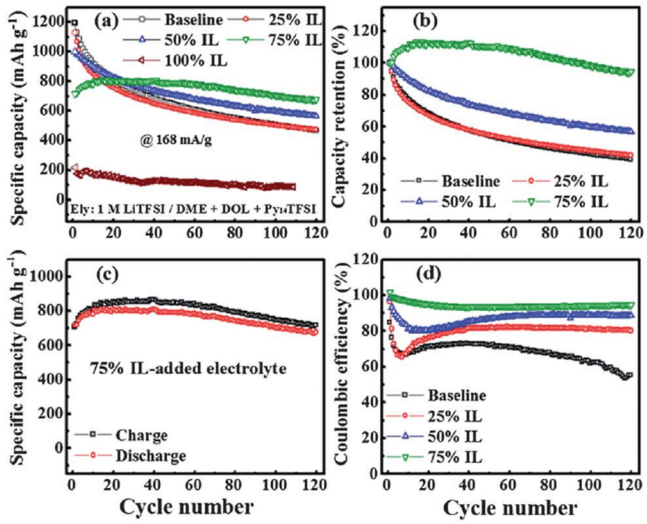

Figure 21. Cycling performance of Li−S cells with electrolyte of 1 mol dm^{-3} Li[TFSA] in DME/DOL + [C_4mpyr][TFSA] at 0.1 C. Reprinted with permission from ref 232. Copyright 2013 Royal Society of Chemistry.

was formed on the lithium anode in the electrolyte containing 75% IL, and it effectively mitigates the shuttle mechanism, leading to stable cycling and high Coulombic efficiency.[232] Byon et al. showed a trade-off between solubility and diffusion rate of Li_2S_m in the mixtures of low-viscous DME and [PP13][TFSA] in their recent work.[233] An optimized composition ratio of DME/[PP13][TFSA] (1/2 volume ratio) allowed large capacity (~1000 mAh g^{-1} at 0.2 C on the first cycle) and good capacity retention (~90% capacity retention after 50 cycles). In a recent development by Xia et al., the electrolyte composed of a ternary mixture, [PP13][TFSA]/DME/DOL (2/1/1, v/v), containing 1 mol dm^{-3} Li[TFSA] and 0.2 mol dm^{-3} $LiNO_3$ achieved high capacity of 1200 mAh g^{-1} and zero self-discharge upon resting a full-charged cell for 2 days.[199] This promising Li−S battery with low self-discharge rates relies on both improvements in control of polysulfide diffusion by addition of the IL and stabilization of lithium metal anode by $LiNO_3$ and the IL additives.

Mixing an IL and molecular solvents was also useful for enhancing conductivity of the Li_2S_m sparingly soluble electrolyte for Li−S batteries (Figure 17 right). To this end, the additional molecular solvent should exhibit low solubility of Li_2S_m and S_8 and stability with respect to the lithium metal anode. The solvate IL [Li(G4)][TFSA] blended with a low-polarity, nonflammable hydrofluoroether, 1,1,2,2−tetrafluoroethyl 2,2,3,3−tetrafluoropropyl ether (HFE) has been

DOI: 10.1021/acs.chemrev.6b00504
Chem. Rev. 2017, 117, 7190−7239

proposed as the electrolyte for the Li–S battery.[234] The [Li(G4)][TFSA]/HFE (1/4 in molar ratio) electrolyte showed an improved conductivity of ~5 mS cm^{-1} and enhanced Li^+ transport property as well as further suppressing the Li_2S_m dissolution. The solvate cation $[Li(G4)]^+$ was found to be stable even in the mixed electrolyte, as confirmed by diffusion measurement of the glyme and Li^+, and thus uncoordinated G4 molecules, required for dissolving Li_2S_m, did not exist. The solubility of S_8 and Li_2S_m was even lower in the [Li(G4)]-[TFSA]/HFE electrolyte than in neat [Li(G4)][TFSA] because Li_2S_m are insoluble in the low polarity HFE (Figure 22). The addition of HFE provided a good cycle stability,

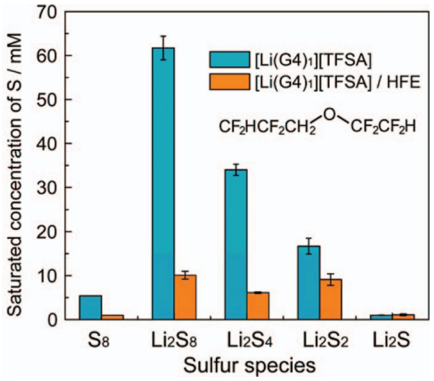

Figure 22. Comparison of S_8 and Li_2S_m solubility limits in [Li(G4)][TFSA] and [Li(G4)][TFSA]/HFE (molar ratio of [Li-(G4)][TFSA]/HFE = 1/4) at 30 °C. The structure of HFE is shown in the inset. Reprinted with permission from ref 234. Copyright 2013 The Electrochemical Society.

higher Coulombic efficiency, and smaller overpotential upon charge–discharge (i.e., greater energy efficiency). As shown in Figure 23, the poor rate capability of a Li–S cell with [Li(G4)][TFSA] was greatly improved by mixing HFE with [Li(G4)][TFSA].

3.6. Outlook for Li–S Battery Electrolytes

Although limited numbers of ILs have been tested as electrolyte components for Li–S cells, the above studies reveal that ILs play multiple roles in improving the IL-S cell performance using either the Li_2S_m highly soluble or the Li_2S_m sparingly soluble electrolytes. Dissolution of Li_2S_m can be inhibited by the addition of ILs having weakly coordinating anions such as $[TFSA]^-$. Recent studies well-controlled the solubility of Li_2S_m by adding the optimized amount of ILs to organic electrolyte for improving the battery performance. The organic cations of ILs could stabilize the solubilized S_m^{2-} in the Li_2S_m highly soluble electrolyte, which appears to mitigate the formation of electrochemically inaccessible, low-order Li_2S_m precipitates in the Li–S cells. Moreover, some ILs or ions were found to form an effective SEI film on the lithium metal anode, which also prevented the parasitic redox shuttling. The Li salt-glyme solvate ILs were highly soluble even in low-polar molecular solvents such as HFE, and they behave as a supporting salt in the Li_2S_m sparingly soluble electrolytes. The solvate IL/HFE mixture realized a very low solubility of S_8 and Li_2S_m less than 10 mmol dm^{-3} (atomic S basis) and greatly improved Li–S battery performances.

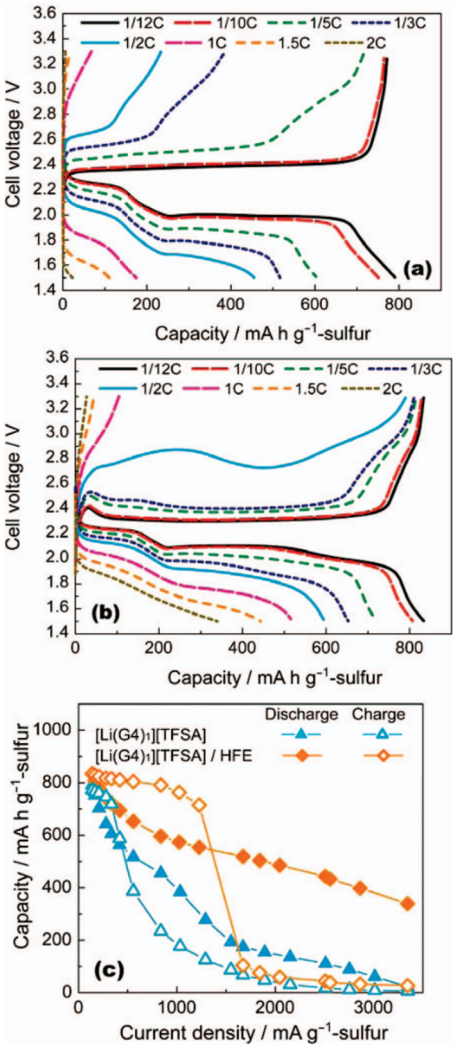

Figure 23. Discharge and charge curves of Li–S cells measured at various current densities with the (a) $[Li(G4)_1][TFSA]$ and (b) Li[TFSA]/G4/HFE = 1:1:4 electrolytes at 30 °C. The cells were charged up to 3.3 V at a rate of 1/12C prior to each discharge test. The cells were discharged down to 1.5 V at a low current density with a rate of 1/12C prior to each charge test. (c) Comparison of discharge and charge rate capabilities for Li–S cells with $[Li(G4)_1][TFSA]$ and Li[TFSA]/G4/HFE = 1:1:4 electrolytes. Reprinted with permission from ref 234. Copyright 2013 The Electrochemical Society.

4. LITHIUM–OXYGEN (LI–O_2) BATTERY ELECTROLYTES

4.1. Non-Aqueous Lithium-O_2 Battery

The nonaqueous lithium air battery has been widely proposed as a very promising technology for energy storage, due in part to a high theoretical gravimetric energy density.[235−238] As a result, a large number of research programs have been launched to investigate the fundamental electrochemistry and to attempt development of a functioning battery system. Figure 24 shows a sketch of the main battery components. The air cathode, typically a conductive porous carbon, allows the oxygen to enter the cell (very similar to a fuel cell electrode) and contact the electrolyte. The electrolyte allows the transport of lithium ions across the cell, with a lithium anode providing a lightweight negative electrode.

DOI: 10.1021/acs.chemrev.6b00504
Chem. Rev. 2017, 117, 7190−7239

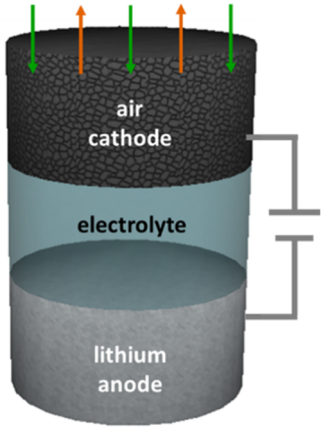

Figure 24. Lithium−air battery schematic.

The lithium−air battery is based on the reversible electrochemical conversion reactions of lithium and oxygen. The first step, the formation of the superoxide (eq 1) has been widely studied in aprotic media.[239−248] The stability (lifetime) of the superoxide is solvent-dependent, and the presence of trace protons tends to induce disproportionation to the peroxide (eqs 2 and 3).[244] In the strict absence of available protons, and presence of lithium, the reaction pathway (eq 4−7) is directed toward the production of lithium peroxide (Li_2O_2), which is now widely accepted to be the main product of the discharge reaction, with very few reports suggesting further reduction (and breaking of the O−O bond) to generate lithium

$$O_2 + e^- \rightarrow O_2^{\cdot -} \quad (1)$$

$$H^+ + O_2^{\cdot -} \rightarrow HO_2^{\cdot} \quad (2)$$

$$2HO_2^{\cdot} \rightarrow H_2O_2 + O_2 \quad (3)$$

$$Li^+ + O_2^{\cdot -} \rightarrow LiO_2^{\cdot} \quad (4)$$

$$Li^+ + O_2 + e^- \rightarrow LiO_2^{\cdot} \quad (5)$$

$$2LiO_2^{\cdot} \rightarrow Li_2O_2 + O_2 \quad (6)$$

$$Li^+ + LiO_2^{\cdot} + e^- \rightarrow Li_2O_2 \quad (7)$$

oxide (Li_2O). One limitation is the poor energy efficiency (i.e., large overpotential) on cycling. Although this may be inherent for conversion batteries,[249] for the lithium−air system it is often attributed to the poor conductivity of the main discharge product, Li_2O_2.[250] A variety of strategies have been considered to overcome this problem, including the use of catalysts/promoters,[251−253] solubilizing the discharge product,[254] and the use of redox mediators.[255−258]

Another major topic has been the search for a stable electrolyte solvent.[259,260] Early interest was devoted toward using conventional lithium-ion battery electrolyte solvents such as propylene carbonate; however, careful study revealed the deleterious irreversible reaction of the superoxide with this solvent.[248,261,262] Subsequently, further research has focused on more stable solvents including polyethers (such as tetraglyme and PEO) and DMSO, which show improved stability compared to the alkyl carbonates but may be unstable upon long-term cycling.[263−266]

4.2. Merits and Limitations of ILs for Li−O_2 Batteries

ILs offer several potential advantages as electrolytes for the lithium−air battery electrolyte. Aside from the ease with which the physicochemical properties may be tuned with astute choice of anion or cation structure, many conventional ILs offer a wide electrochemical window and low volatility (see section 2.2), and thus may more easily accommodate the large overpotential upon charging often observed for these batteries without degradation.

The design of a practical lithium−air battery may take one of two major directions, as was outlined by Gallagher et al.,[267] and shown in Figure 25: (i) an open system, where the cathode

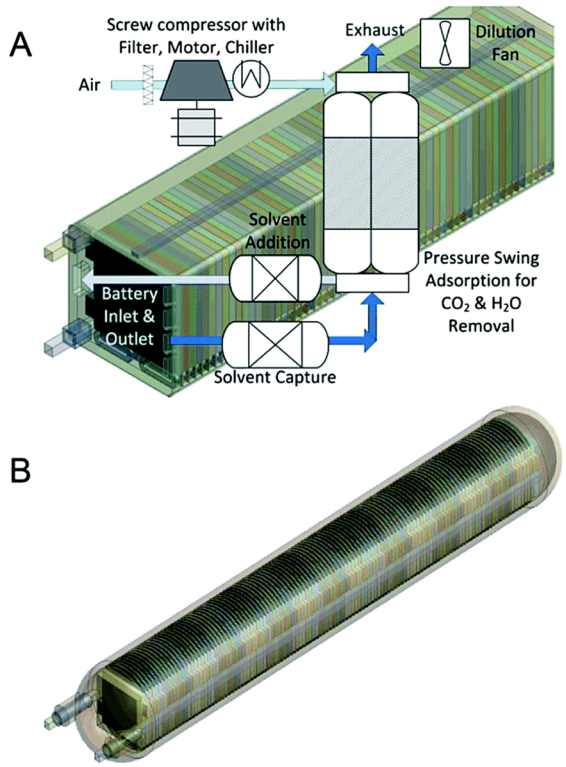

Figure 25. (A) Required components for open-architecture Li/O_2 battery. (B) Closed architecture design for Li/O_2 battery where the cell-stack is enclosed within a pressure vessel. Reprinted with permission from ref 267. Copyright 2014 Royal Society of Chemistry.

and/or electrolyte are exposed to atmosphere, with a possible requirement for separation of oxygen from the other air components and (ii) a closed system, where the oxygen is supplied from a sealed tank akin to recently commercialized fuel cell vehicle technologies such as the Toyota MIRAI.[268] As described in section 2: Li/Na ion battery electrolytes, the use of an IL as electrolyte offers advantages in terms of safety when applied to electrochemical storage devices, where the volatile electrolyte solvents may be replaced with the low volatility IL. In addition, for the open system, the low volatility of the electrolyte would also offer a possibility to exclude the "solvent capture" and separation system (required to recover evaporating solvent), with consequent energy savings.

4.3. O_2 Reduction and Diffusion

For a comprehensive overview of the generation of superoxide in ILs, the interested reader is directed to the recent review by AlNashef et al.[269] This section will give a brief summary of the

DOI: 10.1021/acs.chemrev.6b00504
Chem. Rev. 2017, 117, 7190−7239

reduction of oxygen in particular with a focus on features relevant to the lithium−air battery system.

Compton et al. reported on the reduction of oxygen from mixtures of oxygen and nitrogen and a larger diffusion coefficient (determined from chronoamperometry on a gold microelectrode) for oxygen than the superoxide radical anion.[270] That difference was more marked for the more viscous of the two ILs studied ([N_{6222}][TFSA] > [C_2mim][TFSA]). The authors also commented on the asymmetry of the peaks observed in the cyclic voltammograms, which they attributed to a difference in the diffusion of the two species, dioxygen being almost spherical, and the superoxide radical anion being virtually planar. Their work was later extended to pyrrolidinium- and piperidinium- based ILs.[271] Voltammograms for [N_{6222}][TFSA] are shown Figure 26. Oxygen (and

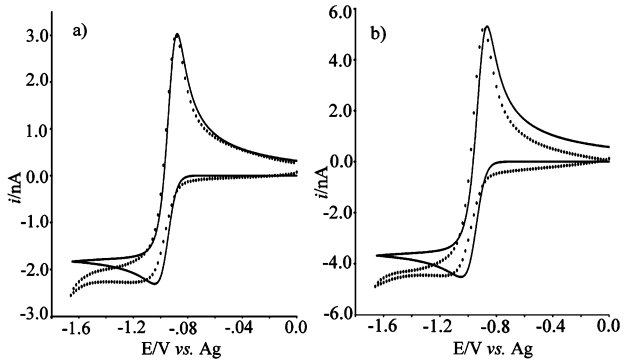

Figure 26. Comparison of experimental and simulated voltammograms (1 V s^{-1} scan rate) for the reduction of oxygen in [N_{6222}][TFSA] in (a) 50% O_2:50% N_2 and (b) 90% O_2:10% N_2 gas mixtures. The closed circles represent experimental data and the solid line represents simulated data. Reprinted with permission from ref 270. Copyright 2003 American Chemical Society.

superoxide) solubility and diffusion are key for good rate capability and present a limitation for ILs, for which the solubility and diffusion of oxygen tend to be lower than for conventional aprotic electrolyte solvents.

Mastragostino et al. reported on the cyclic voltammetry of oxygen in pyrrolidinium-based ILs in the presence of lithium salt and noted that in the presence of lithium cations the ORR is irreversible.[272] The authors ascribed the irreversibility to the high Lewis acidity of Li^+, which could not be attenuated even with addition of strongly coordinating ligands. Subsequent to this report, a large number of groups have focused on pyrrolidinium- and piperidinium-based ILs.

Abraham et al. reported a similar effect for an imidazolium-based IL ([C_2mim][TFSA])[273] and later with a pyrrolidinium-based IL ([C_4mpyr][TFSA]).[274] The corresponding CV curves are shown in Figure 27 (left), with the corresponding assignments in Figure 27 (right). Interestingly, the authors suggest that there are two distinct oxygen reduction peaks observed during the cathodic sweep, one relating to the reduction of oxygen in the presence of lithium ion to form the lithium superoxide (C1) and the second relating to the direct reduction of oxygen and subsequent formation of an ion pair with the pyrrolidinium cation (C2). In using incrementally higher potential limits for the cathodic sweep (inset of Figure 3a, (left), the authors inferred the identity of peaks in the anodic sweep.

The formation of an ion pair between the IL cation and superoxide radical anion, $R^+O_2^{\bullet-}$, is believed to be critical in ensuring the stability of the oxygen reduction product, which otherwise would tend to react rapidly with acidic protons (according to eqs 2 and 3), or via nucleophilic attack,[275−277] and decompose. Thus, ILs may play a role in prevention of decomposition reactions (with organic electrolytes and carbon-based electrodes) that hinder the development of these batteries. However, due to formation of an ion pair with the

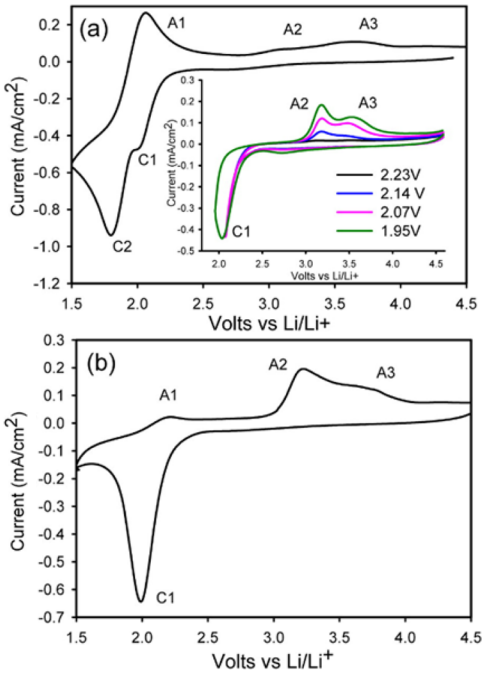

ORR

1. $Li^+ + O_2 + e^- \rightarrow LiO_2$ C1
2. $2LiO_2 \rightarrow Li_2O_2 + O_2$ (chemical)
3. $PYR^+ + O_2 + e^- \rightarrow PYR^+\text{--}O_2^-$ C2

OER

4. $PYR^+\text{--}O_2^- \rightarrow PYR^+ + O_2 + e^-$ A1
5. $LiO_2 \rightarrow Li^+ + O_2 + e^-$ A2
6. $Li_2O_2 \rightarrow 2Li^+ + O_2 + 2e^-$ A3

Figure 27. (Left) Cyclic voltammograms (CVs) at 100 mV/s on Au electrode. (a) 0.025 M Li[TFSA] in [C_4mpyr][TFSA]. Inset: CVs at various cathodic limits of 1.95 V and higher. (b) 0.025 M Li[TFSA] in [C_2mim][TFSA]. (Right) Proposed assignment of peaks. Reprinted from ref 274. Copyright 2012 American Chemical Society.

DOI: 10.1021/acs.chemrev.6b00504
Chem. Rev. 2017, 117, 7190−7239

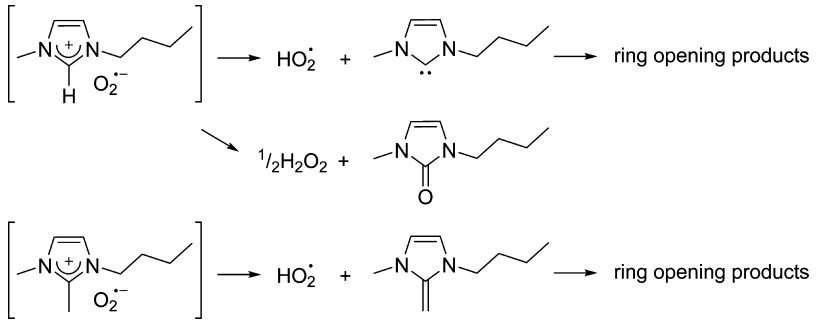

Figure 28. Proposed reactions for imidazolium cation and superoxide ion pairs, after Ohsaka et al.[279] and AlNashef et al.[282]

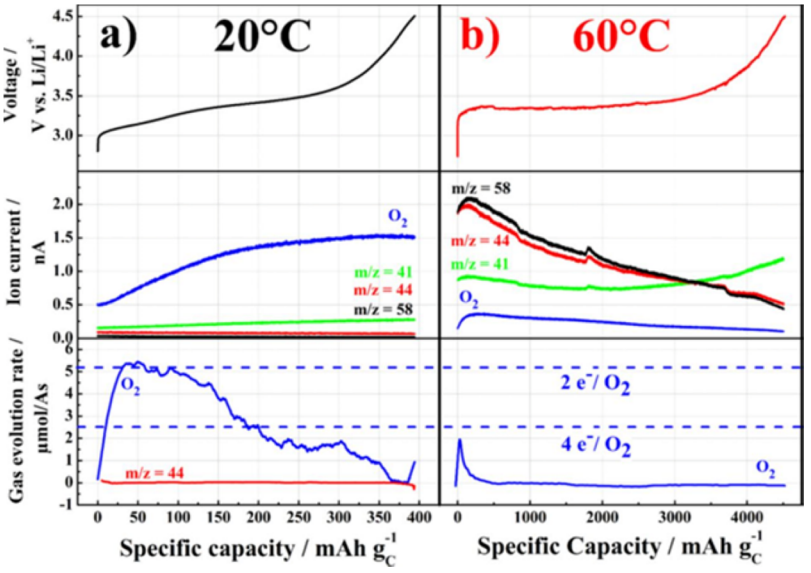

Figure 29. Online electrochemical mass spectrometry analysis of the first charge (120 mA g^{-1}C or 78.3 μA) of Li-Vulcan cells under argon atmosphere following the prior discharge under O_2 in [C_4mpyr][TFSA] with 10 wt % Li[TFSA] at (a) 20 °C and (b) 60 °C. (Top) Charge profile. (Middle) Ion currents of selected masses from the mass spectrometer (m/z = 32, O_2; m/z = 41, propenyl; m/z = 44, CO_2 and/or amines; m/z = 58, amines) which shows the accumulation of reaction products inside the cell. (Bottom) Gas evolution rate of oxygen. Reprinted with permission from ref 294. Copyright 2014 The Electrochemical Society.

cation, it is clear that the stability of the cation itself becomes critical.

4.4. Selection of Stable Ionic Liquids and Cycling Performances

The possible instability of an imidazolium-based IL ([C_2mim][TFSA]) was suggested by Katayama et al., where expansion of the cyclic voltammogram potential scan range revealed irreversibility,[278] and subsequently by others.[279−281] The proposed reaction sequence is shown in Figure 28, the imidazolium cation forms an ion pair with the superoxide radical anion, and subsequent H-abstraction leads to the carbene or methylene-imidazole, respectively. Further work by AlNashef et al. demonstrated the formation of an imidazolone product (perhaps via the carbine as an intermediate) from bulk electrolysis.[282] These reactions have obvious analogies for imidazolium-based ILs with strongly basic anions, for which carbene formation (proton abstraction from the C2-position by the strongly basic counteranion such as acetate) and subsequent reactions with S_8, Se, and CO_2 have been reported.[283,284] Despite these reports, various imidazolium ILs have been studied for the lithium−air battery.[273,274,285−287]

Further study on pyrrolidinium- and piperidinium-based ILs was conducted by Iba et al.[288−291] These ILs showed improved stability, and the authors observed the most promising performance with [DEME][TFSA]. [C_4mpyr][TFSA] has also been studied further as reported by Passerini and Scrosati et al.,[292] who demonstrated improved cycling capabilities (although at limited capacities). The stability of this IL was also probed by in situ Raman spectroscopy,[281] and its use as a component of a gel polymer electrolyte has also been demonstrated.[293] However, Gasteiger and co-workers have suggested instability upon prolonged cycling, reaction between superoxide and cation, and reduction of the pyrrolidinium cation on the lithium anode (see Figure 29).[294−296]

Subsequently, Vegge et al. presented a similar study, comparing several pyrrolidinium- and piperidinium-based ILs. Interestingly, in their study, the [C_4mpyr][TFSA] showed relatively high stability and performance but deterioration upon cycling.[297] Phosphonium-based ILs have also been considered, with some evidence for proton abstraction from the cation.[298−301] Further study is needed to clarify the stabilities and capabilities of these and other potentially stable ILs for long-term electrochemical energy storage in the lithium−air cell.

DOI: 10.1021/acs.chemrev.6b00504
Chem. Rev. 2017, 117, 7190−7239

4.5. Presence of Water

While recent publications have brought to light other, potentially more positive roles for water in these cells under certain limited conditions,[295,302−304] the presence of water can be broadly assumed to be detrimental to the overall cell performance, due to reaction of water with the lithium anode and discharge products (Li_2O_2) at the cathode.[305−307] In earlier work, Kuboki et al. studied the application of hydrophobic ILs for a lithium-air cell, wherein the hydrophobic ILs provided a means to limit water ingress into the cell and thus partially protect the lithium anode and cathode.[287] In another study, [C_2mim][TFSA] was employed as a component of the cathode to prevent water ingress.[286] However, as the ILs employed in these studies were all imidazolium-based, the stability in the presence of reduced oxygen species is unclear (see section 4.3).

More recently, Forsyth et al. investigated the stability of the superoxide radical anion in [P_{66614}]Cl in the presence of water, see Figure 30.[308] The authors suggest that the presence of a strong ion pairing between the superoxide radical anion and [P_{66614}]$^+$ cation may act to prevent the chemical disproportionation of the superoxide which would otherwise be promoted in the presence of water (eqs 2 and 3). In a recent report, this cation was applied in a systematic study varying the ionic liquid components, aimed at reducing the inherent water content of the ionic liquid.[309]

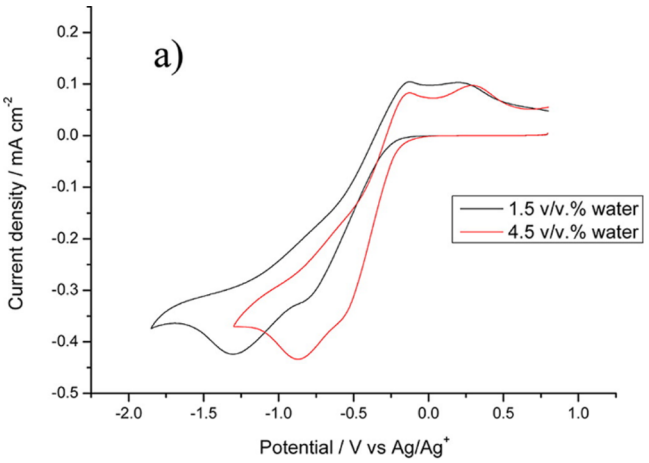

Figure 30. Cyclic voltammograms for ORR in ionic liquid [P_{66614}]Cl with water content of 1.5 and 4.5% v/v using GC as the working electrode. Reprinted from ref 308. Copyright 2013 American Chemical Society.

4.6. Advanced Systems

Several groups have reported on blending ILs with conventional organic electrolyte solvents.[310−312] These systems tend to show improved diffusion coefficients for oxygen and likely higher lithium-ion conductivities, and thus may offer a compromise between attractive features of both systems. However, the long-term stability still remains questionable.

We recently reported on the application of solvate ILs (see section 2.3.1.) for the lithium−air battery,[309,313] where we commented on the importance of discharge depth in determining the effectiveness of a particular solvent system.[313] By using such solvate ILs, despite the presence of the glyme molecule, the solubility of superoxide may be limited, ensuring full reduction occurs in direct contact with the electrode, preventing material losses. Nazar et al. also reported a related "chelate IL".[314]

Further work has been undertaken to develop flow-type cells, as shown in Figure 31.[315−317] Such designs offer the possibility to improve the oxygen transport in the system, thus overcoming one of the main obstacles for ILs to be used in the lithium−air battery.

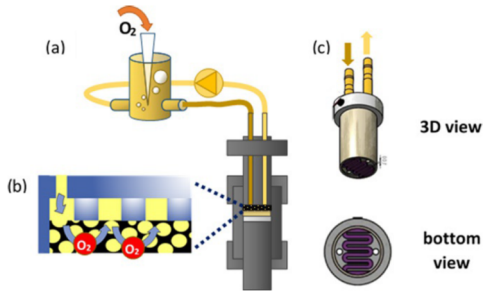

Figure 31. Schematic of flow cell apparatus. (a) Representation of the oxygen bubbling device, the peristaltic pump and the prototype cell, connected with silicone tubes; (b) magnification of the cathode area, showing the O_2-saturated electrolyte pathway across the porous carbon and the flow field plate; (c) 3D and bottom view of the cathode rod. Reprinted with permission from ref 317. Copyright 2016 Wiley.

Recently, Addison et al. reported the use of molten salts at higher temperatures ($LiNO_3$−KNO_3, $LiNO_3$−KNO_2−$CsNO_3$).[318] The absence of any organic components in the electrolyte invokes an enhanced stability for the electrolyte. Limitations remain; however, the carbon electrode is still present and shows some instability, generating Li_2CO_3. This, and the rather high temperatures, should be addressed to fulfill the promise of this interesting strategy. Alternatively, high temperatures may offer promise for more conventional ILs, where the rate capability might be substantially enhanced.[319]

4.7. Outlook for Li−O_2 Battery Electrolytes

Although efforts have been made to study the anode for the lithium−air battery using conventional organic electrolytes such as glymes and DMSO,[320−323] this has not been undertaken to a great extent in ILs. Further study on stability of ILs in this system should therefore focus not only on reactions with the superoxide but also take into account potential side-reactions at the Li metal surface.

The use of redox mediators has been well-reported for conventional aprotic electrolytes in this system,[255−258] but comprehensive studies have not been reported for ILs, and little modeling has been performed for IL electrolytes, compared to organic solvents.[324] These and other fundamental parameters must be studied to fully characterize the potential of ILs in this system.

5. FUEL CELL ELECTROLYTES

5.1. Conventional Fuel Cell Electrolytes

Fuel cells are energy conversion systems, which directly transform the Gibbs energy change of chemical reaction into electric energy. They have attracted much attention as next generation energy devices, since they emit only water and achieve high energy conversion efficiency. Recently, polymer electrolyte fuel cells (PEFC) for fuel cell vehicles and domestic cogeneration systems were commercialized. In a fuel cell system, the hydrogen oxidation reaction (HOR) occurs at the

DOI: 10.1021/acs.chemrev.6b00504
Chem. Rev. 2017, 117, 7190−7239

anode, while the oxygen reduction reaction (ORR) simultaneously occurs at the cathode; the difference in Gibbs energy between both electrode reactions is output as electric energy. In order to achieve high energy conversion efficiency, over potentials for both reactions should be lowered. This is currently achieved by using a Pt electrode catalyst at both electrodes. For the proton conducting membranes used to separate the electrodes, high thermal and chemical stability, high mechanical strength, and a gas barrier property in addition to high H^+-conductivity are required. At present, perfluorinated sulfonic acid membranes, typically Nafion (DuPont), are widely employed in spite of their high cost.[325] Although much effort has been devoted to developing hydrocarbon polymer membranes to replace Nafion,[326−329] Nafion still has superiority in its properties and durability.

Nonhumidifying operation of a PEFC at intermediate temperatures has been of great interest for many researchers, since it offers many benefits such as elimination of a water management system, efficient utilization of waste heat, efficient cooling by a smaller radiator, enhanced catalytic activity of Pt, reduced poisoning of Pt by CO, and so forth. In order to design such a system, new proton conducting electrolytes as alternatives to hydrated acid systems such as Nafion must be developed. One possible candidate is phosphoric acid (H_3PO_4) doped polybenzimidazole (PBI). Savinell et al. reported fuel cell operation at 160 °C without humidification using a H_3PO_4/PBI composite membrane.[330] However, H_3PO_4/PBI composite membranes cannot be used at lower temperature due to high over potential. Protic ionic liquids (PILs) have been focused on as another candidate, since they exhibit excellent thermal stability and proton conductivity without additional solvents.[331−350]

5.2. Properties of Protic Ionic Liquids

PILs are defined as ILs having active protons (exchangeable and reactive) in their chemical structures. Typical PILs are synthesized by a neutralization reaction (proton transfer reaction) between a Brønsted acid and Brønsted base (Scheme 1). ILs having anions with active protons such as HSO_4^- and $H_2PO_4^-$ can also be categorized as PILs. If ions in PILs having an active proton are highly mobile and readily involved in electrode reactions, the PILs can be candidates for proton conductors in fuel cells. Although many cations and anions can be used to form PILs, selection of chemical structure is actually limited due to strict requirements for the proton conductor in fuel cells. Significant properties for the electrolyte in a fuel cell system are thermal stability, proton conductivity, and electrochemical activity.

Scheme 1. Acid−Base Equilibrium in PILs[a]

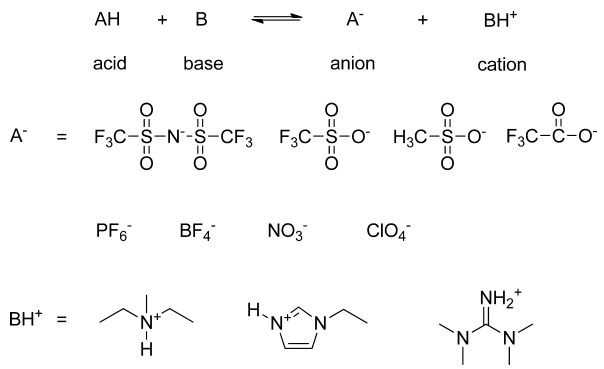

[a] A^- and BH^+ are representative anions and cations comprising PILs, respectively.

5.2.1. Thermal Stability. PILs prepared by neutralization reactions are in acid−base equilibrium. They include not only ionic species (anion and cation) but also neutral species (acid and base) according to the equilibrium constants, which are roughly determined by the difference in pK_a values between the acid and base (ΔpK_a). Angell and his co-workers first reported a linear relationship between excess boiling point (ΔT_b) and ΔpK_a (Figure 32).[331] Watanabe et al. reported thermal stability

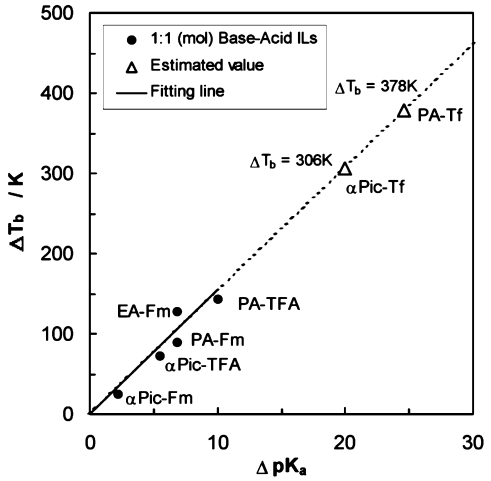

Figure 32. Relation between excess boiling point (ΔT_b) and ΔpK_a. The ΔT_b value is determined as the difference between the measured boiling point and the value, at 1:1, of the linear connection between pure acid and pure base boiling points. EA, ethylamine; PA, propylamine; αPic, 2-methylpyridine; Tf, trifluoromethanesulfonic acid; TFA, trifluoroacetic acid; Fm, formic acid. Reproduced from ref 331. Copyright 2003 American Chemical Society.

of many PILs by thermogravimetry.[332] Weight loss of PILs comes from evaporation of neutral species. Since the difference in Gibbs energy before and after neutralization becomes larger with increasing ΔpK_a, the equilibrium shift to neutral species requires higher temperature with increasing ΔpK_a. They found that the requirement in the magnitude of ΔpK_a for PILs that have sufficient thermal stability is higher than 15.[333] Dai et al. reported thermally stable PILs prepared from superacids and organic superbases such as phosphazenes and guanidines (Figure 33a).[334] Watanabe el al. explored thermal stability of PILs based on 1,8-diazabicyclo[5.4.0]undec-7-ene (DBU) and found that [DBU][TFSA] has a very high thermal decomposition temperature (T_d = 451 °C), which is higher than that of a thermally stable aprotic IL, [C_2mim][TFSA] (Figure 33b).[333]

5.2.2. Proton Conductivity. In hydrated acid systems such as Nafion, the hydronium cation (H_3O^+) is generated by proton transfer reaction from the acid to water, and water also plays an important role as a mediator of proton conduction. Two proton conduction mechanisms have been generally accepted: the vehicle mechanism is conduction by migration of H_3O^+, while Grotthuss mechanism is conduction by proton hopping across the hydrogen bonding network composed of H_3O^+ and water molecules (Figure 34). In actual systems both mechanisms frequently coexist. A Walden plot is a simple way to diagnose the proton transport property of various electrolyte

DOI: 10.1021/acs.chemrev.6b00504
Chem. Rev. 2017, 117, 7190−7239

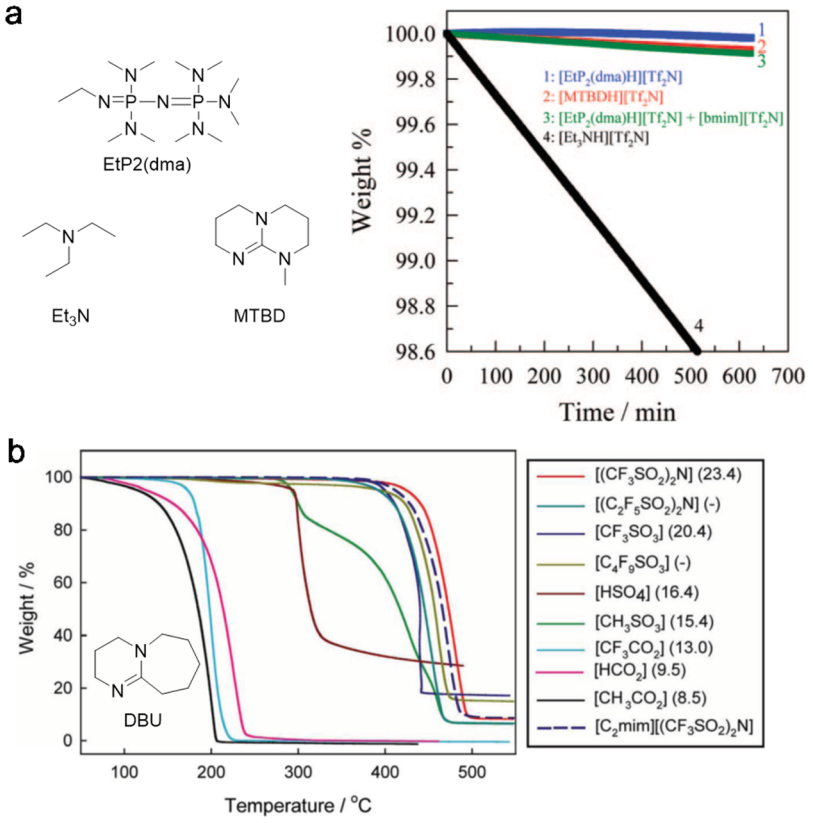

Figure 33. (a) Isothemal thermogravimetry of superbase-based PILs under N_2 at 150 °C. Reproduced from ref 334. Copyright 2009 American Chemical Society. (b) Thermogravimetry curves of [DBU]-based PILs at 10 K min^{-1} under N_2; the number in parentheses corresponds to ΔpK_a of constituent acid and base. Reproduced with permission from ref 333. Copyright 2012 Royal Society of Chemistry.

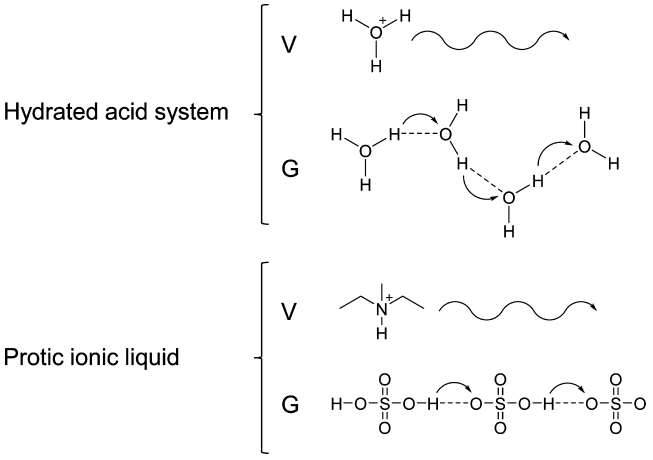

Figure 34. Schematic presentation of proton conduction mechanism in hydrated acid systems and protic ILs. V and G denotes vehicle mechanism and Grotthuss mechanism, respectively. Grotthuss mechanism is achieved by proton hopping followed by reorientation of proton mediator. Grotthuss mechanism is less affected by viscosity, compared with vehicle mechanism.

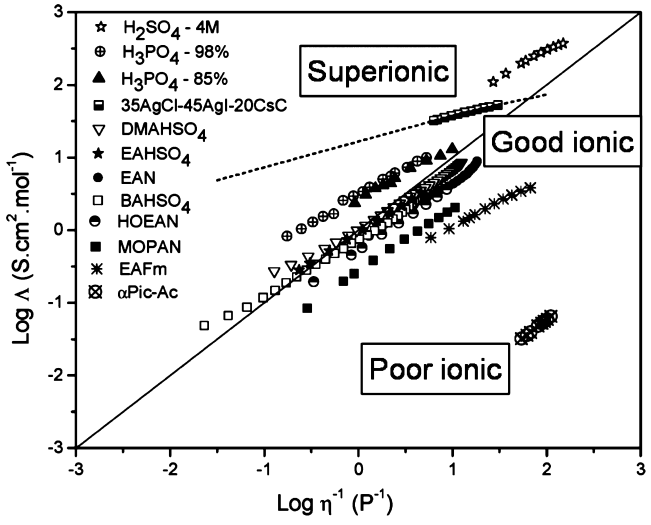

Figure 35. Walden plot for various electrolyte materials. $DMAHSO_4$, dimethylammonium hydrogensulfate; EAN, ethylammonium nitrate; $BAHSO_4$, butylammonium hydrogensulfate; HOEAN, hydroxyethylammonium nitrate; MOPAN, 3-methoxypropylammonium nitrate; EAFm, ethylammonium formate; and αPic-Ac, 2-metylpyridium acetate. Reproduced from ref 338. Copyright 2007 American Chemical Society.

materials (Figure 35).[331,338] In the Walden plot, the solid line with slope = 1 is the ideal line observed for 1 M KCl aqueous solution as a model of the vehicle conduction with complete dissociation. If an electrolyte does not completely dissociate and the Grotthuss mechanism is not involved, the plots lie below the ideal line. On the other hand, when the Grotthuss mechanism is involved in the conduction, which is less affected by viscosity compared to the vehicle mechanism, the plots tend to lie above the ideal line. Angell et al. classified electrolytes whose Walden plots lie much lower than the ideal line as poor electrolytes, while those with the Walden plots close to the ideal line but lower than it are named as good electrolytes. They also categorized electrolyte materials whose Walden plots

DOI: 10.1021/acs.chemrev.6b00504
Chem. Rev. 2017, 117, 7190−7239

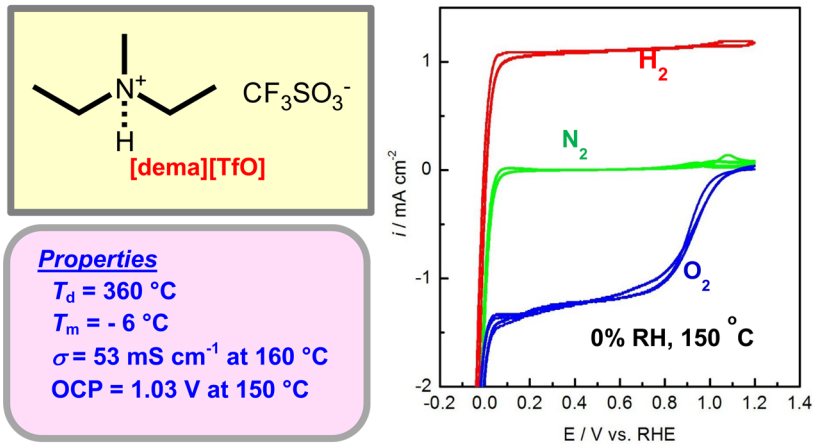

Figure 36. Physicochemical and electrochemical properties of [dema][TfO]. Cyclic voltammetry (right) was measured at a bright Pt-wire electrode (WE) vs a reversible hydrogen electrode (RHE) with a two-compartment glass cell under dry N_2, H_2, or O_2 gas bubbling atmosphere at 10 mV s^{-1}. The counter electrode (CE) was a platinized Pt wire; the RHE was a Pt wire in a H_2-sparged solution, placed close to the WE through a Luggin capillary. Redrawn after ref 332.

lie above the ideal line as superionic electrolytes (Figure 35).[331,338]

Diethylmethylammonium trifluoromethanesulfonate ([dema][TfO]) is a typical PIL having preferable properties as a fuel cell electrolyte [T_m = −6 °C, T_d = 360 °C, σ (ionic conductivity) = 53 mS cm^{-1} at 160 °C, and OCV (open circuit potential for a Grove-type $H_2|O_2$ cell with Pt electrodes) = 1.03 V at 150 °C] (Figure 36).[332] In such PILs, proton transport is carried out by migration of the cations that have active protons. In the case of [dema][TfO], the ΔpK_a is sufficient (17.5) to complete the proton transfer reaction. Consequently, there is no proton receiving site in the structure, and thus proton conduction occurs by the vehicle mechanism. On the other hand, PILs having such anions as HSO_4^- and $H_2PO_3^-$ exhibit proton conduction not only by the vehicle mechanism but also by the Grotthuss mechanism, since these anions have both proton-donating and -accepting sites in their structures and form a hydrogen-bonding network (Figure 34).[337] Walden plots of such systems lie above the ideal line (Figure 35).[338] However, ionic conductivity of electrolyte materials is more or less dominated by their viscosity, thus it should be noted that PILs with a Grotthuss mechanism contribution to their ionic conduction are not always superior to PILs with only the vehicle mechanism. Actually, [dema]HSO_4 and [dema]H_2PO_4 have lower ionic conductivity than [dema][TfO] at the same temperature due to high viscosity derived from the hydrogen-bonding network, even though the Grotthuss mechanism is exhibited for the two former ILs. Additionally, certain PILs, with low ΔpK_a or containing a stoichiometric excess of base, exhibit high proton conductivity by the Grotthuss mechanism, due to the presence of a proton accepting base (proton vacancy). However, thermal stability simultaneously becomes worse due to the existence of a larger amount of neutral species.[339,340]

In PILs, both the cation and anion are generally mobile, and thus ionic conductivity is not always equal to proton conductivity. For certain PILs, the self-diffusion coefficient of cation and anion were measured by PGSE-NMR (pulse-field gradient spin echo NMR), which indicates that the cation has slightly higher but similar self-diffusion coefficient to that of anion (Table 3).[346]

Table 3. Diffusion Coefficients of Ions in PILs, Which Were Estimated by PGSE-NMR Techniques.[346]

PILs[a]		$D \times 10^6$ (cm^2 s^{-1}[b]) 30 °C	130 °C
[dema][TfO]	cation	0.479	4.91
	anion	0.365	5.14
[adma][TfO]	cation	0.493	5.77
	anion	0.424	5.13
[mdpa][TfO]	cation	0.501	5.95
	anion	0.420	5.11

[a]Abbreviations of cations are as follows: [dema] = diethylmethylammonium, [adma] = allyldimethylammonium, and [mdma] = methyldipropylammonium. [b]Self-diffusion coefficient measured by PGSE-NMR techniques.

5.2.3. Electrochemical Activity. Electrode reactions of a $H_2|O_2$ fuel cell using aqueous acidic electrolytes can be written as follows.

$$\text{anode: } H_2 + 2H_2O \rightarrow 2H_3O^+ + 2e^-$$

$$\text{cathode: } 1/2O_2 + 2H_3O^+ + 2e^- \rightarrow 3H_2O$$

$$\text{total: } H_2 + 1/2O_2 \rightarrow H_2O$$

In typical PILs, the proton exists as a component of a cationic structure (BH^+), where proton is bound to the heteroatom (N, P, S, etc.) of base (B). Accordingly, possible fuel cell reactions in PILs can be written as follows:

$$\text{anode: } H_2 + 2B \rightarrow 2BH^+ + 2e^-$$

$$\text{cathode: } 1/2O_2 + 2BH^+ + 2e^- \rightarrow H_2O + 2B$$

$$\text{total: } H_2 + 1/2O_2 \rightarrow H_2O$$

Neutral acid, if present, may also contribute to the anodic reaction instead of BH^+. Figure 36 shows cyclic voltammetry for the hydrogen oxidation reaction (HOR) and oxygen reduction reaction (ORR) in [dema][TfO]. Fuel cell reactions in PILs are greatly affected by the nature of PILs (Table 4),[332] as indicated by the great change in the open circuit potentials (OCP). It was revealed that trifluoromethanesulfonate salts tend to show high OCP, while HSO_4 salts and [TFSA] salts

DOI: 10.1021/acs.chemrev.6b00504
Chem. Rev. 2017, 117, 7190−7239

Table 4. Open Circuit Potential (OCP) for $H_2|O_2$ Fuel Cells Using Pt Electrodes and PILs at 150 °C[332]

PILs[a]	OCP/V	PILs	OCP/V
[dema][TFSA]	0.77	[EPp][TfO]	1.08
[im][TFSA]	0.57	[tea][MS]	0.80
[dema][TfO]	1.03	[dea][MS]	0.81
[dmea][TfO]	1.01	[dema]HSO_4	0.89
[tea][TfO]	0.94	[EPp]HSO_4	0.79

[a]Abbreviations of cations are as follows: [im] = imidazolium, [dmea] = dimethylethylammonium, [tea] = triethylammonium, [Epp] = *N*-ethylpiperidinium, and [dea] = diethylammonium.

show relatively low OCP. The OCP has been correlated with ΔpK_a of PILs and tends to have a maximum at a certain value of ΔpK_a (Figure 37a).[348] Interestingly, mixtures of [dema]-HSO_4 and [dema][TFSA] show a higher OCP than the component ILs, comparable to [dema][TfO] (Figure 37b).[349] The former observation has been interpreted in terms of N−H bond strength, electrode poisoning by a trace amount of neutral amine, and the anion-exchange effect.[332,349] The N−H bond strength increases with ΔpK_a.[335] Strong N−H bonds may retard the ORR, resulting in a low OCP. However, weak N−H bonds (low ΔpK_a) indicate incomplete proton transfer reactions and the presence of neutral amine, also resulting in a low OCP. Kanzaki et al. reported acid base equilibrium constants in PILs, which were determined by potentiometric titration techniques.[350] ΔpK_a is of course a metric of the equilibrium constants, but it is based on acidity in aqueous media. Therefore, ΔpK_a is affected by the hydration effect. According to their report, the estimated equilibrium constant for ethylammonium nitrate is lower than that derived from ΔpK_a by a factor of 2, which indicates that there are in fact more neutral species in PILs than estimated by ΔpK_a. The mixing effect on OCP might be understandable if anion-exchange reactions are fast enough to average the N−H bond strength.

5.3. Membrane Fabrication

PILs for fuel cell applications should be fabricated as thin films. There are two possible ways to obtain thin films including PILs: one is impregnation of PILs into porous membranes and another is fabricating dense composite membranes by using polymer matrixes. On the basis of the fact that the fuel cell system is an open system, the latter way is preferable, since PILs can easily be leaked out from the membrane in the former.

5.3.1. Poly(vinylidene fluoride) (PVDF) Based Composite Membranes. PVDF and its copolymers are chemically and electrochemically stable crystalline polymers with T_m of 140−160 °C and can be processed into mechanically strong thin membranes. When they are processed by using a solution casting method, morphology of the resulting membrane is strongly dependent on the casting solvent, ranging from porous to dense membranes.[351] PVDF composite membranes including aprotic ILs and acids were reported by Scrosati et al.[352] and Sekhon et al.[353] Zhou fabricated composite membranes where HSO_4^- salts are impregnated into porous PVDF membranes and achieved a polarization current of 170 mA cm^{-2} at 50 °C in fuel cell operation using the membranes.[354]

5.3.2. Nafion-Based Composite Membranes. IL composite membranes based on perfluorosulfonic acid membranes, typically Nafion, have also been examined by several researchers. Doyle fabricated composite membranes consisting of DOW membrane or Nafion membranes by immersing them into ILs. Ionic conductivities in excess of 0.1 S/cm at 180 °C have been demonstrated using [C_4mim][TfO].[355] Comparisons between the IL-swollen membrane and the neat liquid itself indicate substantial proton mobility in these composites.

Iojoiu and her co-workers have explored ionic conductivity of Nafion-based composite membranes in detail.[356−362] They fabricated composite membranes, consisting of triethylamine (TEA)-based-PILs and Nafion, by an immersing method and estimated ionic conductivity of the membranes. The order of ionic conductivity of the composite membranes is MS-TEA > PFBu-TEA > TF-TEA, which is different from that of neat PILs (TF-TEA > MS-TEA ≫ PFBuTEA) (Figure 38).[361] From broadband electric spectroscopy, they explain the discrepancy in terms of differences in the interaction between PILs and Nafion and resulting nanophase separation structures.

Computational simulation of this system has also been performed.[363,364] Zhou et al. reported computational simulation of nanophase separation of [C_4mim]BF_4/Nafion composite membrane (Figure 39).[363] The diffusion coefficient of the cation in the composite membrane is calculated to be two times higher than that of the anion due to interaction between the PIL and Nafion, while the diffusion coefficients of both ions in neat [C_4mim]BF_4 are similar.

5.3.3. Block Polymer-Based Composite Membranes. Interesting attempts have been made for the fabrication of composite membranes having well-developed nanophase separation of ionic and nonionic domains by using block

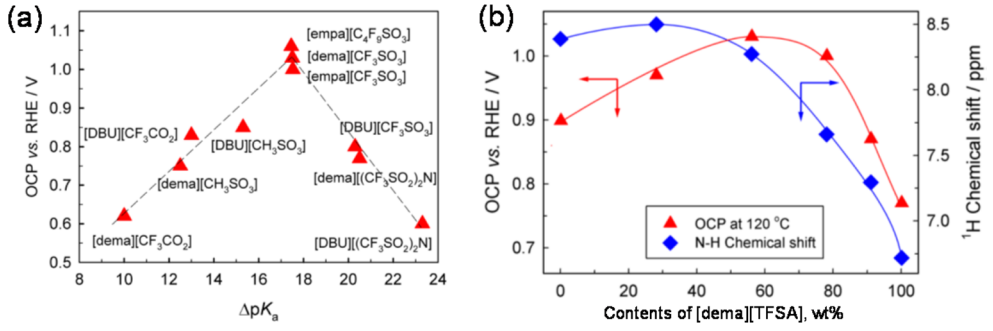

Figure 37. (a) Open circuit potential (OCP) for $H_2|O_2$ fuel cells using Pt electrodes in PILs at 150 °C as a function of ΔpK_a. Reproduced with permission from ref 348. Copyright 2013 Royal Society of Chemistry. (b) OCP for $H_2|O_2$ fuel cells using Pt electrodes at 120 °C and chemical shift of N−H proton in [dema] as a function of compositions of [dema][TFSA] and [dema]HSO_4 binary mixtures; [empa]: ethylmethylpropylammonium. Reproduced from ref 349. Copyright 2014 American Chemical Society.

DOI: 10.1021/acs.chemrev.6b00504
Chem. Rev. 2017, 117, 7190−7239

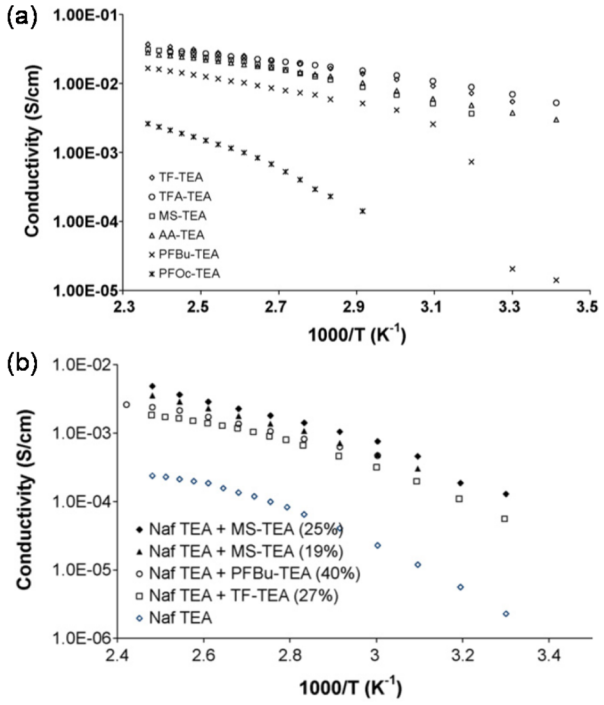

Figure 38. (a) Ionic conductivity of PILs and (b) their Nafion composite membranes. TEA, triethylamine; TF, trifluoromethanesulfonic acid; TFA, trifluoroacetic acid; MS, methanesulfonic acid; AA, acetic acid; PFBu, perfluorobutanesulfonic acid; PFOc, perfluorooctanesulfonic acid; and Naf, Nafion. Reproduced with permission from ref 361. Copyright 2010 Elsevier.

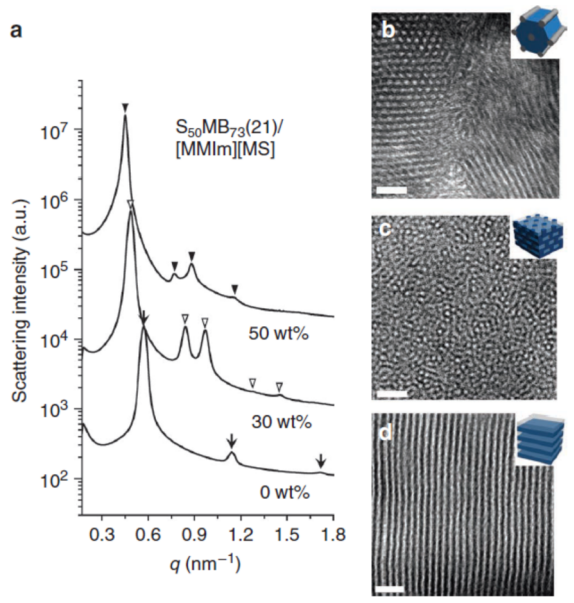

Figure 40. Morphologies of $[C_1mim][MS]$/poly(styrenesulfonate-*b*-methylbutylene) composite membranes as a function of IL content. (a) SAXS profiles and cross-sectional TEM images composite membranes containing (b) 0 wt %, (c) 30 wt %, and (d) 50 wt % of $[C_1mim][MS]$. [MMIm] = $[C_1mim]$. Reproduced with permission from ref 365. Copyright 2010 Nature Publishing Group.

copolymers. Park et al. fabricated the composite membranes consisting of $[C_1mim][MS]$ or $[C_4mim]BF_4$ and poly(styrenesulfonate-*b*-methylbutyene) block copolymer (SMB), and a comparison with Nafion-based membranes was made. The SMB-based composite membranes form well-developed lamellar or cylinder structures (Figure 40); their ionic conductivity obeys the order: $[C_1mim][MS]$/SMB > $[C_4mim]BF_4$/SMB, while Nafion-based membranes show the opposite tendency. Additionally, $[C_1mim][MS]$/SMB membranes exhibit much higher ionic conductivity than Nafion-based membranes. This difference is explained in terms of well-developed nanophase separation of SMB-based membranes and proton hopping via the SO_3^- moiety in the polymer and the anion in the PIL.[365] Hoarfrost et al. prepared composite membranes consisting of poly(styrene-*b*-vinylpyridine) block copolymer and [im][TFSA] ([im]: imidazolium) and claimed that proton hopping occurs more effectively in PIL confined in a nanosize domain of polymer matrix than that in the bulk.[366]

5.3.4. Aromatic Polymer Based Composite Membranes. Aromatic polymers such as polyimide and polybenzimidazole are known as super engineering plastics and have superior thermal and chemical stability, mechanical strength, and membrane formability. Due to their favorable properties,

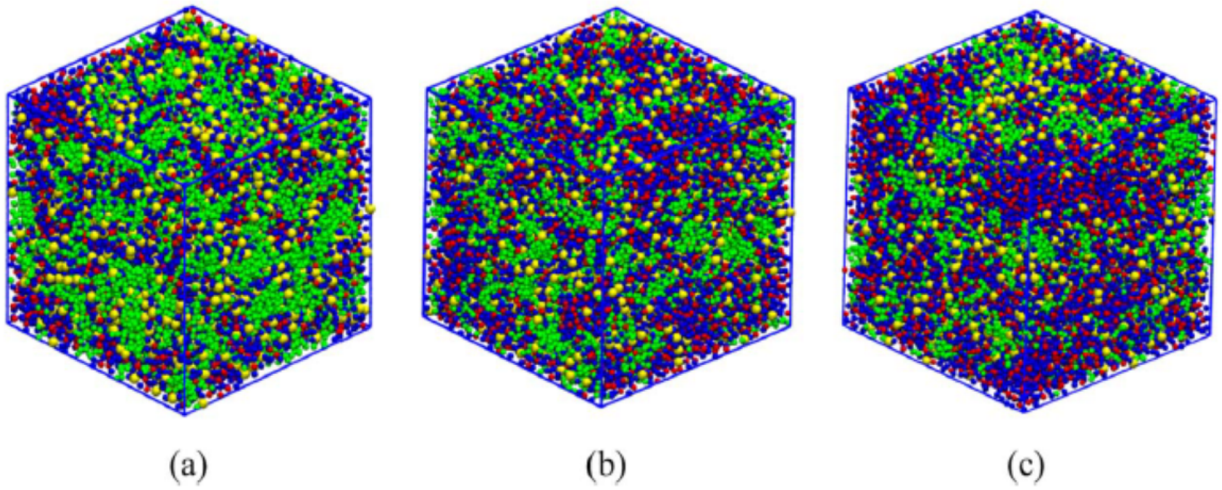

Figure 39. Computational simulation of $[C_4mim]BF_4$/Nafion composites with a different fraction of IL: (a) 45%, (b) 52%, and (c) 57%. Color representations: green, Nafion back bones; yellow, Nafion pendant charged groups; blue, cations; and red, anions. Reproduced with permission from ref 363. Copyright 2013 John Wiley & Sons, Inc.

DOI: 10.1021/acs.chemrev.6b00504
Chem. Rev. 2017, 117, 7190−7239

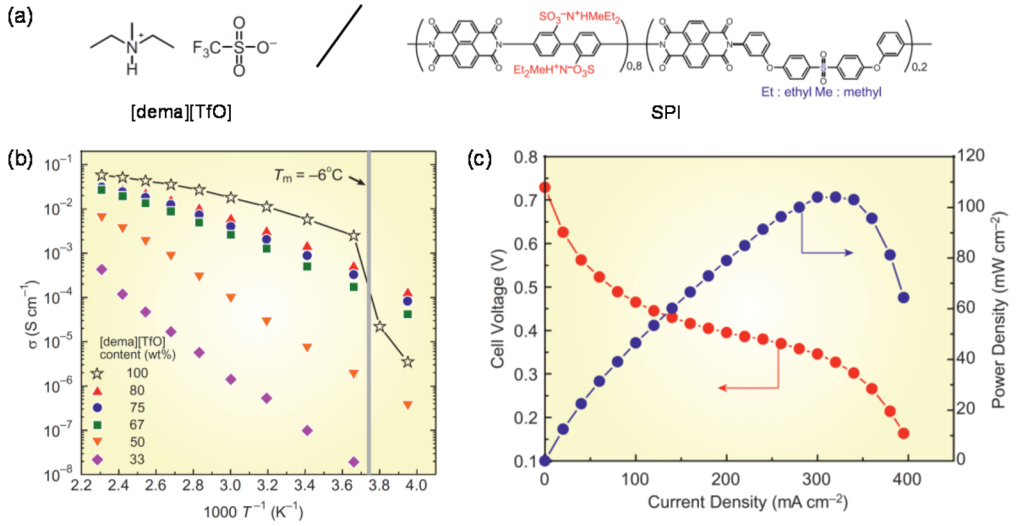

Figure 41. (a) Chemical structure of [dema][TfO]/SPI, (b) ionic conductivity under anhydrous conditions, and (c) nonhumidifying fuel cell performance at 120 °C using [dema][TfO]/SPI composite membranes. Reproduced with permission from ref 370. Copyright 2013 Materials Research Society.

these polymers, modified with acid groups, have been widely studied as alternatives to Nafion for fuel cell application. Polyimides with substituted sulfonated groups (SPI) (Figure 41a) are found to have good compatibility with PILs and gives uniform, thin, and mechanically strong composite membranes. The resulting composite membranes, [dema][TfO]/SPI, exhibit acceptable ionic conductivity (Figure 41b).[367,368] Multiblock copolyimides consisting of ionic and nonionic segments have higher PIL-retaining abilities than random copolyimides with the same ion-exchange capacity and exhibit higher ionic conductivity even at the same PILs content.[369] From AFM observations, nanophase separation of ionic and nonionic domains in the composite membranes is found to be more developed in the multiblock copolyimides compared with that of the random copolyimides.[369] In nonhumidifying fuel cell operation using [dema][TfO]/SPI composite membranes at 120 °C, the maximum current and power densities of ca. 400 mA cm^{-2} and 110 mW/cm^2 are reported (Figure 41c).[370]

Another example is the composite membranes based on polybenzimidazoles (PBIs). Mamlouk et al. observed polarization current density of 70 mA cm^{-2} at 150 °C in nonhumidifying fuel cell operation using diethylammonium hydrogenesulate ([dea]HSO_4)/PBI composite membranes.[371]

5.4. Outlook for Fuel Cell Electrolytes

Requirements for the proton conductors in a nonhumidifying fuel cell system are extremely severe. Chemical, electrochemical, and thermal stabilities are basic requirements for PILs, as well as favorable transport properties and facile electrode reactions. For matrix polymers of the composite membranes, mechanical strength and stability are needed in addition to the above-mentioned stabilities. Leakage of PILs from the composite membranes is still a severe drawback for the composite systems. Materials satisfactory to such requirements have not been developed yet. However, fuel cell membranes operable under nonhumidifying conditions and at above 100 °C are considered to be dream membranes, and there is enough scope for further investigation.

6. ELECTROACTIVE CARBONS FROM IONIC LIQUIDS

6.1. N-Doped Carbon Materials

Carbon materials owing to their unique features in terms of high surface area, excellent electric and thermal conductivity, high chemical stability, and low cost have attracted significant attention in diverse areas such as environmental treatment, catalysis, sensing, separation, gas capture/separation, and particularly, electrochemical energy conversion/storage.[372,373] In general, carbon materials can be prepared by the carbonization of carbon-containing precursors. The structure and composition of the precursors are critical to the preparation process and the structure and properties of the final carbons. Incorporation of electron-donating or electron-withdrawing foreign elements such as N, B, S, and P into the carbon structures provides a simple and effective way to tune and control physicochemical properties of the carbon materials. Particularly, N-doping can modulate the electronic structure of the carbons via conjugation between the nitrogen lone-pair and π-system of the carbon lattice and generate additional functional groups on the carbon surface, which thereby enhances their electrical conductivity, basicity, oxidation stability, and (electrochemically and chemically) catalytic activity for potential applications.[374−378] The resultant N-doped carbon materials (NDCs), particularly those with both high N content and graphitic degree, exhibit very high conductivity[379,380] because of the increase in electron density at the Fermi level and allowing the electrons to reach the conduction band.[381−383] NDCs also show outstanding oxidative stability, even at elevated temperatures,[379,384] and can chemically activate oxygen while not reacting themselves.[385] As a nanostructured high surface support for noble platinum, NDC was even able to survive the conditions of the Periana reaction, which involves high pressure oxygen in foaming sulfuric acid above 200 °C.[386]

Normally, NDCs are synthesized according to the following strategies: postmodification of the as-prepared carbon materials or in situ carbonization of specific precursors. The former method requires additional heteroatom-containing agents such as ammonia gas and is uncontrollable in terms of both the amount and distribution of dopants.[387,388] In contrast, in situ

DOI: 10.1021/acs.chemrev.6b00504
Chem. Rev. 2017, 117, 7190−7239

carbonization of heteroatom-containing carbon precursors such as polyacrylonitrile usually yields more homogeneously distributed heteroatom atoms throughout the material.[374] Since most organic compounds are completely evaporated or decomposed into gaseous products during high-temperature carbonization, precursors currently available for NDCs are limited to natural or synthetic polymers. The polymer precursors-related procedures are multistep and time-consuming. Meanwhile, direct carbonization of such precursors always lead to low N content.[389,390]

6.2. New Concept: From Ionic Liquids to N-Doped Carbons

Because of their unique features such as a carbon-rich nature, negligible vapor pressure, and high thermal stability, ILs composed of organic cations and inorganic/organic anions have shown great promise as versatile small-molecular and low-vapor-pressure carbon precursors, instead of conventional polymers. Carbon materialization of ILs can be readily carried out without applied pressure. The intrinsic nitrogen-containing nature of most ILs offer the possibility to yield NDCs in situ without additional doping agents. Moreover, the structures and properties of the final carbon materials can be easily controlled at the molecular level through rational design of the ionic precursors by virtue of their structural diversity.[391−394] Since most conventional ILs under inert atmosphere and ambient pressure afford no suitable carbons due to the lack of stable intermediate polymeric structures and the eventual formation of volatile vapors during thermal decomposition,[395,396] the IL precursors being investigated in the early stage are mainly focused on specific ILs containing cross-linkable moieties.[379,396] As pioneered by Dai et al. in 2009,[396] various intrinsic NDCs were obtained by direct carbonization of aprotic ILs containing nitrile/cyano moieties in either cations or anions.[379,391,393,397−401] Nitrogen heteroatoms are believed to be homogeneously distributed in the obtained NDCs because of the one-step carbonization from a single precursor. The key to successful carbonization of these task-specific ILs in atmospheric pressure is that the nitrile groups undergo cross-linking reactions and form intermediate amorphous polytriazine networks through cyclotrimerization of nitrile groups (Figure 42).[402] Another advantage is that the liquid state of ILs at

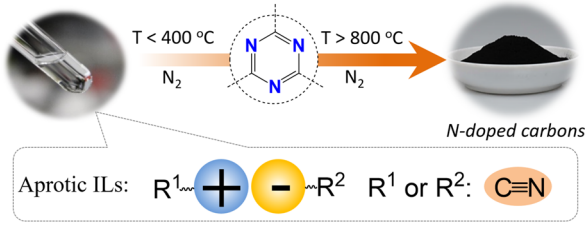

Figure 42. Schematic representation of synthesis of NDCs from nitrile/cyano-containing aprotic ILs.

ambient conditions will facilitate the production of seamless continuous carbon films.[396] However, the wide application of these nitrile/cyano-containing ILs is strongly hampered by their complicated synthesis, high cost, and relatively low carbon yield (<13% at 1000 °C). In order to address this issue, many efforts have been devoted to developing new IL precursors for carbonization, mainly focused on the following candidates: poly(ionic liquid)s (poly-ILs), deep-eutectic solvents (DESs), protic ILs and salts (PILs/PSs).

Poly-ILs owing to their polymeric nature as carbon precursors have the following merits.[403−406] First, poly-ILs can be processed into various shapes, which leads to monolithic carbon materials such as membranes, tubes, hollow spheres, and foams with a full preservation of the shape of the precursors.[407−411] Such well-defined morphologies are inaccessible via monomers or small molecule based ILs. Second, poly-ILs always show improved carbon yield as opposed to conventional ILs.[412] Third, known favorable interactions between polar IL monomers and inorganic templates make it possible to coat poly-ILs on the template surface homogeneously by in situ polymerization, thus producing more advanced porous carbons such as hollow carbon spheres or carbon-encapsulated structures.[408,413−417] In addition to poly-ILs that require complicated syntheses, DESs, which share many characteristics with conventional ILs,[418−420] have also been proposed as a new class of IL precursors recently. Monte and co-workers have contributed extensively to this research area and showed that low cost DESs (if combined with polycondensation of resorcinol−formaldehyde gels) are highly desirable to produce bulk monolithic carbons with hierarchical and interconnected porous structures.[421−429] However, it should be noted that direct carbonization of DES itself in most cases gives rise to no carbon residues.[422] A possible explanation is that the hydrogen-bond strength between the hydrogen donors and acceptors in DESs is insufficient to render the DESs thermally stable prior to preliminary polymerization and carbonization at high temperature. Besides poly-ILs and DESs, a more attractive type of IL precursor is the low-cost and easily prepared N-containing PILs/PSs developed very recently mainly by Zhang in the Watanabe group.[380,384,391,430−433] Employment of such PILs/PSs as single and versatile precursors for the facile direct carbonization, without additional catalyst, prepolymerization or other complex techniques can overcome the drawbacks related to cyano/nitrile-containing aprotic IL precursors such as a multistep and time-consuming synthesis, rigorous purification, metal impurities (e.g., Li, Na, or Ag, possibly from metathesis), and high cost.[395,396] As seen in Figure 43a, the entire procedure of a PILs/PSs-involved process is quite simple and easy to carry out, involving only two steps: neutralization and carbonization. The concept is validated by the comparative study of thermal gravimetric analysis (TGA) of both the parent base and PILs/PSs. As seen in Figure 43b, all of the parent amines are completely evaporated or decomposed below 400 °C, while the corresponding PILs/PSs were indeed converted to carbon residues, with carbon yield strongly dependent on the structure of the PILs/PSs. Very importantly, the structure and properties (N content, conductivity, graphitic degree, and porosity) of the obtained carbons can be finely modulated by varying the precursor structure.

As a matter of fact, other than the specific IL precursors mentioned above, conventional ILs without any cross-linkable functional groups can also be considered as potential precursors if they are confined in nanospace.[434−440] The matrixes for nanoconfinement can be either inorganic or organic materials, such as silica gel[434] and cyclodextrin.[439] For example, when a noncarbonizable IL, [C_4mim][TFSA] (char residue was not obtained by direct carbonization of the bulk IL), was confined into an oxide framework via an in situ nonhydrolytic sol−gel process, carbon materials with substantial yield were achieved after carbonization.[434] It is believed that aromatization of the in situ-formed fragments through dehydrogenation reactions is considerably enhanced, and evaporative loss of intermediate

DOI: 10.1021/acs.chemrev.6b00504
Chem. Rev. 2017, 117, 7190−7239

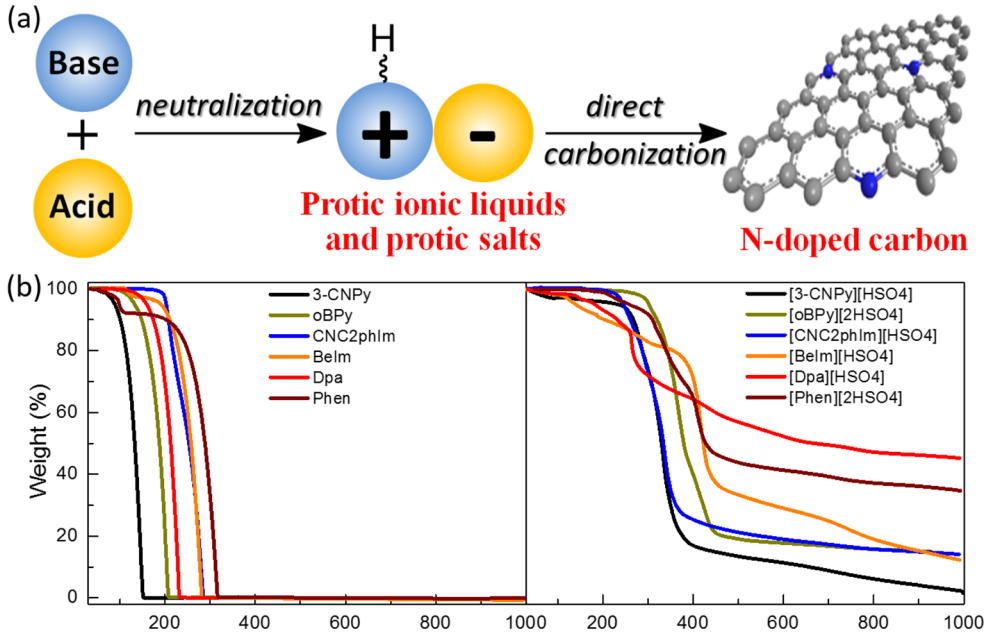

Figure 43. (a) Schematic representation of synthesis of NDCs by direct carbonization of PILs/PSs. (b) TGA curves of typical PILs/PSs as well as their parent amines. 3-CNPy: 3-cyanopyridine, oBPy: 2,2′-bipyridine, CNC2phIm: 1-cyanoethyl-2-phenylimidazole, BeIm: benzimidazole, DPa: diphenylamine, Phen: phenanthroline. These abbreviations in brackets denote the corresponding protonated ammoniums. Reprinted from ref 384 and 380, respectively. Copyright 2014 American Chemical Society.

species (other than hydrogen gas) is suppressed by the nanoconfinement effect. The improved carbon yield of ILs confined in β-cyclodextrin or cucurbituril further validate the concept of nanoconfinement-assisted carbonization.[439]

In addition to developing new potential IL precursors, another method to make full use of IL precursors but lower the cost is to use ILs as surface-coating agents or N-containing dopants for carbonization.[438,441−444] In such cases, the required amount of ILs is greatly reduced, while the attractive features of IL-derived NDCs, such as high conductivities and high nitrogen contents, remains. Noteworthy is that conventionally non-carbonizable ILs can also been explored as dopants for fabrication of heteroatom-doped carbon, although the resultant carbon yield is relatively lower than that of nitrile-containing ILs. Owing to the fluidic feature of the IL precursors coupled with their high nitrogen contents and graphitic structures of the resultant carbons, [DCA]-based ILs, especially [C_2mim][DCA]), have been intensively exploited to decorate the surfaces of bulk materials such as $Li_4Ti_5O_{12}$,[445,446] Pt/XC-72 catalyst,[447] and carbon nanotubes (CNTs)[448] with a thin layer of IL-derived NDCs. This thin layer was expected to protect the pristine materials while at the same time facilitate the electron transfer across the encapsulated shell. [DCA]-based ILs have also been frequently used as a N-containing agent for N doping for non-N-containing precursors such as graphene and graphene oxide.[449−453] It should be noted that using ILs in some cases not only leads to heteroatom incorporation into the framework but also modulates the carbon microstructure.[453]

6.3. Structure and Properties of Ionic-Liquid-Derived N-Doped Carbons

Compared to conventional precursors, the structural diversity of ILs, especially the easily obtained PILs/PSs, offers the possibility to easily control the structure and properties of the final carbon materials, which may result in NDCs with very attractive properties such as high N content, high graphitic degree, high conductivity, high oxidation ability, and meso-porous structure.[384,449,454] The IL structure is beneficial to nitrogen fixation in the carbon materials, and most of the highly nitrogen-doped carbons reported to date seem to be derived from IL precursors. For example, direct carbonization of [C_2mim][DCA] (39.5 wt % N) with an N/C molar ratio of 0.63:1 produced NDCs characterized by a very high nitrogen content, up to 10.4 wt % at 1000 °C.[379] This value could be further improved to about 12.0 wt % through cocarbonization of the same IL with naturally N-rich compounds; this ultrahigh nitrogen content should be the highest value for NDCs obtained by in situ N-doping.[455] Similarly, PIL of 3-cyanopyridinium hydrogen sulfate ([3-CNPy][HSO_4]), despite their relatively low N/C value of 0.33:1, has been shown to produce NDCs with nitrogen content of up to 11.91 wt % at 1000 °C.[384] This value, to our knowledge, was the highest value for NDCs obtained from a single precursor. The obtained high nitrogen contents are very important because N-doping in the carbon lattice can significantly alter or improve the physicochemical properties of carbon materials,[374,456,457] and moreover, it was generally accepted that for most NDCs with given porosity and graphitic structure, the higher the nitrogen content of the carbon material, the better performance it may exhibit. By virtue of the wide availability and easy synthesis of PILs/PSs, Watanabe and co-workers observed a linear or polynomial relationship between the N/C molar ratio and the N content of carbons. On the basis of this relationship, the upper limit of nitrogen content in carbon materials that might be achieved has been estimated for the first time.[458] The estimated upper limit for the nitrogen content of NDCs was found to be strongly related to the carbonization temperature. For example, maximally, one can dope 14.3 wt % of nitrogen into carbon obtained at 1000 °C, while this value can theoretically be increased to 21.7 wt % at 900 °C.[458] Indeed, such upper limits have never been achieved experimentally for NDCs prepared through either in situ carbonization or post-treatment. Other than the N-monodoped carbons, dual- or

DOI: 10.1021/acs.chemrev.6b00504
Chem. Rev. 2017, 117, 7190−7239

multidoped carbons such as N, S-codoped, N, B-codoped, N, P-codoped, and even Fe (or Co), N-codoped carbons, can be achieved by carbonization of ILs containing heteroatoms other than N, such as B,[399,459] S,[400,438,449] P,[384] and metallic atoms,[460,461] etc. in the cationic or anionic backbone of ILs (Figure 44).

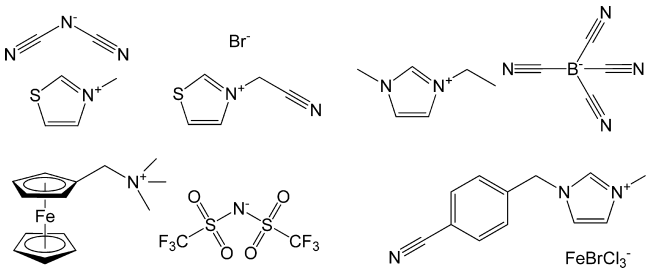

Figure 44. Chemical structure of typical IL precursors containing heteroatoms other than nitrogen.

Some IL-derived NDCs with very high N contents were found to have a high graphitic degree.[379,449] Graphitic order with bent layer planes and weak edge termination are randomly oriented but uniformly present throughout the entire carbon structure in $[C_2mim][DCA]$[379] and 3-cyanopyridinium hydrogen sulfate ($[3\text{-CNPy}][HSO_4]$)-derived NDCs,[380] while graphene layers in the 1-(2-cyanoethyl)-2-phenylimidazole hydrogen sulfate ($[CNC_2phIm][HSO_4]$)-derived carbon are mostly arranged in one direction. The graphitelike microstructures observed for the highly N-doped carbons without additional graphitization requirements such as complex graphite-like precursors,[462,463] catalytic graphitization,[464] chemical vapor deposition,[465] or very high temperature,[466] are interesting, since it was generally accepted that incorporation of large number of N atoms in carbon lattice would result in amorphization of the graphitic network, which may lead to a bent carbon structure with relatively long interlayer distance.[381,382] A combined Raman and X-ray photoelectron spectroscopy (XPS) analysis suggested that the high percentages of pyridinic N with planar structures (in contrast to quaternary N with a "out of plane" bonding configuration[467]) in these highly N-doped carbons relax the N content-induced amorphization, thus resulting in more graphitic structure with short interlayer distances.[449] IL-derived NDCs with a combination of very high N content and high graphitic degree have been shown to result in very high conductivity, even higher than that of the graphite.[379,449] The high graphitic degree in such IL-derived NDCs also helps to improve the thermal stability against oxidation.[379,384] The oxidation temperatures of $[CNC_2phIm][HSO_4]$- and $[3\text{-CNPy}][HSO_4]$-derived NDCs recorded in air are significantly higher than those of furfuryl alcohol and sucrose-derived carbons, and even graphite, CNTs.[468−470]

To maximize the potential applications of IL-derived NDCs, it is essential to introduce pores into NDCs since high porosity facilitates mass transport and diffusion, providing abundant

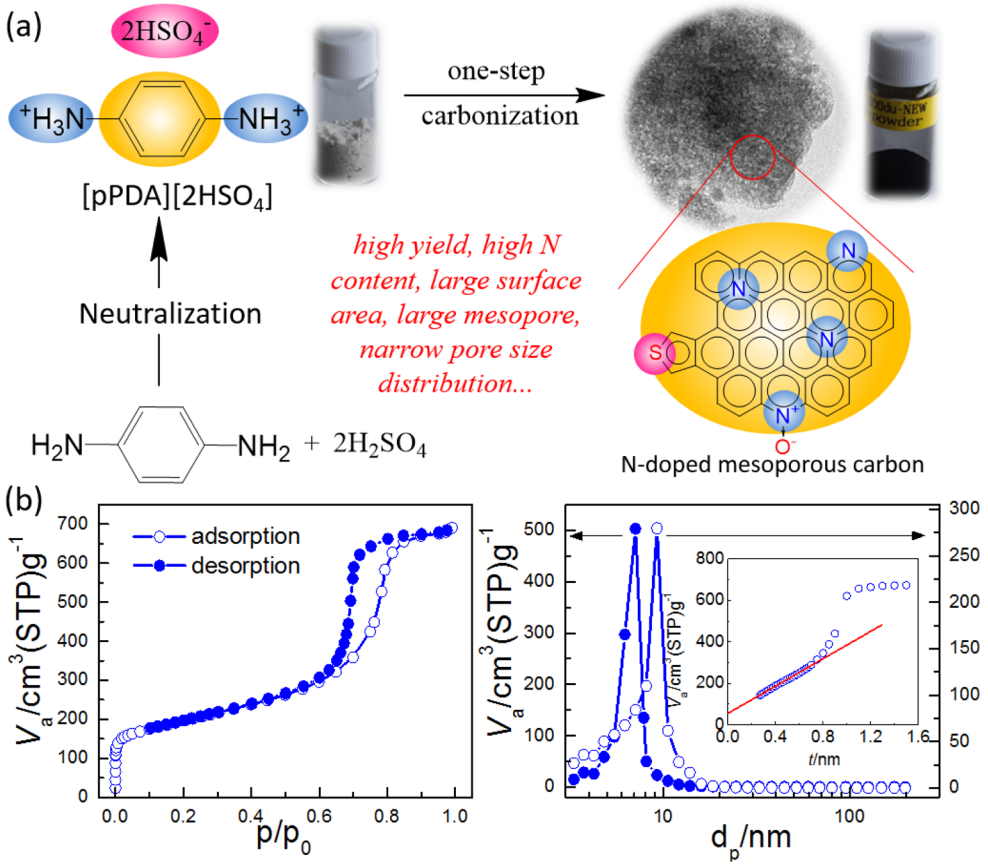

Figure 45. (a) Schematic representation of template-free synthesis of mesoporous NDCs by direct carbonization of *p*-phenylenediammonium dihydrogensulfate ($[pPDA][2HSO_4]$). (b) Nitrogen sorption isotherms and pore size distributions of mesoporous NDC obtained by direct carbonization of $[pPDA][2HSO_4]$ at 1000 °C. The inset in (b) shows the *t*-plot. Reprinted with permission from ref 433. Copyright 2015 Elsevier.

DOI: 10.1021/acs.chemrev.6b00504
Chem. Rev. 2017, 117, 7190−7239

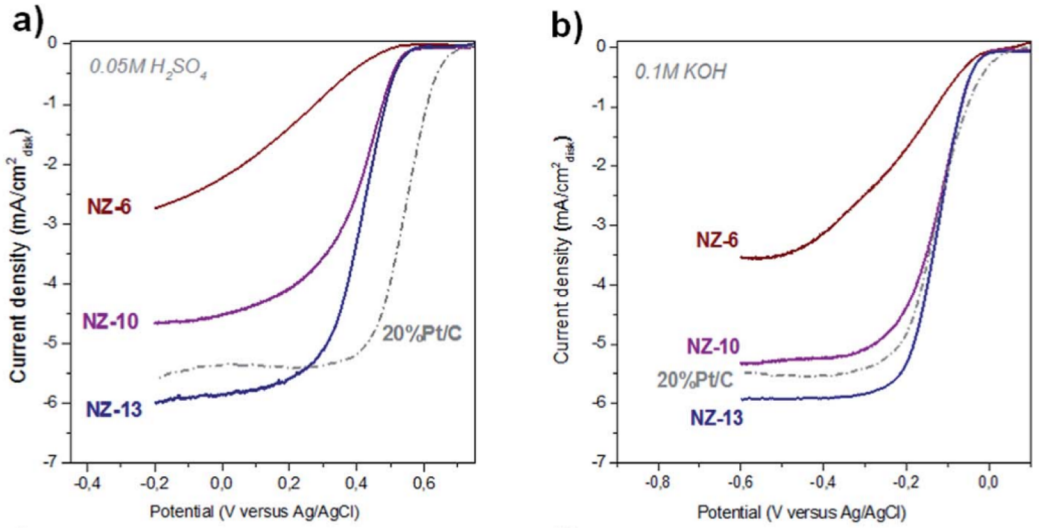

Figure 46. Linear sweep voltammetry (LSV) polarization curves of metal-free porous NDC (NZ-X) catalysts obtained by carbonization of $[C_2mim][DCA]$ mixed with different mass ratio (X) of salt melt ($NaCl/ZnCl_2$) to IL at 1000 °C in (a) O_2 saturated 0.05 M H_2SO_4 and (b) O_2 saturated 0.1 M KOH. LSV curves were recorded at scan rate 10 mV s^{-1} and at rotation speed 1600 rpm. For all measurements, the catalyst loading is around 0.21 mg cm^{-2} (including Pt/C catalyst). Reprinted with permission from ref 498. Copyright 2014 Royal Society of Chemistry.

active sites for efficient processes such as chemical catalysis and electrocatalysis. Various porous NDCs with multiscale pore structures have been specifically designed by template or template-free carbonization of ILs, including microporous, ordered/disordered mesoporous, macroporous, and hierarchical porous carbons. Notably, mesopores were generated by direct carbonization of either aprotic nitrile-containing imidazolium ILs paired with bulky anions such as [TFSA] or [BETA][396,471,472] or specific PIL/PSs.[433] For example, direct carbonization of 1-cyanomethyl-3-methylimidazolium bis(trifluoromethylsulfonyl)amide ([MCNIm][TFSA]) produced mesoporous NDCs with surface areas of up to 780 m^2 g^{-1}; the bulky anions are expected to undergo partial decomposition and behave as a self-template during carbonization.[396] The cation structure was found to have a profound influence on the final mesoporous structure and thus the surface area.[396,471] Very interestingly, mesoporous NDCs with high carbon yield, high nitrogen content, and excellent mesoporosity can be obtained by one-step carbonization of a protic salt, *p*-phenylenediamine bisulfate ($[pPDA][2HSO_4]$). As shown in Figure 45b, the nitrogen sorption analysis of NDC obtained at 1000 °C exhibits a typical type IV isotherm with a well-defined H2 hysteresis loop (p/p_o = 0.6−0.9), suggesting the presence of large mesopores with a very narrow size distribution, as confirmed by the corresponding pore size distribution (9.2 and 7.0 nm, respectively, for adsorption and desorption branches) and TEM images (Figure 45). The high mesoporosity of this carbon was evidenced by the large mesoporous surface area (508 m^2 g^{-1}) calculated by *t*-plot analysis (Figure 45b, inset). Intensive analysis indicated that the template-free fabrication of mesoporous NDCs was realized by the hydrogen-bond-assisted self-assembled structure. During carbonization, $[pPDA][2HSO_4]$ served as an "all-in-one" precursor; the anion $[HSO_4]^-$ acted as not only a self-oxidant to accelerate the polymerization of pPDA but also a unique self-template and porogen, while the cation $[pPDA]^+$ acted as a self-reductive agent and polymerizable monomer, as well as the carbon and nitrogen source.[433]

Although a few specific ILs can generate mesoporous NDCs via direct carbonization, as mentioned above, most ILs, especially those that can yield carbons with high N content and high conductivity, result in nonporous structures or very low surface area via template-free carbonization. For example, direct carbonization of $[C_2mim][DCA]$ at 800 °C produces a NDC with surface area as low as 3.41 m^2 g^{-1}.[473] Therefore, a conventional templating method has to be adopted in order to introduce pores in the IL-derived NDCs. The easy carbonization of ILs at ambient pressure, high thermal stability, and the favorable interactions between most ILs and inorganic surfaces[402,417,474] may assist the facile incorporation of ILs into the voids of templates with a homogeneous coverage and produce advanced porous NDCs. ILs also provide the opportunity to greatly reduce the synthesis time of templated carbons as the impregnation step can be carried out at reduced pressure. The external templates used for IL precursors can be mesoporous silica,[379,455] colloidal silica,[430,455,475] silica gel,[434] noncarbonizable inorganic eutectic salts,[476−479] metal−organic frameworks (MOFs),[480] etc. For example, $[C_2mim][DCA]$ in the presence of SBA-15[379,481−485] or LUDOX HS-40 (12 nm silica nanoparticles)[379,400,402,455,475,486−488] can give rise to exclusively (ordered or disordered) mesoporous NDCs with surface areas close to or above 1000 m^2 g^{-1}, while at the same time, maintaining their high N contents.

6.4. Applications of Ionic-Liquid-Derived N-Doped Carbons

6.4.1. Electrocatalysts. Owing to the unique features including high N content and conductivity, designable porosity, etc., IL-derived NDCs, especially porous NDCs, have found potential applications in electrochemical energy storage and/or conversion, particularly as electrocatalysts for oxygen reduction reaction (ORR). The high N content is expected to endow these electroactive carbons with not only high conductivity, which is beneficial to the electron transfer during electrocatalysis, but also abundant N dopants that create favorable positive sites for O_2 on the adjacent carbons owing to the electronegativity difference between N and C.[456] The developed pores in these electroactive carbons likely facilitate efficient mass transport and diffusion of reagents and products,

DOI: 10.1021/acs.chemrev.6b00504
Chem. Rev. 2017, 117, 7190−7239

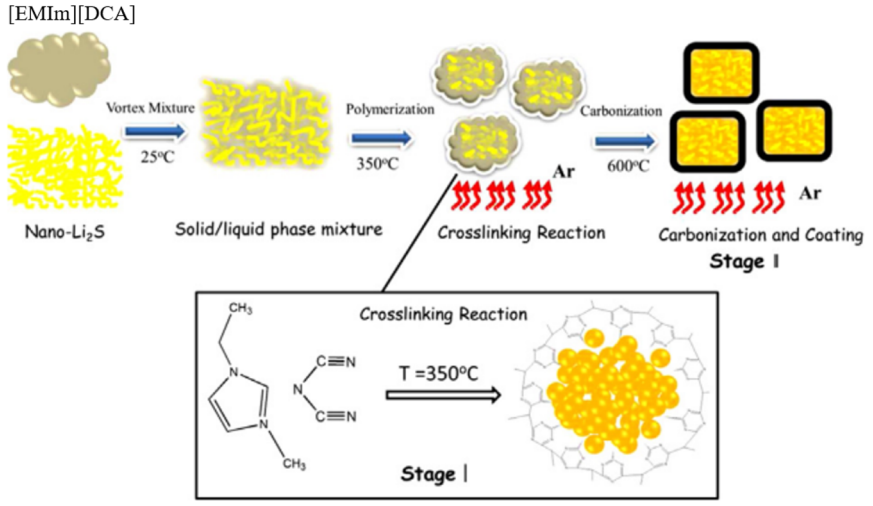

Figure 47. Schematic of preparing carbon cage encapsulated nanoclusters Li_2S composite for Li−S batteries. [EMIm] = [C_2mim]. Reprinted with permission from ref 512. Copyright 2015 Elsevier.

providing a large amount of accessible active sites for electrocatalysis. There are many IL-derived NDCs as metal-free electrocatalysts that exhibited excellent ORR activity.[438,440,449,455,489−498] For example, a series of carbons possessing both high nitrogen content and large surface area were obtained through cocarbonization of [C_2mim][DCA] and nucleobases such as adenine, guanine, cytosine, thymine, and uracil at 1000 °C, wherein the IL behaves as a carbon and nitrogen source for carbonization, while the nucleobases act as high N-content additives. Compared to the nonporous carbon derived from solely [C_2mim][DCA] under the same conditions (N 10.8 wt %), this hard templating method produced mesoporous NDCs with nitrogen contents of up to 12.0 wt % and large surface areas of up to 1553 $m^2\ g^{-1}$. As judged from the polarization curve on a rotating disk electrode (RDE), most of these carbons exhibit very high ORR activities, with onset potential, half-wave potential as well limiting diffusion current density being close to that of the commercial Pt/C. Through analysis of the plateau currents through Koutecky−Levich (K−L) plots, one of the obtained carbons has proven to undergo a four-electron reduction process of O_2, thus yielding water as the main product, as is the case for the Pt-based catalyst. However, these electrocatalysts only operate well in alkaline electrolyte and tend to perform poorly in acidic electrolyte. For example, for the best performing NDC in 0.1 M KOH, when employed in a 0.1 $HClO_4$ aqueous solution, a high overpotential of 197 mV as compared with Pt/C is observed.[455] Simply lowering the carbonization temperature of the above process from 1000 to 800 °C results in a much smaller surface area (~320 $m^2\ g^{-1}$). Interestingly, the obtained mesoporous NDC is highly active for the selective electrochemical reduction of oxygen to hydrogen peroxide ($O_2 + 2H^+ + 2e^- \rightarrow H_2O_2$) even in an acidic medium (0.1 M $HClO_4$). Such a nearly ideal two-electron process for the ORR was ascribed to a combination of the increased nitrogen content, the "radical" character of NDC, and the pyrrolic N sites within the carbon material.[475]

Replacing the silica template by a more easily removable "salt template" such as the eutectic salt mixture of NaCl/$ZnCl_2$ was found to not only simplify the whole synthetic process but also result in a highly efficient ORR electrocatalyst in both alkaline (0.1 M KOH) and acidic (0.05 M H_2SO_4) electrolytes.[498] Particularly, when the mass ratio of salt melt to IL is 13, the as-prepared sample NC-NZ-13 (carbonized at 1000 °C) shows outstanding activity with a half-wave potential equal to the Pt/C catalyst at the same loading. A high electrocatalytic activity was also observed in acidic medium (Figure 46). Moreover, both K−L plots and rotating ring-disk electrode (RRDE) data revealed that the transferred electron number was close to 4 at different potentials in both electrolytes. The observed exceptional electrocatalytic activity of NC-NZ-13 is ascribed to the combination of the aerogel-like structure with an improved porosity together with a high catalytically active surface. The small size of primary particles along with the relatively small stacking of the graphitic carbon increased the concentration of accessible active sites. Furthermore, the aerogel-like morphology provides a wide interstitial pore system which decreases the diffusion limitations while the particle interconnection is sufficient to maintain high electrical conductivity.[498]

Instead of the sophisticated templating method, template-free carbonization of either protic ILs[449] or specific cyano/nitrile-containing ILs can also yield porous NDCs as metal-free electroctalysts.[489] For example, direct carbonization of amino-acetonitrile hydrogen sulfate results in a N,S-codoped porous carbon with high surface area (1380 $m^2\ g^{-1}$), which showed excellent electrocatalytic activity toward ORR, with both onset and half-wave potential being very close to that of commercial Pt/C. The calculated peroxide yield was <15%, and the average electron-transfer number was >3.7.[449] In contrast, hierarchical micro- and meso-porous NDCs resulting from specific cyano/nitrile-containing ILs showed a much inferior ORR activity, while both the ORR activity and kinetics were found to be strongly correlated with the pore size distribution.[489] Other than metal-free NDCs, IL-derived Fe-, N-, or Co-, N-codoped carbon electrocatalysts were also found to be highly efficient for ORR. Such carbon materials are usually obtained by carbonization of either task-specific ILs (Figure 44) containing a metal ion in either the cations[461] or anions[460] or ILs in the presence of metal-containing precursors.[473,499] In addition to ORR, IL-derived NDCs can be used as electrocatalysts for oxygen evolution reaction (OER),[500,501] hydrogen evolution reaction (HER),[502] and methanol oxidation.[413,416,447,503−505] More attractively, a mesoporous NDC obtained by carbonization of N-butyl-3-methylpyridinium dicyanamide with LUDOXHS-40

DOI: 10.1021/acs.chemrev.6b00504
Chem. Rev. 2017, 117, 7190−7239

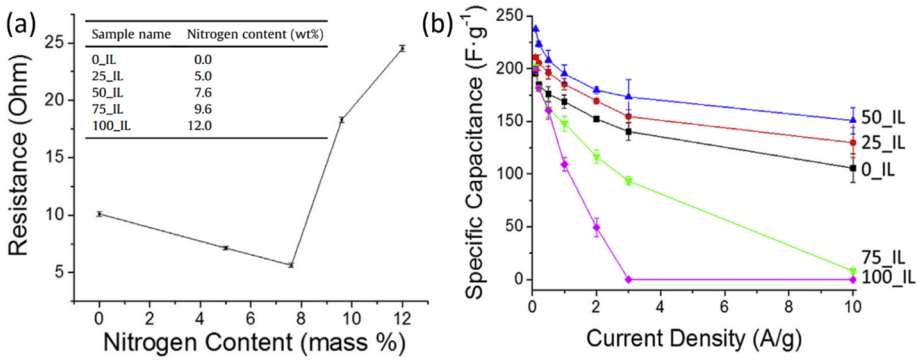

Figure 48. Porous NDCs obtained by carbonization of mixture of [C_2mim][DCA] and phenol-formaldehyde resol in the presence of silica spheres template for supercapacitors. (a) Cell resistance calculated from the Ohmic drop of each cell correlated to the nitrogen content of NDCs. Inset shows the correlations between N content of NDCs and the IL content in this precursor mixture. (b) Average specific capacitance of the carbon materials over a range of rates. Reprinted with permission from ref 442. Copyright 2015 Elsevier.

template can serve as a bifunctional metal-free catalyst for ORR and OER.[501]

6.4.2. Lithium Battery Electrodes. IL-derived NDCs have also found potential applications as electrodes for Li-ion batteries,[445,450,502,506−510] Li-sulfur batteries,[511−513] and Li−air (oxygen) batteries.[500,501,514] For example, they can be directly used as anode materials for Li-ion batteries, demonstrating an initial discharging capacity of more than 3000 mA h g^{-1} at a current density of 1 A g^{-1}, with nearly 100% capacity retention after 100 cycles. Nevertheless, less than half of the initial discharging capacity can be obtained in the following charging process.[515] The very low initial Coulombic efficiency (<50%) was attributed to their high surface areas and irreversible Li insertion in the vicinity of residual hydrogen atoms in carbonaceous materials.[516]

An alternative route to improve the initial Coulombic efficiency is to use ILs as precursors to form a NDC coating in situ on state-of-the-art anode materials for Li-ion batteries.[445,446] For example, simply mixing $Li_4Ti_5O_{12}$ and [C_2mim][DCA] with a subsequent carbonization at 600 °C created a NDC-coated porous anode, which clearly showed higher rate capability and charge/discharge capacities than the pristine $Li_4Ti_5O_{12}$ and $Li_4Ti_5O_{12}$ coated with a sugar-derived non-N-doped carbon. Undoubtedly, the improved performance originated from the significant electron transfer from the $Li_4Ti_5O_{12}$ surface to the NDC coating layer and the improved interfacial stability.[445] Using either cyano/nitrile-containing ILs or noncarbonizable ILs as precursors, the IL-based carbon coating method can be applied to a series of cathode or anode materials such as metal oxides,[414,506,517,518] $LiFePO_4$,[508] and $Li_3V_2(PO_4)_3$.[506]

The same concept can also be extended to Li−S batteries.[512] Li−S batteries are believed to be one of the most promising "beyond Li-ion" technologies because of their very high theoretical capacities (1672 mA h g^{-1}) and energy densities (2600 Wh kg^{-1} or 2800 Wh L^{-1}). However, their practical application has been dramatically hampered by the electronically insulating nature of sulfur and Li_2S as well as the serious shuttle effect in polysulfide-soluble electrolytes.[203] Using [C_2mim][DCA] as a precursor, Wang et al. successfully encapsulated insulating Li_2S with an uniform and dense NDC cage coating.[512] As illustrated in Figure 47, IL was first penetrated into an agglomerated nano-Li_2S particle and polymerized at low temperature and then carbonized at high temperature. Due to the high mobility of [C_2mim][DCA], it is easy to achieve sufficient immersion and therefore form a uniform carbon coating on Li_2S. Meanwhile, the oxygen-free nature of [C_2mim][DCA] would effectively avoid the generation of H_2O and thus avoid the side reaction between Li_2S and H_2O in the pyrolysis process. The resultant dense NDC layers on the Li_2S nanoclusters not only shortened the lithium ion diffusion distance and lowered charge transfer resistance but also entrapped the intermediate product within the carbon cage, thus preventing the shuttle effect of lithium polysulfides. As a result, compared to commercial micro-Li_2S and pure nano-Li_2S, the NDC-coated nano-Li_2S cathode displays a high utilization of active material (826 mAh g^{-1} at 0.1 C), long cycling stability (82% of capacity retention after 500 cycles at 1 C) with near 100% Coulombic efficiency.[512]

6.4.3. Supercapacitor Electrodes. Supercapacitors have attracted considerable interest in both academia and industry because of their distinct advantages such as higher power density induced by a fast charging/discharging rate and a long cycle life when compared to batteries and fuel cells.[519] Unlike simple porous carbons, whose supercapacitor performance is limited as its charge storage mechanism mainly depends on adsorption of electrolytes onto the surface, NDCs afford an additional mechanism of charge storage known as pseudocapacitance, in which the charge is stored through a rapid surface reaction.[520,521] Incorporating N atoms into the carbon lattice is also able to partially modify the hydrophobic surface of carbon materials and enhance the wettability and thus the specific capacitance.[522−524] IL-derived NDCs are therefore considered to be promising electrode materials for supercapacitors. Generally, they were obtained by direct carbonization of ILs,[471,525] templated carbonization of ILs,[453,479,485] or IL-doped carbonization.[442−444,449,451] Through direct carbonization of [C_2mim][DCA] (IL-C) with subsequent chemical activation (KOH) of the IL-C carbon, Roh et al. obtained a NDC (IL-AC) with large surface area and partial graphitic structure. Since KOH activation always deteriorates the graphitic structure, the graphitic features of IL-AC were unexpected and were ascribed to the following reasons: (i) the intrinsically high graphitic degree of IL-C contributed to the formation of graphitic features of IL-AC to some extent and (ii) the exclusion of nitrogen during activation contributes to the partial collapse of the overall structure, leading to a graphitic structure and nanopores in IL-AC. As expected, this highly nanoporous and partially graphitic IL-AC showed specific capacitance of 180, 174, and 172 F g^{-1} at current densities of 0.1, 0.2, and 1.0 mA

DOI: 10.1021/acs.chemrev.6b00504
Chem. Rev. 2017, 117, 7190−7239

cm^{-2}, respectively, much higher than that of the commercial activated carbon and IL-C.[525] In the case of electrode materials obtained by IL-doped carbonization, the IL content in the precursor mixture was found to greatly affect the resistance, structural integrity, and specific capacitance of the porous electrodes, as exemplified by mesoporous NDCs obtained by direct carbonization of [C_2mim][DCA] and phenol-formaldehyde resol in the presence of silica spheres template.[442] As shown in Figure 48, with increasing the IL content from 0 (0_IL) to 100% (100_IL), then N content monotonously increased, reaching a maximum of 12.0 wt % in 100_IL. Interestingly, the lowest resistance was observed when 50% IL was doped in the precursor mixture, while at higher nitrogen content, the resistance increases significantly (Figure 48a), which could be due to the loss of the bicontinuous structure and the smaller graphitic domains, as confirmed by nitrogen sorption isotherms and Raman spectra. Correspondingly, the specific capacitances of 50_IL are higher than all of the other carbons in the whole current density range from 0.1 to 10 A g^{-1} (Figure 48b). Its specific capacitance is 237 F g^{-1} at 0.1 A g^{-1} and over 190 F g^{-1} after 1100 cycles at 1 A g^{-1}.[442] DES-derived carbons are also promising for supercapacitors because porous carbon monoliths can easily be formed if combining DESs with traditional organic precursors such as poly(furfuryl alcohol) and resorcinol. Introducing dopants such as CNTs[428] or phosphate heteroatoms[423] have proven to improve the electrical conductivity or broaden the operational voltage window of the electrode, respectively.

7. ENDING REMARKS AND OUTLOOK

We have reviewed in this article applications of ionic liquids to energy storage and conversion materials and devices by specifically focusing on the applications as electrolyte materials for Li/Na ion batteries, Li-sulfur batteries, Li-oxygen batteries, and nonhumidified fuel cells and as carbon precursors for electrode catalysts of fuel cells and electrode materials for batteries and supercapacitors. The number of publications on those topics is greatly increasing reflecting the strong demand for a sustainable society. Due to characteristic properties such as nonvolatility, high thermal stability, and high ionic conductivity, ionic liquids appear to meet the strong demand. However, for further development, specific applications for which these characteristic properties become unique (i.e., not easily achieved by other materials) must be explored.

In the initial stage of the study on the electrolyte materials for Li ion batteries, special attention was paid to the nonvolatility and the resulting low flammability of ionic liquids, for which safety issues of the batteries would be greatly improved. However, it was immediately discovered that the performance of the batteries is frequently impaired even if the safety issues can be improved. Application of ionic liquids to electrolytes of "beyond Li ion" batteries appears to utilize unique properties of ionic liquids. For instance, in Li-sulfur batteries, the quite low coordinating properties of ionic liquids are exploited in order to suppress the dissolution of the electroactive materials into the electrolytes. For Li-oxygen batteries that are open to oxygen (air), nonvolatility of electrolytes seems to be a prerequisite for the electrolyte materials. These two examples utilize unique properties of ionic liquids, and no other materials appear to be easily adopted. The fuel cell electrolytes exploit the electrochemical activity of protic ionic liquids for fuel cell reactions as well as taking advantage of the high thermal stability. Precursors of carbon materials are conventionally natural and synthetic polymers. However, the finding that certain ionic liquids can be precursors of carbon materials opened up their unique applications. Their liquid state allows them to be easily coated and homogeneously carbonized on any surfaces. Such processing has not been possible for the conventional polymer precursors.

The importance of energy storage and conversion materials and devices will enhance even more in the future. Through strong demands for research and consideration of ILs unique properties, we will be able to identify indispensable applications for ILs.

AUTHOR INFORMATION

Corresponding Author

*E-mail: mwatanab@ynu.ac.jp.

ORCID

Masayoshi Watanabe: 0000-0003-4092-6150

Notes

The authors declare no competing financial interest.

Biographies

Masayoshi Watanabe is a Professor of Yokohama National University. He received his B.S., M.S., and Ph.D. degrees from Waseda University. After working with Prof. Royce W. Murray at Univerity of North Carolina, Chapel Hill (1988−1990), he moved to Yokohama National University in 1992 and was promoted to a full Professor in 1998. He received the Award of the Society of Polymer Science, Japan, in 2006, and the Award of The Electrochemical Society of Japan (Takei Award) and ECS Max Bredig Award in 2016. His current research interests are the materials design of ionic liquids and polymers for electrochemical applications and phase-behavior and self-assembly of polymers and colloids in ionic liquids.

Morgan L. Thomas received his Ph.D. in 2008 with Prof. Martyn Poliakoff at the University of Nottingham (U.K.). After postdoctoral/research associate experience with Prof. Walter Leitner at RWTH Aachen (Germany), Prof. Janusz Kozinski and Prof. Ian Butler at the University of Saskatchewan, York University, and McGill University (Canada), and Prof Hye-Ryung Byon at RIKEN (Japan), he joined the Watanabe's group at Yokohama National University (Japan) in 2014. His research interests are in clean chemical, material, and energy technologies, with a particular interest in solvent and electrolyte systems.

Shiguo Zhang received Ph.D. from the Lanzhou Institute of Chemical Physics, Chinese Academy of Sciences, in 2011. From 2011 to 2012, he was a research assistant in Lanzhou Institute of Chemical Physics. In April 2012, he joined Prof. Masayoshi Watanabe's group as a postdoctoral researcher at Yokohama National University. He joined the faculty as a professor at Hunan University in 2016. His current research interests are ionic liquids, carbon materials, and electrochemical energy conversion/storage. He has published more than 50 scientific papers in international journals.

Kazuhide Ueno received his Ph.D. degrees in 2009 with Prof. M. Watanabe from Yokohama National University. He was a postdoctoral fellow at Tohoku University working with Prof. K. Kurihara, at Arizona State University working with Prof. C. Austen Angell, and at Yokohama National University. In 2015, he was appointed as an assistant professor at Yamaguchi University. His research interests include ionic liquid-based soft materials and battery electrolytes.

DOI: 10.1021/acs.chemrev.6b00504
Chem. Rev. 2017, 117, 7190−7239

Tomohiro Yasuda received his Ph.D. degree in 2007 with Prof. K. Miyatake from University of Yamanashi. He was then a postdoctoral fellow at Yokohama National University working with Prof. M. Watanabe. In 2015, he was appointed as associate professor at Hokkaido University. His research interests include fuel cells, polymer electrolytes, and ionic liquids.

Kaoru Dokko is a Professor of Yokohama National University. He received Ph.D. from Tohoku University in 2001 under the supervision of Prof. Isamu Uchida. He then did his postdoctoral research at Case Western Reserve University with Prof. Daniel A. Scherson and at Tokyo Metropolitan University with Prof. Kiyoshi Kanamura and joined Yokohama National University in 2008. His current research interests are the physicochemical properties of concentrated electrolytes, nanostructured materials for energy conversion and storage, and electrochemical reaction process in electrochemical devices.

REFERENCES

(1) Tarascon, J.-M.; Armand, M. Issues and Challenges Facing Rechargeable Lithium Batteries. *Nature* **2001**, *414*, 359−367.
(2) Armand, M.; Tarascon, J.-M. Building Better Batteries. *Nature* **2008**, *451*, 652−657.
(3) Goodenough, J. B.; Kim, Y. Challenges for Rechargeable Li Batteries. *Chem. Mater.* **2010**, *22*, 587−603.
(4) Xu, K. Nonaqueous Liquid Electrolytes for Lithium-Based Rechargeable Batteries. *Chem. Rev.* **2004**, *104*, 4303−4418.
(5) Xu, K. Electrolytes and Interphases in Li-Ion Batteries and Beyond. *Chem. Rev.* **2014**, *114*, 11503−11618.
(6) Yabuuchi, N.; Kubota, K.; Dahbi, M.; Komaba, S. Research Development on Sodium-Ion Batteries. *Chem. Rev.* **2014**, *114*, 11636−11682.
(7) *Electrochemical Aspects of Ionic Liquids*; Ohno, H., Ed.; John & Wiley Sons, Inc.: Hoboken, NJ, 2005.
(8) *Electrolytes for Lithium and Lithium-Ion Batteries*; Jow, R. T., Xu, K., Borodin, O., Ue, M., Eds.; Springer: New York, 2014.
(9) Armand, M.; Endres, F.; MacFarlane, D. R.; Ohno, H.; Scrosati, B. Ionic-liquid Materials for the Electrochemical Challenges of the Future. *Nat. Mater.* **2009**, *8*, 621−629.
(10) Navarra, M. A. Ionic Liquids as Safe Electrolyte Components for Li-Metal and Li-Ion Batteries. *MRS Bull.* **2013**, *38*, 548−553.
(11) MacFarlane, D. R.; Tachikawa, N.; Forsyth, M.; Pringle, J. M.; Howlett, P. C.; Elliott, G. D.; Davis, J. H.; Watanabe, M.; Simon, P.; Angell, C. A. Energy Applications of Ionic Liquids. *Energy Environ. Sci.* **2014**, *7*, 232−250.
(12) MacFarlane, D. R.; Forsyth, M.; Howlett, P. C.; Kar, M.; Passerini, S.; Pringle, J. M.; Ohno, H.; Watanabe, M.; Yan, F.; Zheng, W.; et al. Ionic Liquids and Their Solid-State Analogues as Materials for Energy Generation and Storage. *Nat. Rev. Mater.* **2016**, *1*, 15005.
(13) Wang, Y.; Zaghib, K.; Guerfi, A.; Bazito, F. F. C.; Torresi, R. M.; Dahn, J. R. Accelerating Rate Calorimetry Studies of the Reactions Between Ionic Liquids and Charged Lithium Ion Battery Electrode Materials. *Electrochim. Acta* **2007**, *52*, 6346−6352.
(14) Sakaebe, H.; Matsumoto, H.; Tatsumi, K. Application of Room Temperature Ionic Liquids to Li Batteries. *Electrochim. Acta* **2007**, *53*, 1048−1054.
(15) Nakagawa, H.; Fujino, Y.; Kozono, S.; Katayama, Y.; Nukuda, T.; Sakaebe, H.; Matsumoto, H.; Tatsumi, K. Application of Nonflammable Electrolyte with Room Temperature Ionic Liquids (RTILs) for Lithium-Ion Cells. *J. Power Sources* **2007**, *174*, 1021−1026.
(16) Guerfi, A.; Dontigny, M.; Charest, P.; Petitclerc, M.; Lagacé, M.; Vijh, A.; Zaghib, K. Improved Electrolytes for Li-Ion Batteries: Mixtures of Ionic Liquid and Organic Electrolyte with Enhanced Safety and Electrochemical Performance. *J. Power Sources* **2010**, *195*, 845−852.
(17) Lombardo, L.; Brutti, S.; Navarra, M. A.; Panero, S.; Reale, P. Mixtures of Ionic Liquid - Alkylcarbonates as Electrolytes for Safe Lithium-Ion Batteries. *J. Power Sources* **2013**, *227*, 8−14.
(18) Carlin, R. T.; Fuller, J.; Hedenskoog, M. Reversible Lithium-Graphite Anodes in Room-Temperature Chloroaluminate Melts. *J. Electrochem. Soc.* **1994**, *141*, L21−L22.
(19) Carlin, R. T.; Delong, H. C.; Fuller, J.; Trulove, P. C. Dual Intercalating Molten Electrolyte Batteries. *J. Electrochem. Soc.* **1994**, *141*, L73−L76.
(20) Fuller, J.; Osteryoung, R. A.; Carlin, R. T. Rechargeable Lithium and Sodium Anodes in Chloroaluminate Molten-Salts Containing Thionyl Chloride. *J. Electrochem. Soc.* **1995**, *142*, 3632−3636.
(21) Carlin, R. T.; Fuller, J.; Kuhn, W. K.; Lysaght, M. J.; Trulove, P. C. Electrochemistry of Room-Temperature Chloroaluminate Molten Salts at Graphitic and Nongraphitic Electrodes. *J. Appl. Electrochem.* **1996**, *26*, 1147−1160.
(22) Fung, Y. S.; Zhou, R. Q. Room Temperature Molten Salt as Medium for Lithium Battery. *J. Power Sources* **1999**, *81*−*82*, 891−895.
(23) Koura, N.; Etoh, K.; Idemoto, Y.; Matsumoto, F. Electrochemical Behavior of Graphite-Lithium Intercalation Electrode in $AlCl_3$-EMIC-LiCl-$SOCl_2$ Room-Temperature Molten Salt. *Chem. Lett.* **2001**, *30*, 1320−1321.
(24) Campbell, A. N.; Kartzmark, E. M.; Nagarajan, M. K. The Binary (Anhydrous) Systems $NaNO_3$−$LiNO_3$, $LiClO_3$−$NaClO_3$, $LiClO_3$−$LiNO_3$, $NaNO_3$−$NaClO_3$ and the Quaternary System $NaNO_3$−$LiNO_3$−$LiClO_3$−$NaClO_3$. *Can. J. Chem.* **1962**, *40*, 1258−1265.
(25) Liu, C.; Angell, C. A. Phase equilibria, high conductivity ambient temperature liquids, and glasses in the pseudo-halide systems A1C13-MSCN (M = Li, Na, K). *Solid State Ionics* **1996**, *86*−*88*, 467−473.
(26) Tokuda, H.; Watanabe, M. Characterization and Ionic Transport Properties of Nano-Composite Electrolytes Containing a Lithium Salt of a Superweak Aluminate Anion. *Electrochim. Acta* **2003**, *48*, 2085−2091.
(27) Tokuda, H.; Tabata, S. I.; Susan, M. A. B. H.; Hayamizu, K.; Watanabe, M. Design of Polymer Electrolytes Based on a Lithium Salt of a Weakly Coordinating Anion to Realize High Ionic Conductivity with Fast Charge-Transfer Reaction. *J. Phys. Chem. B* **2004**, *108*, 11995−12002.
(28) Fujinami, T.; Buzoujima, Y. Novel Lithium Salts Exhibiting High Lithium Ion Transference Numbers in Polymer Electrolytes. *J. Power Sources* **2003**, *119*−*121*, 438−441.
(29) Tao, R.; Miyamoto, D.; Aoki, T.; Fujinami, T. Novel Liquid Lithium Borates Characterized with High Lithium Ion Transference Numbers. *J. Power Sources* **2004**, *135*, 267−272.
(30) Shobukawa, H.; Tokuda, H.; Tabata, S.; Watanabe, M. Preparation and Transport Properties of Novel Lithium Ionic Liquids. *Electrochim. Acta* **2004**, *50*, 305−309.
(31) Shobukawa, H.; Tokuda, H.; Susan, M. A. B. H.; Watanabe, M. Ion Transport Properties of Lithium Ionic Liquids and Their Ion Gels. *Electrochim. Acta* **2005**, *50*, 3872−3877.
(32) Tokuda, H.; Watanabe, M. Physicochemical Properties and Structures of Ionic Liquids and Their Utilization for Lithium Rechargeable Batteries. *Battery Technology (Committee of Battery Technology, Electrochemical Society of Japan)* **2008**, *20*, 65−71.
(33) Zech, O.; Kellermeier, M.; Thomaier, S.; Maurer, E.; Klein, R.; Schreiner, C.; Kunz, W. Alkali Metal Oligoether Carboxylates-A New Class of Ionic Liquids. *Chem. - Eur. J.* **2009**, *15*, 1341−1345.
(34) Zech, O.; Hunger, J.; Sangoro, J. R.; Iacob, C.; Kremer, F.; Kunz, W.; Buchner, R. Correlation between Polarity Parameters and Dielectric Properties of [Na][TOTO]-A Sodium Ionic Liquid. *Phys. Chem. Chem. Phys.* **2010**, *12*, 14341−14350.
(35) Padhi, A. K.; Nanjundaswamy, K. S.; Goodenough, J. B. Phospho-Olivines as Positive-Electrode Materials for Rechargeable Lithium Batteries. *J. Electrochem. Soc.* **1997**, *144*, 1188−1194.
(36) Hagiwara, R.; Tamaki, K.; Kubota, K.; Goto, T.; Nohira, T. Thermal Properties of Mixed Alkali Bis(trifluoromethylsulfonyl)-amides. *J. Chem. Eng. Data* **2008**, *53*, 355−358.
(37) Kubota, K.; Nohira, T.; Goto, T.; Hagiwara, R. Ternary Phase Diagrams of Alkali Bis(trifluoromethylsulfonyl)amides. *J. Chem. Eng. Data* **2008**, *53*, 2144−2147.
(38) Kubota, K.; Tamaki, K.; Nohira, T.; Goto, T.; Hagiwara, R. Electrochemical Properties of Alkali Bis(trifluoromethylsulfonyl)-

DOI: 10.1021/acs.chemrev.6b00504
Chem. Rev. 2017, 117, 7190−7239

amides and Their Eutectic Mixtures. *Electrochim. Acta* **2010**, *55*, 1113−1119.
(39) Watarai, A.; Kubota, K.; Yamagata, M.; Goto, T.; Nohira, T.; Hagiwara, R.; Ui, K.; Kumagai, N. A Rechargeable Lithium Metal Battery Operating at Intermediate Temperatures using Molten Alkali Bis(trifluoromethylsulfonyl)amide Mixture as an Electrolyte. *J. Power Sources* **2008**, *183*, 724−729.
(40) Kubota, K.; Nohira, T.; Hagiwara, R. Thermal Properties of Alkali Bis(fluorosulfonyl)amides and Their Binary Mixtures. *J. Chem. Eng. Data* **2010**, *55*, 3142−3146.
(41) Kubota, K.; Nohira, T.; Goto, T.; Hagiwara, R. Novel Inorganic Ionic Liquids Possessing Low Melting Temperatures and Wide Electrochemical Windows: Binary Mixtures of Alkali Bis(fluorosulfonyl)amides. *Electrochem. Commun.* **2008**, *10*, 1886−1888.
(42) Kubota, K.; Nohira, T.; Hagiwara, R. New Inorganic Ionic Liquids Possessing Low Melting Temperatures and Wide Electrochemical Windows: Ternary Mixtures of Alkali Bis(fluorosulfonyl)amides. *Electrochim. Acta* **2012**, *66*, 320−324.
(43) Fukunaga, A.; Nohira, T.; Kozawa, Y.; Hagiwara, R.; Sakai, S.; Nitta, K.; Inazawa, S. Intermediate-Temperature Ionic Liquid NaFSA-KFSA and its Application to Sodium Secondary Batteries. *J. Power Sources* **2012**, *209*, 52−56.
(44) Yamamoto, T.; Nohira, T.; Hagiwara, R.; Fukunaga, A.; Sakai, S.; Nitta, K.; Inazawa, S. Charge−Discharge Behavior of Tin Negative Electrode for a Sodium Secondary Battery using Intermediate Temperature Ionic Liquid Sodium Bis(fluorosulfonyl)amide−Potassium Bis(fluorosulfonyl)amide. *J. Power Sources* **2012**, *217*, 479−484.
(45) Komaba, S.; Takei, C.; Nakayama, T.; Ogata, A.; Yabuuchi, N. Electrochemical Intercalation Activity of Layered $NaCrO_2$ vs. $LiCrO_2$. *Electrochem. Commun.* **2010**, *12*, 355−358.
(46) Kubota, K.; Matsumoto, H. Investigation of an Intermediate Temperature Molten Lithium Salt Based on Fluorosulfonyl-(trifluoromethylsulfonyl)amide as a Solvent-Free Lithium Battery Electrolyte. *J. Phys. Chem. C* **2013**, *117*, 18829−18836.
(47) Kubota, K.; Matsumoto, H. Electrolyte Performance of LiFTA-CsFTA Molten Salt for Lithium Secondary Battery. *ECS Trans.* **2013**, *50*, 339−345.
(48) Kubota, K.; Matsumoto, H. Solvent Free Lithium Molten Salt as Electrolyte of Lithium Secondary Battery. *ECS Trans.* **2014**, *62*, 231−234.
(49) Kubota, K.; Matsumoto, H. Cation Mixtures of Alkali Metal (Fluorosulfonyl) (trifluoromethylsulfonyl)Amide as Electrolytes for Lithium Secondary Battery. *J. Electrochem. Soc.* **2014**, *161*, A902−A907.
(50) Matsumoto, H.; Yanagida, M.; Tanimoto, K.; Kojima, T.; Tamiya, Y.; Miyazaki, Y. In *Molten Salt XII: The Electrochemical Proceedings*; Trulove, P. C., De Long, H. C., Deki, S., Stafford, G. R., Eds.; The Electrochemical Society: Pennington, NJ, 2000.
(51) Matsumoto, H.; Sakaebe, H.; Tatsumi, K. Preparation of Room Temperature Ionic Liquids based on Aliphatic Onium Cations and Asymmetric Amide Anions and their Electrochemical Properties as a Lithium Battery Electrolyte. *J. Power Sources* **2005**, *146*, 45−50.
(52) MacFarlane, D. R.; Meakin, P.; Sun, J.; Amini, N.; Forsyth, M. Pyrrolidinium Imides: A New Family of Molten Salts and Conductive Plastic Crystal Phases. *J. Phys. Chem. B* **1999**, *103*, 4164−4170.
(53) Howlett, P. C.; MacFarlane, D. R.; Hollenkamp, A. F. High Lithium Metal Cycling Efficiency in a Room-Temperature Ionic Liquid. *Electrochem. Solid-State Lett.* **2004**, *7*, A97−A101.
(54) Fernicola, A.; Croce, F.; Scrosati, B.; Watanabe, T.; Ohno, H. LiTFSI-BEPyTFSI as an Improved Ionic Liquid Electrolyte for Rechargeable Lithium Batteries. *J. Power Sources* **2007**, *174*, 342−348.
(55) Sakaebe, H.; Matsumoto, H. *N*-Methyl-*N*-propylpiperidinium bis(trifluoromethanesulfonyl)imide (PP13−TFSI) − Novel Electrolyte Base for Li Battery. *Electrochem. Commun.* **2003**, *5*, 594−598.
(56) Tsunashima, K.; Sugiya, M. Physical and Electrochemical Properties of Low-Viscosity Phosphonium Ionic Liquids as Potential Electrolytes. *Electrochem. Commun.* **2007**, *9*, 2353−2358.
(57) Girard, G. M. A.; Hilder, M.; Zhu, H.; Nucciarone, D.; Whitbread, K.; Zavorine, S.; Moser, M.; Forsyth, M.; MacFarlane, D. R.; Howlett, P. C. Electrochemical and Physicochemical Properties of Small Phosphonium Cation Ionic Liquid Electrolytes with High Lithium Salt Content. *Phys. Chem. Chem. Phys.* **2015**, *17*, 8706−8713.
(58) Nakagawa, H.; Izuchi, S.; Kuwana, K.; Nukuda, T.; Aihara, Y. Liquid and Polymer Gel Electrolytes for Lithium Batteries Composed of Room-Temperature Molten Salt Doped by Lithium Salt. *J. Electrochem. Soc.* **2003**, *150*, A695−A700.
(59) Garcia, B.; Lavallee, S.; Perron, G.; Michot, C.; Armand, M. Room Temperature Molten Salts as Lithium Battery Electrolyte. *Electrochim. Acta* **2004**, *49*, 4583−4588.
(60) Koch, V. R.; Nanjundiah, C.; Battista Appetecchi, G.; Scrosati, B. The Interfacial Stability of Li with Two New Solvent-Free Ionic Liquids: 1,2-Dimethyl-3-propylimidazolium Imide and Methide. *J. Electrochem. Soc.* **1995**, *142*, L116−L118.
(61) Seki, S.; Kobayashi, Y.; Miyashiro, H.; Ohno, Y.; Usami, A.; Mita, Y.; Kihira, N.; Watanabe, M.; Terada, N. Lithium Secondary Batteries Using Modified-Imidazolium Room-Temperature Ionic Liquid. *J. Phys. Chem. B* **2006**, *110*, 10228−10230.
(62) Seki, S.; Ohno, Y.; Kobayashi, Y.; Miyashiro, H.; Usami, A.; Mita, Y.; Tokuda, H.; Watanabe, M.; Hayamizu, K.; Tsuzuki, S.; et al. Imidazolium-Based Room-Temperature Ionic Liquid for Lithium Secondary Batteries - Effects of Lithium Salt Concentration. *J. Electrochem. Soc.* **2007**, *154*, A173−A177.
(63) Seki, S.; Mita, Y.; Tokuda, H.; Ohno, Y.; Kobayashi, Y.; Usami, A.; Watanabe, M.; Terada, N.; Miyashiro, H. Effects of Alkyl Chain in Imidazolium-Type Room-Temperature Ionic Liquids as Lithium Secondary Battery Electrolytes. *Electrochem. Solid-State Lett.* **2007**, *10*, A237−A240.
(64) Tokuda, H.; Hayamizu, K.; Ishii, K.; Susan, M. A. B. H.; Watanabe, M. Physicochemical Properties and Structures of Room Temperature Ionic Liquids. 2. Variation of Alkyl Chain Length in Imidazolium Cation. *J. Phys. Chem. B* **2005**, *109*, 6103−6110.
(65) Matsumoto, H.; Sakaebe, H.; Tatsumi, K. Li/$LiCoO_2$ Cell Performance Using Ionic Liquids Composed of *N*,*N*-Diethyl-*N*-methyl-N-(2-methoxyethyl)ammonium - Effect of Anionic Structure. *ECS Trans* **2008**, *16*, 59−66.
(66) Sato, T.; Maruo, T.; Marukane, S.; Takagi, K. Ionic Liquids Containing Carbonate Solvent as Electrolytes for Lithium Ion Cells. *J. Power Sources* **2004**, *138*, 253−261.
(67) Tsuzuki, S.; Hayamizu, K.; Seki, S.; Ohno, Y.; Kobayashi, Y.; Miyashiro, H. Quaternary Ammonium Room-Temperature Ionic Liquid Including an Oxygen Atom in Side Chain/Lithium Salt Binary Electrolytes: *ab initio* Molecular Orbital Calculations of Interactions Between Ions. *J. Phys. Chem. B* **2008**, *112*, 9914−9920.
(68) Seki, S.; Kobayashi, Y.; Miyashiro, H.; Ohno, Y.; Mita, Y.; Usami, A.; Terada, N.; Watanabe, M. Reversibility of Lithium Secondary Batteries Using a Room-Temperature Ionic Liquid Mixture and Lithium Metal. *Electrochem. Solid-State Lett.* **2005**, *8*, A577−A578.
(69) Seki, S.; Kobayashi, Y.; Miyashiro, H.; Ohno, Y.; Usami, A.; Mita, Y.; Watanabe, M.; Terada, N. Highly Reversible Lithium Metal Secondary Battery Using a Room Temperature Ionic Liquid/Lithium Salt Mixture and a Surface-Coated Cathode Active Material. *Chem. Commun.* **2006**, *42*, 544−545.
(70) Seki, S.; Ohno, Y.; Miyashiro, H.; Kobayashi, Y.; Usami, A.; Mita, Y.; Terada, N.; Hayamizu, K.; Tsuzuki, S.; Watanabe, M. Quaternary Ammonium Room-Temperature Ionic Liquid/Lithium Salt Binary Electrolytes: Electrochemical Study. *J. Electrochem. Soc.* **2008**, *155*, A421−A427.
(71) Shimizu, M.; Usui, H.; Matsumoto, K.; Nokami, T.; Itoh, T.; Sakaguchi, H. Effect of Cation Structure of Ionic Liquids on Anode Properties of Si Electrodes for LIB. *J. Electrochem. Soc.* **2014**, *161*, A1765−A1771.
(72) Shimizu, M.; Usui, H.; Sakaguchi, H. Functional Ionic Liquids for Enhancement of Li-Ion Transfer: the Effect of Cation Structure on the Charge-Discharge Performance of the $Li_4Ti_5O_{12}$ Electrode. *Phys. Chem. Chem. Phys.* **2016**, *18*, 5139−5147.
(73) Ueno, K.; Tokuda, H.; Watanabe, M. Ionicity in Ionic Liquids: Correlation with Ionic Structure and Physicochemical Properties. *Phys. Chem. Chem. Phys.* **2010**, *12*, 1649−1658.

DOI: 10.1021/acs.chemrev.6b00504
Chem. Rev. 2017, 117, 7190−7239

(74) Umebayashi, Y.; Mori, S.; Fujii, K.; Tsuzuki, S.; Seki, S.; Hayamizu, K.; Ishiguro, S. Raman Spectroscopic Studies and *ab initio* Calculations on Conformational Isomerism of 1-butyl-3-methylimidazolium bis-(trifluoromethanesulfonyl)amide Solvated to a Lithium Ion in Ionic Liquids: Effects of the Second Solvation Sphere of the Lithium Ion. *J. Phys. Chem. B* **2010**, *114*, 6513−6521.
(75) Hayamizu, K. Temperature Dependence of Self-Diffusion Coefficients of Ions and Solvents in Ethylene Carbonate, Propylene Carbonate, and Diethyl Carbonate Single Solutions and Ethylene Carbonate + Diethyl Carbonate Binary Solutions of $LiPF_6$ Studied by NMR. *J. Chem. Eng. Data* **2012**, *57*, 2012−2017.
(76) Yoshida, K.; Tsuchiya, M.; Tachikawa, N.; Dokko, K.; Watanabe, M. Correlation between Battery Performance and Lithium Ion Diffusion in Glyme-Lithium Bis(trifluoromethanesulfonyl)amide Equimolar Complexes. *J. Electrochem. Soc.* **2012**, *159*, A1005−A1012.
(77) Zhou, Z. B.; Matsumoto, H.; Tatsumi, K. Low-Melting, Low-Viscous, Hydrophobic Ionic Liquids: Aliphatic Quaternary Ammonium Salts with Perfluoroalkyltrifluoroborates. *Chem. - Eur. J.* **2005**, *11*, 752−766.
(78) Zhou, Z. B.; Matsumoto, H.; Tatsumi, K. Cyclic Quaternary Ammonium Ionic Liquids with Perfluoroalkyltrifluoroborates: Synthesis, Characterization, and Properties. *Chem. - Eur. J.* **2006**, *12*, 2196−2212.
(79) Mizushima, K.; Jones, P. C.; Wiseman, P. J.; Goodenough, J. B. Li_xCoO_2 (0 < x<-1): A New Cathode Material for Batteries of High Energy Density. *Mater. Res. Bull.* **1980**, *15*, 783−789.
(80) Matsumoto, H.; Sakaebe, H.; Tatsumi, K.; Kikuta, M.; Ishiko, E.; Kono, M. Fast Cycling of $Li/LiCoO_2$ Cell with Low-Viscosity Ionic Liquids based on Bis(fluorosulfonyl)imide $[FSI]^-$. *J. Power Sources* **2006**, *160*, 1308−1313.
(81) Ishikawa, M.; Sugimoto, T.; Kikuta, M.; Ishiko, E.; Kono, M. Pure Ionic Liquid Electrolytes Compatible with a Graphitized Carbon Negative Electrode in Rechargeable Lithium-Ion Batteries. *J. Power Sources* **2006**, *162*, 658−662.
(82) Guerfi, A.; Duchesne, S.; Kobayashi, Y.; Vijh, A.; Zaghib, K. LiFePO4 and Graphite Electrodes with Ionic Liquids based on Bis(fluorosulfonyl)imide $(FSI)^-$ for Li-Ion Batteries. *J. Power Sources* **2008**, *175*, 866−873.
(83) Seki, S.; Kobayashi, Y.; Miyashiro, H.; Ohno, Y.; Mita, Y.; Terada, N.; Charest, P.; Guerfi, A.; Zaghib, K. Compatibility of *N*-Methyl-*N*-propylpyrrolidinium Cation Room-Temperature Ionic Liquid Electrolytes and Graphite Electrodes. *J. Phys. Chem. C* **2008**, *112*, 16708−16713.
(84) Saint, J.; Best, A. S.; Hollenkamp, A. F.; Kerr, J.; Shin, J.-H.; Doeff, M. M. Compatibility of $Li_xTi_yMn_{1-y}O_2$ (y = 0,0.11) Electrode Materials with Pyrrolidinium-Based Ionic Liquid Electrolyte Systems. *J. Electrochem. Soc.* **2008**, *155*, A172−A180.
(85) Sugimoto, T.; Atsumi, Y.; Kikuta, M.; Ishiko, E.; Kono, M.; Ishikawa, M. Ionic Liquid Electrolyte Systems Based on Bis-(fluorosulfonyl)imide for Lithium-Ion Batteries. *J. Power Sources* **2009**, *189*, 802−805.
(86) Balducci, A.; Jeong, S. S.; Kim, G. T.; Passerini, S.; Winter, M.; Schmuck, M.; Appetecchi, G. B.; Marcilla, R.; Mecerreyes, D.; Barsukov, V.; et al. Development of Safe, Green and High Performance Ionic Liquids-based Batteries (ILLIBATT Project). *J. Power Sources* **2011**, *196*, 9719−9730.
(87) Matsui, Y.; Kawaguchi, S.; Sugimoto, T.; Kikuta, M.; Higashizaki, T.; Kono, M.; Yamagata, M.; Ishikawa, M. Charge-Discharge Characteristics of a $LiNi_{1/3}Mn_{1/3}Co_{1/3}O_2$ Cathode in FSI-based Ionic Liquids. *Electrochemistry* **2012**, *80*, 808−811.
(88) Yoon, H.; Howlett, P. C.; Best, A. S.; Forsyth, M.; MacFarlane, D. R. Fast Charge/Discharge of Li Metal Batteries Using an Ionic Liquid Electrolyte. *J. Electrochem. Soc.* **2013**, *160*, A1629−A1637.
(89) Matsui, Y.; Yamagata, M.; Murakami, S.; Saito, Y.; Higashizaki, T.; Ishiko, E.; Kono, M.; Ishikawa, M. Design of an Electrolyte Composition for Stable and Rapid Charging−Discharging of a Graphite Negative Electrode in a Bis(fluorosulfonyl)imide-based Ionic Liquid. *J. Power Sources* **2015**, *279*, 766−773.
(90) Ishihara, Y.; Miyazaki, K.; Fukutsuka, T.; Abe, T. Lithium-Ion Transfer at the Interface between High Potential Negative Electrodes and Ionic Liquids. *J. Electrochem. Soc.* **2014**, *161*, A1939−A1942.
(91) Sagane, F.; Abe, T.; Ogumi, Z. Electrochemical Analysis of Lithium-Ion Transfer Reaction through the Interface between Ceramic Electrolyte and Ionic Liquids. *J. Electrochem. Soc.* **2012**, *159*, A1766−A1769.
(92) Zheng, H.; Zhang, H.; Fu, Y.; Abe, T.; Ogumi, Z. Temperature Effects on the Electrochemical Behavior of Spinel $LiMn_2O_4$ in Quaternary Ammonium-Based Ionic Liquid Electrolyte. *J. Phys. Chem. B* **2005**, *109*, 13676−13684.
(93) Zheng, H.; Qin, J.; Zhao, Y.; Abe, T.; Ogumi, Z. Temperature Dependence of the Electrochemical Behavior of LiCoO in Quaternary Ammonium-Based Ionic Liquid Electrolyte. *Solid State Ionics* **2005**, *176*, 2219−2226.
(94) Dahn, J. R. Phase Diagram of Li_xC_6. *Phys. Rev. B: Condens. Matter Mater. Phys.* **1991**, *44*, 9170−9177.
(95) Holzapfel, M.; Jost, C.; Novák, P. Stable Cycling of Graphite in an Ionic Liquid based Electrolyte. *Chem. Commun.* **2004**, *40*, 2098−2099.
(96) Zheng, H.; Jiang, K.; Abe, T.; Ogumi, Z. Electrochemical Intercalation of Lithium into a Natural Graphite Anode in Quaternary Ammonium-Based Ionic Liquid Electrolytes. *Carbon* **2006**, *44*, 203−210.
(97) Balducci, A.; Schmuck, M.; Kern, W.; Rupp, B.; Passerini, S.; Winter, M. Ionic Liquids as Electrolyte in Lithium Batteries: In Situ FTIRs Studies on the Use of Electrolyte Additives. *ECS Trans* **2007**, *11*, 109−114.
(98) Yamagata, M.; Nishigaki, N.; Nishishita, S.; Matsui, Y.; Sugimoto, T.; Kikuta, M.; Higashizaki, T.; Kono, M.; Ishikawa, M. Charge−Discharge Behavior of Graphite Negative Electrodes in Bis(fluorosulfonyl)imide-Based Ionic Liquid and Structural Aspects of Their Electrode/Electrolyte Interfaces. *Electrochim. Acta* **2013**, *110*, 181−190.
(99) Yamagata, M.; Tanaka, K.; Tsuruda, Y.; Sone, Y.; Fukuda, S.; Nakasuka, S.; Kono, M.; Ishikawa, M. The First Lithium-ion Battery with Ionic Liquid Electrolyte Demonstrated in Extreme Environment of Space. *Electrochemistry* **2015**, *83*, 918−924.
(100) Ding, C.; Nohira, T.; Hagiwara, R.; Matsumoto, K.; Okamoto, Y.; Fukunaga, A.; Sakai, S.; Nitta, K.; Inazawa, S. Na[FSA]-$[C_3C_1pyrr][FSA]$ Ionic Liquids as Electrolytes for Sodium Secondary Batteries: Effects of Na Ion Concentration and Operation Temperature. *J. Power Sources* **2014**, *269*, 124−128.
(101) Ding, C. S.; Nohira, T.; Kuroda, K.; Hagiwara, R.; Fukunaga, A.; Sakai, S.; Nitta, K.; Inazawa, S. NaFSA-C_1C_3pyrFSA Ionic Liquids for Sodium Secondary Battery Operating Over a Wide Temperature Range. *J. Power Sources* **2013**, *238*, 296−300.
(102) Fukunaga, A.; Nohira, T.; Hagiwara, R.; Numata, K.; Itani, E.; Sakai, S.; Nitta, K.; Inazawa, S. A Safe and High-Rate Negative Electrode for Sodium-Ion Batteries: Hard Carbon in NaFSA-C_1C_3pyrFSA Ionic Liquid at 363 K. *J. Power Sources* **2014**, *246*, 387−391.
(103) Matsumoto, K.; Hosokawa, T.; Nohira, T.; Hagiwara, R.; Fukunaga, A.; Numata, K.; Itani, E.; Sakai, S.; Nitta, K.; Inazawa, S. The Na[FSA]−$[C_2C_1im][FSA]$ ($C_2C_1im^+$:1-ethyl-3-methylimidazolium and FSA^-:bis(fluorosulfonyl)amide) Ionic Liquid Electrolytes for Sodium Secondary Batteries. *J. Power Sources* **2014**, *265*, 36−39.
(104) Chen, C.-Y.; Matsumoto, K.; Nohira, T.; Ding, C.; Yamamoto, T.; Hagiwara, R. Charge−Discharge Behavior of a $Na_2FeP_2O_7$ Positive Electrode in an Ionic Liquid Electrolyte between 253 and 363K. *Electrochim. Acta* **2014**, *133*, 583−588.
(105) Ding, C.; Nohira, T.; Hagiwara, R.; Fukunaga, A.; Sakai, S.; Nitta, K. Electrochemical Performance of Hard Carbon Negative Electrodes for Ionic Liquid-Based Sodium Ion Batteries Over a Wide Temperature Range. *Electrochim. Acta* **2015**, *176*, 344−349.
(106) Monti, D.; Jónsson, E.; Palacín, M. R.; Johansson, P. Ionic Liquid Based Electrolytes for Sodium-Ion Batteries: Na^+ Solvation and Ionic Conductivity. *J. Power Sources* **2014**, *245*, 630−636.

DOI: 10.1021/acs.chemrev.6b00504
Chem. Rev. 2017, 117, 7190−7239

(107) Chagas, L. G.; Buchholz, D.; Wu, L.; Vortmann, B.; Passerini, S. Unexpected Performance of Layered Sodium-Ion Cathode Material in Ionic Liquid-Based Electrolyte. *J. Power Sources* **2014**, *247*, 377−383.
(108) Yoon, H.; Zhu, H.; Hervault, A.; Armand, M.; MacFarlane, D. R.; Forsyth, M. Physicochemical Properties of *N*-propyl-*N*-methylpyrrolidinium Bis(fluorosulfonyl)imide for Sodium Metal Battery Applications. *Phys. Chem. Chem. Phys.* **2014**, *16*, 12350−12355.
(109) Forsyth, M.; Yoon, H.; Chen, F.; Zhu, H.; MacFarlane, D. R.; Armand, M.; Howlett, P. C. Novel Na+Ion Diffusion Mechanism in Mixed Organic−Inorganic Ionic Liquid Electrolyte Leading to High Na+Transference Number and Stable, High Rate Electrochemical Cycling of Sodium Cells. *J. Phys. Chem. C* **2016**, *120*, 4276−4286.
(110) Wongittharom, N.; Wang, C.-H.; Wang, Y.-C.; Yang, C.-H.; Chang, J.-K. Ionic Liquid Electrolytes with Various Sodium Solutes for Rechargeable Na/NaFePO4 Batteries Operated at Elevated Temperatures. *ACS Appl. Mater. Interfaces* **2014**, *6*, 17564−17570.
(111) Wang, C.-H.; Yeh, Y.-W.; Wongittharom, N.; Wang, Y.-C.; Tseng, C.-J.; Lee, S.-W.; Chang, W.-S.; Chang, J.-K. Rechargeable Na/$Na_{0.44}MnO_2$ Cells with Ionic Liquid Electrolytes Containing Various Sodium Solutes. *J. Power Sources* **2015**, *274*, 1016−1023.
(112) Hasa, I.; Passerini, S.; Hassoun, J. Characteristics of an Ionic Liquid Electrolyte for Sodium-Ion Batteries. *J. Power Sources* **2016**, *303*, 203−207.
(113) Matsumoto, K.; Okamoto, Y.; Nohira, T.; Hagiwara, R. Thermal and Transport Properties of $Na[N(SO_2F)_2]$−[*N*-Methyl-*N*-propylpyrrolidinium][$N(SO_2F)_2$] Ionic Liquids for Na Secondary Batteries. *J. Phys. Chem. C* **2015**, *119*, 7648−7655.
(114) Hosokawa, T.; Matsumoto, K.; Nohira, T.; Hagiwara, R.; Fukunaga, A.; Sakai, S.; Nitta, K. Stability of Ionic Liquids Against Sodium Metal: A Comparative Study of 1-Ethyl-3-methylimidazolium Ionic Liquids with Bis(fluorosulfonyl)amide and Bis(trifluoromethylsulfonyl)amide. *J. Phys. Chem. C* **2016**, *120*, 9628−9636.
(115) MacFarlane, D. R.; Huang, J.; Forsyth, M. Lithium-Doped Plastic Crystal Electrolytes Exhibiting Fast Ion Conduction for Secondary Batteries. *Nature* **1999**, *402*, 792−794.
(116) MacFarlane, D. R.; Forsyth, M. Plastic Crystal Electrolyte Materials: New Perspectives on Solid State Ionics. *Adv. Mater.* **2001**, *13*, 957−966.
(117) Pringle, J. M.; Howlett, P. C.; MacFarlane, D. R.; Forsyth, M. Organic Ionic Plastic Crystals: Recent Advances. *J. Mater. Chem.* **2010**, *20*, 2056−2062.
(118) Alarco, P.-J.; Abu-Lebdeh, Y.; Ravet, N.; Armand, M. Lithium Conducting Pyrazolium Imides Plastic Crystals: a New Solid State Electrolyte Matrix. *Solid State Ionics* **2004**, *172*, 53−56.
(119) Zhou, Z.-B.; Matsumoto, H. Lithium-Doped, Organic Ionic Plastic Crystal Electrolytes Exhibiting High Ambient-Temperature Conductivities. *Electrochem. Commun.* **2007**, *9*, 1017−1022.
(120) Henderson, W. A.; Seo, D. M.; Zhou, Q.; Boyle, P. D.; Shin, J.-H.; De Long, H. C.; Trulove, P. C.; Passerini, S. An Alternative Ionic Conductivity Mechanism for Plastic Crystalline Salt-Lithium Salt Electrolyte Mixtures. *Adv. Energy Mater.* **2012**, *2*, 1343−1350.
(121) Romanenko, K.; Jin, L.; Howlett, P.; Forsyth, M. In Situ MRI of Operating Solid-State Lithium Metal Cells Based on Ionic Plastic Crystal Electrolytes. *Chem. Mater.* **2016**, *28*, 2844−2851.
(122) Abu-Lebdeh, Y.; Abouimrane, A.; Alarco, P.-J.; Armand, M. Ionic Liquid and Plastic Crystalline Phases of Pyrazolium Imide Salts as Electrolytes for Rechargeable Lithium-Ion Batteries. *J. Power Sources* **2006**, *154*, 255−261.
(123) Armel, V.; Velayutham, D.; Sun, J.; Howlett, P. C.; Forsyth, M.; MacFarlane, D. R.; Pringle, J. M. Ionic Liquids and Organic Ionic Plastic Crystals Utilizing Small Phosphonium Cations. *J. Mater. Chem.* **2011**, *21*, 7640−7650.
(124) Sunarso, J.; Shekibi, Y.; Efthimiadis, J.; Jin, L.; Pringle, J. M.; Hollenkamp, A. F.; MacFarlane, D. R.; Forsyth, M.; Howlett, P. C. Optimising Organic Ionic Plastic Crystal Electrolyte for All Solid-State and Higher than Ambient Temperature Lithium Batteries. *J. Solid State Electrochem.* **2012**, *16*, 1841−1848.
(125) Jin, L. Y.; Howlett, P. C.; Pringle, J. M.; Janikowski, J.; Armand, M.; MacFarlane, D. R.; Forsyth, M. An Organic Ionic Plastic Crystal Electrolyte for Rate Capability and Stability of Ambient Temperature Lithium Batteries. *Energy Environ. Sci.* **2014**, *7*, 3352−3361.
(126) Brouillette, D.; Irish, D. E.; Taylor, N. J.; Perron, G.; Odziemkowski, M.; Desnoyers, J. E. Stable Solvates in Solution of Lithium Bis(trifluoromethylsulfone)imide in Glymes and Other Aprotic Solvents: Phase Diagrams, Crystallography and Raman Spectroscopy. *Phys. Chem. Chem. Phys.* **2002**, *4*, 6063−6071.
(127) Henderson, W. A. Glyme-Lithium Salt Phase Behavior. *J. Phys. Chem. B* **2006**, *110*, 13177−13183.
(128) Pappenfus, T. M.; Henderson, W. A.; Owens, B. B.; Mann, K. R.; Smyrl, W. H. Complexes of Lithium Imide Salts with Tetraglyme and Their Polyelectrolyte Composite Materials. *J. Electrochem. Soc.* **2004**, *151*, A209−A215.
(129) Tamura, T.; Yoshida, K.; Hachida, T.; Tsuchiya, M.; Nakamura, M.; Kazue, Y.; Tachikawa, N.; Dokko, K.; Watanabe, M. Physicochemical Properties of Glyme−Li Salt Complexes as a New Family of Room-Temperature Ionic Liquids. *Chem. Lett.* **2010**, *39*, 753−755.
(130) Yoshida, K.; Nakamura, M.; Kazue, Y.; Tachikawa, N.; Tsuzuki, S.; Seki, S.; Dokko, K.; Watanabe, M. Oxidative-Stability Enhancement and Charge Transport Mechanism in Glyme-Lithium Salt Equimolar Complexes. *J. Am. Chem. Soc.* **2011**, *133*, 13121−13129.
(131) Ueno, K.; Yoshida, K.; Tsuchiya, M.; Tachikawa, N.; Dokko, K.; Watanabe, M. Glyme-Lithium Salt Equimolar Molten Mixtures: Concentrated Solutions or Solvate Ionic Liquids? *J. Phys. Chem. B* **2012**, *116*, 11323−11331.
(132) Ueno, K.; Tatara, R.; Tsuzuki, S.; Saito, S.; Doi, H.; Yoshida, K.; Mandai, T.; Matsugami, M.; Umebayashi, Y.; Dokko, K.; et al. Li^+ Solvation in Glyme-Li Salt Solvate Ionic Liquids. *Phys. Chem. Chem. Phys.* **2015**, *17*, 8248−8257.
(133) Zhang, C.; Ueno, K.; Yamazaki, A.; Yoshida, K.; Moon, H.; Mandai, T.; Umebayashi, Y.; Dokko, K.; Watanabe, M. Chelate Effects in Glyme/Lithium Bis(trifluoromethanesulfonyl)amide Solvate Ionic Liquids, Part 1: Stability of Solvate Cations and Correlation with Electrolyte Properties. *J. Phys. Chem. B* **2014**, *118*, 5144−5153.
(134) Mandai, T.; Yoshida, K.; Ueno, K.; Dokko, K.; Watanabe, M. Criteria for Solvate Ionic Liquids. *Phys. Chem. Chem. Phys.* **2014**, *16*, 8761−8772.
(135) Angell, C. A. Electrical Conductance of Concentrated Aqueous Solutions and Molten Salts: Correlation through Free Volume Transport Model. *J. Phys. Chem.* **1965**, *69*, 2137.
(136) Angell, C. A. A New Class of Molten Salt Mixtures The Hydrated Dipositive Ion as an Independent Cation Species. *J. Electrochem. Soc.* **1965**, *112*, 1224−1227.
(137) Angell, C. A.; Ansari, Y.; Zhao, Z. Ionic Liquids: Past, Present and Future. *Faraday Discuss.* **2012**, *154*, 9−27.
(138) Moon, H.; Tatara, R.; Mandai, T.; Ueno, K.; Yoshida, K.; Tachikawa, N.; Yasuda, T.; Dokko, K.; Watanabe, M. Mechanism of Li Ion Desolvation at the Interface of Graphite Electrode and Glyme−Li Salt Solvate Ionic Liquids. *J. Phys. Chem. C* **2014**, *118*, 20246−20256.
(139) Seki, S.; Takei, K.; Miyashiro, H.; Watanabe, M. Physicochemical and Electrochemical Properties of Glyme-LiN$(SO_2F)_2$ Complex for Safe Lithium-ion Secondary Battery Electrolyte. *J. Electrochem. Soc.* **2011**, *158*, A769−A774.
(140) Mandai, T.; Nozawa, R.; Tsuzuki, S.; Yoshida, K.; Ueno, K.; Dokko, K.; Watanabe, M. Phase Diagrams and Solvate Structures of Binary Mixtures of Glymes and Na Salts. *J. Phys. Chem. B* **2013**, *117*, 15072−15085.
(141) Mandai, T.; Yoshida, K.; Tsuzuki, S.; Nozawa, R.; Masu, H.; Ueno, K.; Dokko, K.; Watanabe, M. Effect of Ionic Size on Solvate Stability of Glyme-based Solvate Ionic Liquids. *J. Phys. Chem. B* **2015**, *119*, 1523−1534.
(142) Terada, S.; Mandai, T.; Nozawa, R.; Yoshida, K.; Ueno, K.; Tsuzuki, S.; Dokko, K.; Watanabe, M. Physicochemical Properties of Pentaglyme-Sodium Bis(trifluoromethanesulfonyl)amide Solvate Ionic Liquid. *Phys. Chem. Chem. Phys.* **2014**, *16*, 11737−11746.

DOI: 10.1021/acs.chemrev.6b00504
Chem. Rev. 2017, 117, 7190−7239

(143) Ueno, K.; Murai, J.; Ikeda, K.; Tsuzuki, S.; Tsuchiya, M.; Tatara, R.; Mandai, T.; Umebayashi, Y.; Dokko, K.; Watanabe, M. Li^+ Solvation and Ionic Transport in Lithium Solvate Ionic Liquids Diluted by Molecular Solvents. *J. Phys. Chem. C* **2016**, *120*, 15792−15802.
(144) Saito, S.; Watanabe, H.; Ueno, K.; Mandai, T.; Seki, S.; Tsuzuki, S.; Kameda, Y.; Dokko, K.; Watanabe, M.; Umebayashi, Y. Li(+) Local Structure in Hydrofluoroether Diluted Li-Glyme Solvate Ionic Liquid. *J. Phys. Chem. B* **2016**, *120*, 3378−3387.
(145) Achiha, T.; Nakajima, T.; Ohzawa, Y.; Koh, M.; Yamauchi, A.; Kagawa, M.; Aoyama, H. Thermal Stability and Electrochemical Properties of Fluorine Compounds as Nonflammable Solvents for Lithium-Ion Batteries. *J. Electrochem. Soc.* **2010**, *157*, A707−A712.
(146) Moon, H.; Mandai, T.; Tatara, R.; Ueno, K.; Yamazaki, A.; Yoshida, K.; Seki, S.; Dokko, K.; Watanabe, M. Solvent Activity in Electrolyte Solutions Controls Electrochemical Reactions in Li-Ion and Li-Sulfur Batteries. *J. Phys. Chem. C* **2015**, *119*, 3957−3970.
(147) Jeong, S.-K.; Inaba, M.; Iriyama, Y.; Abe, T.; Ogumi, Z. Electrochemical Intercalation of Lithium Ion within Graphite from Propylene Carbonate Solutions. *Electrochem. Solid-State Lett.* **2003**, *6*, A13−A15.
(148) Jeong, S.-K.; Inaba, M.; Iriyama, Y.; Abe, T.; Ogumi, Z. Interfacial Reactions Between Graphite Electrodes and Propylene Carbonate-based Solutions: Electrolyte-Concentration Dependence of Electrochemical Lithium Intercalation Reaction. *J. Power Sources* **2008**, *175*, 540−546.
(149) Nie, M.; Abraham, D. P.; Seo, D. M.; Chen, Y.; Bose, A.; Lucht, B. L. Role of Solution Structure in Solid Electrolyte Interphase Formation on Graphite with $LiPF_6$ in Propylene Carbonate. *J. Phys. Chem. C* **2013**, *117*, 25381−25389.
(150) Yamada, Y.; Takazawa, Y.; Miyazaki, K.; Abe, T. Electrochemical Lithium Intercalation into Graphite in Dimethyl Sulfoxide-Based Electrolytes: Effect of Solvation Structure of Lithium Ion. *J. Phys. Chem. C* **2010**, *114*, 11680−11685.
(151) Yamada, Y.; Yaegashi, M.; Abe, T.; Yamada, A. A Superconcentrated Ether Electrolyte for Fast-Charging Li-ion Batteries. *Chem. Commun.* **2013**, *49*, 11194−11196.
(152) Yamada, Y.; Furukawa, K.; Sodeyama, K.; Kikuchi, K.; Yaegashi, M.; Tateyama, Y.; Yamada, A. Unusual Stability of Acetonitrile-Based Superconcentrated Electrolytes for Fast-Charging Lithium-Ion Batteries. *J. Am. Chem. Soc.* **2014**, *136*, 5039−5046.
(153) Yamada, Y.; Usui, K.; Chiang, C. H.; Kikuchi, K.; Furukawa, K.; Yamada, A. General Observation of Lithium Intercalation into Graphite in Ethylene-Carbonate-free Superconcentrated Electrolytes. *ACS Appl. Mater. Interfaces* **2014**, *6*, 10892−10899.
(154) Petibon, R.; Aiken, C. P.; Ma, L.; Xiong, D.; Dahn, J. R. The Use of Ethyl Acetate as a Sole Solvent in Highly Concentrated Electrolyte for Li-Ion Batteries. *Electrochim. Acta* **2015**, *154*, 287−293.
(155) Suo, L.; Hu, Y. S.; Li, H.; Armand, M.; Chen, L. A New Class of Solvent-in-Salt Electrolyte for High-Energy Rechargeable Metallic Lithium Batteries. *Nat. Commun.* **2013**, *4*, 1481.
(156) Qian, J.; Henderson, W. A.; Xu, W.; Bhattacharya, P.; Engelhard, M.; Borodin, O.; Zhang, J. G. High Rate and Stable Cycling of Lithium Metal Anode. *Nat. Commun.* **2015**, *6*, 6362.
(157) McOwen, D. W.; Seo, D. M.; Borodin, O.; Vatamanu, J.; Boyle, P. D.; Henderson, W. A. Concentrated Electrolytes: Decrypting Electrolyte Properties and Reassessing Al Corrosion Mechanisms. *Energy Environ. Sci.* **2014**, *7*, 416−426.
(158) Zhang, C.; Yamazaki, A.; Murai, J.; Park, J.-W.; Mandai, T.; Ueno, K.; Dokko, K.; Watanabe, M. Chelate Effects in Glyme/Lithium Bis(trifluoromethanesulfonyl)amide Solvate Ionic Liquids, Part 2: Importance of Solvate-Structure Stability for Electrolytes of Lithium Batteries. *J. Phys. Chem. C* **2014**, *118*, 17362−17373.
(159) Yamada, Y.; Chiang, C. H.; Sodeyama, K.; Wang, J.; Tateyama, Y.; Yamada, A. Corrosion Prevention Mechanism of Aluminum Metal in Superconcentrated Electrolytes. *ChemElectroChem* **2015**, *2*, 1687−1694.
(160) Wang, J.; Yamada, Y.; Sodeyama, K.; Chiang, C. H.; Tateyama, Y.; Yamada, A. Superconcentrated Electrolytes for a High-Voltage Lithium-Ion Battery. *Nat. Commun.* **2016**, *7*, 12032.
(161) Doi, T.; Masuhara, R.; Hashinokuchi, M.; Shimizu, Y.; Inaba, M. Concentrated $LiPF_6$/PC Electrolyte Solutions for 5-V Li-$Ni_{0.5}Mn_{1.5}O_4$ Positive Electrode in Lithium-Ion Batteries. *Electrochim. Acta* **2016**, *209*, 219−224.
(162) Yamada, Y.; Yamada, A. Review—Superconcentrated Electrolytes for Lithium Batteries. *J. Electrochem. Soc.* **2015**, *162*, A2406−A2423.
(163) Suo, L.; Borodin, O.; Gao, T.; Olguin, M.; Ho, J.; Fan, X.; Luo, C.; Wang, C.; Xu, K. "Water-in-Salt" Electrolyte Enables High-Voltage Aqueous Lithium-Ion Chemistries. *Science* **2015**, *350*, 938−943.
(164) Suo, L.; Han, F.; Fan, X.; Liu, H.; Xu, K.; Wang, C. Water-in-Salt" Electrolytes Enable Green and Safe Li-Ion Batteries for Large Scale Electric Energy Storage Applications. *J. Mater. Chem. A* **2016**, *4*, 6639−6644.
(165) Suo, L.; Borodin, O.; Sun, W.; Fan, X.; Yang, C.; Wang, F.; Gao, T.; Ma, Z.; Schroeder, M.; von Cresce, A.; et al. Advanced High-Voltage Aqueous Lithium-Ion Battery Enabled by "Water-in-Bisalt" Electrolyte. *Angew. Chem., Int. Ed.* **2016**, *55*, 7136−7141.
(166) Miyazaki, K.; Shimada, T.; Ito, S.; Yokoyama, Y.; Fukutsuka, T.; Abe, T. Enhanced Resistance to Oxidative Decomposition of Aqueous Electrolytes for Aqueous Lithium-Ion Batteries. *Chem. Commun.* **2016**, *52*, 4979−4982.
(167) Yamada, Y.; Usui, K.; Sodeyama, K.; Ko, S.; Tateyama, Y.; Yamada, A. Hydrate-Melt Electrolytes for High-Energy-Density Aqueous Batteries. *Nature Energy* **2016**, *1*, 16129.
(168) Angell, C. A.; Liu, C.; Sanchez, E. Rubbery Solid Electrolytes with Dominant Cationic Transport and High Ambient Conductivity. *Nature* **1993**, *362*, 137−139.
(169) Watanabe, M.; Yamada, S.; Sanui, K.; Ogata, N. High Ionic-Conductivity of New Polymer Electrolytes Consisting of Polypyridinium, Pyridinium and Aluminum-Chloride. *J. Chem. Soc., Chem. Commun.* **1993**, *29*, 929−931.
(170) Fuller, J.; Breda, A. C.; Carlin, R. T. Ionic Liquid−Polymer Gel Electrolytes from Hydrophilic and Hydrophobic Ionic Liquids. *J. Electroanal. Chem.* **1998**, *459*, 29−34.
(171) Susan, M. A. B. H.; Kaneko, T.; Noda, A.; Watanabe, M. Ion Gels Prepared by In Situ Radical Polymerization of Vinyl Monomers in an Ionic Liquid and Their Characterization as Polymer Electrolytes. *J. Am. Chem. Soc.* **2005**, *127*, 4976−4983.
(172) Armand, M. Polymer Solid Electrolytes - an Overview. *Solid State Ionics* **1983**, *9−10*, 745−754.
(173) Shin, J.-H.; Henderson, W. A.; Passerini, S. Ionic Liquids to the Rescue? Overcoming the Ionic Conductivity Limitations of Polymer Electrolytes. *Electrochem. Commun.* **2003**, *5*, 1016−1020.
(174) Shin, J.-H.; Henderson, W. A.; Passerini, S. An Elegant Fix for Polymer Electrolytes. *Electrochem. Solid-State Lett.* **2005**, *8*, A125−A127.
(175) Shin, J.-H.; Henderson, W. A.; Passerini, S. PEO-based Polymer Electrolytes with Ionic Liquids and Their Use in Lithium Metal-Polymer Electrolyte Batteries. *J. Electrochem. Soc.* **2005**, *152*, A978−A983.
(176) Shin, J.-H.; Henderson, W. A.; Tizzani, C.; Passerini, S.; Jeong, S.-S.; Kim, K.-W. Characterization of Solvent-Free Polymer Electrolytes Consisting of Ternary PEO−LiTFSI−PYR_{14}TFSI. *J. Electrochem. Soc.* **2006**, *153*, A1649.
(177) Shin, J.-H.; Henderson, W. A.; Appetecchi, G. B.; Alessandrini, F.; Passerini, S. Recent Developments in the ENEA Lithium Metal Battery Project. *Electrochim. Acta* **2005**, *50*, 3859−3865.
(178) Shin, J.-H.; Henderson, W. A.; Scaccia, S.; Prosini, P. P.; Passerini, S. Solid-State Li/$LiFePO_4$ Polymer Electrolyte Batteries Incorporating an Ionic Liquid Cycled at 40 °C. *J. Power Sources* **2006**, *156*, 560−566.
(179) Sivakkumar, S. R.; MacFarlane, D. R.; Forsyth, M.; Kim, D.-W. Ionic Liquid-Based Rechargeable Lithium Metal-Polymer Cells Assembled with Polyaniline/Carbon Nanotube Composite Cathode. *J. Electrochem. Soc.* **2007**, *154*, A834−A838.

DOI: 10.1021/acs.chemrev.6b00504
Chem. Rev. 2017, 117, 7190−7239

(180) Kim, K.-S.; Park, S.-Y.; Choi, S.; Lee, H. Ionic Liquid−Polymer Gel Electrolytes based on Morpholinium Salt and PVdF(HFP) copolymer. *J. Power Sources* **2006**, *155*, 385−390.
(181) Ye, H.; Huang, J.; Xu, J. J.; Khalfan, A.; Greenbaum, S. G. Li Ion Conducting Polymer Gel Electrolytes Based on Ionic Liquid/PVDF-HFP Blends. *J. Electrochem. Soc.* **2007**, *154*, A1048−A1057.
(182) Kim, J.-K.; Manuel, J.; Chauhan, G. S.; Ahn, J.-H.; Ryu, H.-S. Ionic Liquid-based Gel Polymer Electrolyte for $LiMn_{0.4}Fe_{0.6}PO_4$ Cathode Prepared by Electrospinning Technique. *Electrochim. Acta* **2010**, *55*, 1366−1372.
(183) Sirisopanaporn, C.; Fernicola, A.; Scrosati, B. New, Ionic Liquid-Based Membranes for Lithium Battery Application. *J. Power Sources* **2009**, *186*, 490−495.
(184) Navarra, M. A.; Manzi, J.; Lombardo, L.; Panero, S.; Scrosati, B. Ionic Liquid-Based Membranes as Electrolytes for Advanced Lithium Polymer Batteries. *ChemSusChem* **2011**, *4*, 125−130.
(185) Appetecchi, G. B.; Kim, G. T.; Montanino, M.; Alessandrini, F.; Passerini, S. Room Temperature Lithium Polymer Batteries Based on Ionic Liquids. *J. Power Sources* **2011**, *196*, 6703−6709.
(186) Tsurumaki, A.; Navarra, M. A.; Panero, S.; Scrosati, B.; Ohno, H. *N*-n-Butyl-*N*-Methylpyrrolidinium Hexafluorophosphate-Added Electrolyte Solutions and Membranes for Lithium-Secondary Batteries. *J. Power Sources* **2013**, *233*, 104−109.
(187) Abraham, K. M.; Jiang, Z.; Carroll, B. Highly Conductive PEO-like Polymer Electrolytes. *Chem. Mater.* **1997**, *9*, 1978−1988.
(188) Kitazawa, Y.; Iwata, K.; Imaizumi, S.; Ahn, H.; Kim, S. Y.; Ueno, K.; Park, M. J.; Watanabe, M. Gelation of Solvate Ionic Liquid by Self-Assembly of Block Copolymer and Characterization as Polymer Electrolyte. *Macromolecules* **2014**, *47*, 6009−6016.
(189) Borghini, M. C.; Mastroagostino, M.; Passerrini, S.; Scrosati, B. Electrochemical Properties of Polyethylene Oxide-$Li[(CF_3SO_2)_2N]$-Gamma-$LiAlO_2$ Composite Polymer Electrolytes. *J. Electrochem. Soc.* **1995**, *142*, 2118.
(190) Appetecchi, G. B.; Dautzenberg, G.; Scrosati, B. A New Class of Advanced Polymer Electrolytes and Their Relevance in Plastic-like, Rechargeable Lithium Batteries. *J. Electrochem. Soc.* **1996**, *143*, 6−12.
(191) Bruce, P. G.; Freunberger, S. A.; Hardwick, L. J.; Tarascon, J.-M. Li-O_2 and Li-S Batteries with High Energy Storage. *Nat. Mater.* **2011**, *11*, 19−29.
(192) Evers, S.; Nazar, L. F. New Approaches for High Energy Density Lithium−Sulfur Battery Cathodes. *Acc. Chem. Res.* **2013**, *46*, 1135−1143.
(193) Wild, M.; O'Neill, L.; Zhang, T.; Purkayastha, R.; Minton, G.; Marinescu, M.; Offer, G. J. Lithium Sulfur Batteries, a Mechanistic Review. *Energy Environ. Sci.* **2015**, *8*, 3477−3494.
(194) Herbert, D.; Ulam, J. Electric Dry Cells and Storage Batteries. U.S. Patent 3,043,896, 1962.
(195) Manthiram, A.; Fu, Y.; Chung, S.-H.; Zu, C.; Su, Y.-S. Rechargeable Lithium−Sulfur Batteries. *Chem. Rev.* **2014**, *114*, 11751−11787.
(196) Yin, Y.-X.; Xin, S.; Guo, Y.-G.; Wan, L.-J. Lithium−Sulfur Batteries: Electrochemistry, Materials, and Prospects. *Angew. Chem., Int. Ed.* **2013**, *52*, 13186−13200.
(197) Chen, R.; Zhao, T.; Wu, F. From a Historic Review to Horizons Beyond: Lithium-Sulphur Batteries Run on the Wheels. *Chem. Commun.* **2015**, *51*, 18−33.
(198) Zhang, S. S. Liquid Electrolyte Lithium/Sulfur Battery: Fundamental Chemistry, Problems, and Solutions. *J. Power Sources* **2013**, *231*, 153−162.
(199) Wang, L.; Liu, J.; Yuan, S.; Wang, Y.; Xia, Y. To Mitigate Self-Discharge of Lithium-Sulfur Batteries by Optimizing Ionic Liquid Electrolytes. *Energy Environ. Sci.* **2016**, *9*, 224−231.
(200) Zhang, S. S. Role of $LiNO_3$ in Rechargeable Lithium/Sulfur Battery. *Electrochim. Acta* **2012**, *70*, 344−348.
(201) Hagen, M.; Hanselmann, D.; Ahlbrecht, K.; Maça, R.; Gerber, D.; Tübke, J. Lithium−Sulfur Cells: The Gap Between the State-of-the-Art and the Requirements for High Energy Battery Cells. *Adv. Energy Mater.* **2015**, *5*, 1401986.
(202) Yuan, L. X.; Feng, J. K.; Ai, X. P.; Cao, Y. L.; Chen, S. L.; Yang, H. X. Improved Dischargeability and Reversibility of Sulfur Cathode in a Novel Ionic Liquid Electrolyte. *Electrochem. Commun.* **2006**, *8*, 610−614.
(203) Zhang, S.; Ueno, K.; Dokko, K.; Watanabe, M. Recent Advances in Electrolytes for Lithium−Sulfur Batteries. *Adv. Energy Mater.* **2015**, *5*, 1500117.
(204) Scheers, J.; Fantini, S.; Johansson, P. A Review of Electrolytes for Lithium−Sulphur Batteries. *J. Power Sources* **2014**, *255*, 204−218.
(205) Barghamadi, M.; Best, A. S.; Bhatt, A. I.; Hollenkamp, A. F.; Musameh, M.; Rees, R. J.; Ruther, T. Lithium-Sulfur Batteries-The Solution is in the Electrolyte, but is the Electrolyte a Solution? *Energy Environ. Sci.* **2014**, *7*, 3902−3920.
(206) Gao, J.; Lowe, M. A.; Kiya, Y.; Abruña, H. D. Effects of Liquid Electrolytes on the Charge−Discharge Performance of Rechargeable Lithium/Sulfur Batteries: Electrochemical and in-Situ X-ray Absorption Spectroscopic Studies. *J. Phys. Chem. C* **2011**, *115*, 25132−25137.
(207) Park, J.-W.; Ueno, K.; Tachikawa, N.; Dokko, K.; Watanabe, M. Ionic Liquid Electrolytes for Lithium−Sulfur Batteries. *J. Phys. Chem. C* **2013**, *117*, 20531−20541.
(208) Ueno, K.; Park, J.-W.; Yamazaki, A.; Mandai, T.; Tachikawa, N.; Dokko, K.; Watanabe, M. Anionic Effects on Solvate Ionic Liquid Electrolytes in Rechargeable Lithium−Sulfur Batteries. *J. Phys. Chem. C* **2013**, *117*, 20509−20516.
(209) Salitra, G.; Markevich, E.; Rosenman, A.; Talyosef, Y.; Aurbach, D.; Garsuch, A. High-Performance Lithium−Sulfur Batteries Based on Ionic-Liquid Electrolytes with Bis(fluorolsufonyl)imide Anions and Sulfur-Encapsulated Highly Disordered Activated Carbon. *ChemElectroChem* **2014**, *1*, 1492−1496.
(210) Takahashi, T.; Yamagata, M.; Ishikawa, M. A Sulfur−Microporous Carbon Composite Positive Electrode for Lithium/Sulfur and Silicon/Sulfur Rechargeble Batteries. *Prog. Nat. Sci.* **2015**, *25*, 612−621.
(211) Yan, Y.; Yin, Y.; Guo, Y.; Wan, L.-J. Effect of Cations in Ionic Liquids on the Electrochemical Performance of Lithium-Sulfur Batteries. *Sci. China: Chem.* **2014**, *57*, 1564−1569.
(212) Kim, S.; Jung, Y.; Park, S.-J. Effect of Imidazolium Cation on Cycle Life Characteristics of Secondary Lithium−Sulfur Cells using Liquid Electrolytes. *Electrochim. Acta* **2007**, *52*, 2116−2122.
(213) Aurbach, D.; Pollak, E.; Elazari, R.; Salitra, G.; Kelley, C. S.; Affinito, J. On the Surface Chemical Aspects of Very High Energy Density, Rechargeable Li−Sulfur Batteries. *J. Electrochem. Soc.* **2009**, *156*, A694−A702.
(214) Barghamadi, M.; Best, A. S.; Bhatt, A. I.; Hollenkamp, A. F.; Mahon, P. J.; Musameh, M.; Rüther, T. Effect of $LiNO_3$ Additive and Pyrrolidinium Ionic Liquid on the Solid Electrolyte Interphase in the Lithium−Sulfur Battery. *J. Power Sources* **2015**, *295*, 212−220.
(215) Xiong, S.; Xie, K.; Blomberg, E.; Jacobsson, P.; Matic, A. Analysis of the Solid Electrolyte Interphase formed with an Ionic Liquid Electrolyte for Lithium-Sulfur Batteries. *J. Power Sources* **2014**, *252*, 150−155.
(216) Cao, R.; Chen, J.; Han, K. S.; Xu, W.; Mei, D.; Bhattacharya, P.; Engelhard, M. H.; Mueller, K. T.; Liu, J.; Zhang, J.-G. Effect of the Anion Activity on the Stability of Li Metal Anodes in Lithium-Sulfur Batteries. *Adv. Funct. Mater.* **2016**, *26*, 3059−3066.
(217) Hu, J. J.; Long, G. K.; Liu, S.; Li, G. R.; Gao, X. P. A LiFSI-LiTFSI Binary-Salt Electrolyte to Achieve High Capacity and Cycle Stability for a Li-S Battery. *Chem. Commun.* **2014**, *50*, 14647−14650.
(218) Ma, Q.; Tong, B.; Fang, Z.; Qi, X.; Feng, W.; Nie, J.; Hu, Y.-S.; Li, H.; Huang, X.; Chen, L.; et al. Impact of Anionic Structure of Lithium Salt on the Cycling Stability of Lithium-Metal Anode in Li-S Batteries. *J. Electrochem. Soc.* **2016**, *163*, A1776−A1783.
(219) Wu, F.; Zhu, Q.; Chen, R.; Chen, N.; Chen, Y.; Ye, Y.; Qian, J.; Li, L. Ionic Liquid-Based Electrolyte with Binary Lithium Salts for High Performance Lithium−Sulfur Batteries. *J. Power Sources* **2015**, *296*, 10−17.
(220) Xiong, S.; Kai, X.; Hong, X.; Diao, Y. Effect of LiBOB as Additive on Electrochemical Properties of Lithium−Sulfur Batteries. *Ionics* **2012**, *18*, 249−254.

DOI: 10.1021/acs.chemrev.6b00504
Chem. Rev. 2017, 117, 7190−7239

(221) Wang, W.; Wang, Y.; Huang, Y.; Huang, C.; Yu, Z.; Zhang, H.; Wang, A.; Yuan, K. The Electrochemical Performance of Lithium−Sulfur Batteries with $LiClO_4$ DOL/DME Electrolyte. *J. Appl. Electrochem.* **2010**, *40*, 321−325.
(222) Wang, J.; Chew, S. Y.; Zhao, Z. W.; Ashraf, S.; Wexler, D.; Chen, J.; Ng, S. H.; Chou, S. L.; Liu, H. K. Sulfur−Mesoporous Carbon Composites in Conjunction with a Novel Ionic Liquid Electrolyte for Lithium Rechargeable Batteries. *Carbon* **2008**, *46*, 229−235.
(223) Park, J.-W.; Yamauchi, K.; Takashima, E.; Tachikawa, N.; Ueno, K.; Dokko, K.; Watanabe, M. Solvent Effect of Room Temperature Ionic Liquids on Electrochemical Reactions in Lithium−Sulfur Batteries. *J. Phys. Chem. C* **2013**, *117*, 4431−4440.
(224) Shin, E. S.; Kim, K.; Oh, S. H.; Cho, W. I. Polysulfide Dissolution Control: the Common Ion Effect. *Chem. Commun.* **2013**, *49*, 2004−2006.
(225) Tachikawa, N.; Yamauchi, K.; Takashima, E.; Park, J.-W.; Dokko, K.; Watanabe, M. Reversibility of Electrochemical Reactions of Sulfur Supported on Inverse Opal Carbon in Glyme−Li Salt Molten Complex Electrolytes. *Chem. Commun.* **2011**, *47*, 8157−8159.
(226) Barghamadi, M.; Best, A. S.; Bhatt, A. I.; Hollenkamp, A. F.; Mahon, P. J.; Musameh, M.; Rüther, T. Effect of Anion on Behaviour of Li-S Battery Electrolyte Solutions Based on *N*-Methyl-*N*-Butyl-Pyrrolidinium Ionic Liquids. *Electrochim. Acta* **2015**, *180*, 636−644.
(227) Manan, N. S.; Aldous, L.; Alias, Y.; Murray, P.; Yellowlees, L. J.; Lagunas, M. C.; Hardacre, C. Electrochemistry of Sulfur and Polysulfides in Ionic Liquids. *J. Phys. Chem. B* **2011**, *115*, 13873−13879.
(228) Boros, È.; Earle, M. J.; Gîlea, M. A.; Metlen, A.; Mudring, A.-V.; Rieger, F.; Robertson, A. J.; Seddon, K. R.; Tomaszowska, A. A.; Trusov, L.; et al. On the Dissolution of Non-Metallic Solid Elements (Sulfur, Selenium, Tellurium and Phosphorus) in Ionic Liquids. *Chem. Commun.* **2010**, *46*, 716−718.
(229) Zhang, S. S. New Insight into Liquid Electrolyte of Rechargeable Lithium/Sulfur Battery. *Electrochim. Acta* **2013**, *97*, 226−230.
(230) Song, M.-K.; Zhang, Y.; Cairns, E. J. A Long-Life, High-Rate Lithium/Sulfur Cell: A Multifaceted Approach to Enhancing Cell Performance. *Nano Lett.* **2013**, *13*, 5891−5899.
(231) Shin, J. H.; Cairns, E. J. *N*-Methyl-(*n*-butyl) pyrrolidinium bis (trifluoromethanesulfonyl) imide-LiTFSI−poly (ethylene glycol) dimethyl ether Mixture as a Li/S Cell Electrolyte. *J. Power Sources* **2008**, *177*, 537−545.
(232) Zheng, J.; Gu, M.; Chen, H.; Meduri, P.; Engelhard, M. H.; Zhang, J.-G.; Liu, J.; Xiao, J. Ionic Liquid-Enhanced Solid State Electrolyte Interface (SEI) for Lithium−Sulfur Batteries. *J. Mater. Chem. A* **2013**, *1*, 8464−8470.
(233) Wang, L.; Byon, H. R. *N*-Methyl-*N*-propylpiperidinium bis (trifluoromethanesulfonyl) imide-Based Organic Electrolyte for High Performance Lithium−Sulfur Batteries. *J. Power Sources* **2013**, *236*, 207−214.
(234) Dokko, K.; Tachikawa, N.; Yamauchi, K.; Tsuchiya, M.; Yamazaki, A.; Takashima, E.; Park, J.-W.; Ueno, K.; Seki, S.; Serizawa, N.; et al. Solvate Ionic Liquid Electrolyte for Li−S Batteries. *J. Electrochem. Soc.* **2013**, *160*, A1304−A1310.
(235) Grande, L.; Paillard, E.; Hassoun, J.; Park, J. B.; Lee, Y. J.; Sun, Y. K.; Passerini, S.; Scrosati, B. The Lithium/Air Battery: Still an Emerging System or a Practical Reality? *Adv. Mater.* **2015**, *27*, 784−800.
(236) Luntz, A. C.; McCloskey, B. D. Nonaqueous Li-Air Batteries: A Status Report. *Chem. Rev.* **2014**, *114*, 11721−11750.
(237) Christensen, J.; Albertus, P.; Sanchez-Carrera, R. S.; Lohmann, T.; Kozinsky, B.; Liedtke, R.; Ahmed, J.; Kojic, A. A Critical Review of Li/Air Batteries. *J. Electrochem. Soc.* **2012**, *159*, R1.
(238) Black, R.; Adams, B.; Nazar, L. F. Non-Aqueous and Hybrid Li-O2 Batteries. *Adv. Energy Mater.* **2012**, *2*, 801−815.
(239) Vasudevan, D.; Wendt, H. Electroreduction of Oxygen in Aprotic Media. *J. Electroanal. Chem.* **1995**, *392*, 69−74.
(240) Laoire, C. O.; Mukerjee, S.; Abraham, K. M.; Plichta, E. J.; Hendrickson, M. A. Influence of Nonaqueous Solvents on the Electrochemistry of Oxygen in the Rechargeable Lithium−Air Battery. *J. Phys. Chem. C* **2010**, *114*, 9178−9186.
(241) Maricle, D. L.; Hodgson, W. G. Reducion of Oxygen to Superoxide Anion in Aprotic Solvents. *Anal. Chem.* **1965**, *37*, 1562−1565.
(242) Peover, M. E.; White, B. S. The Formation of the Superoxide Ion by Electrolysis of Oxygen in Aprotic Solvents. *Chem. Commun.* **1965**, *1*, 183−184.
(243) Peover, M. E.; White, B. S. Electrolytic Reduction of Oxygen in Aprotic Solvents: The Superoxide Ion. *Electrochim. Acta* **1966**, *11*, 1061−1067.
(244) Chin, D. H.; Chiericato, G.; Nanni, E. J.; Sawyer, D. T. Proton-Induced Disproportionation of Superoxide Ion in Aprotic Media. *J. Am. Chem. Soc.* **1982**, *104*, 1296−1299.
(245) Jain, P. S.; Lal, S. Electrolytic Reduction of Oxygen at Solid Electrodes in Aprotic-Solvents - the Superoxide Ion. *Electrochim. Acta* **1982**, *27*, 759−763.
(246) Andrieux, C. P.; Hapiot, P.; Saveant, J. M. Mechanism of Superoxide Ion Disproportionation in Aprotic-Solvents. *J. Am. Chem. Soc.* **1987**, *109*, 3768−3775.
(247) Afanas'ev, I. B. *Superoxide Ion Chemistry and Biological Implications*; CRC Press: Boca Raton, FL, 1989.
(248) Aurbach, D.; Daroux, M.; Faguy, P.; Yeager, E. The Electrochemistry of Noble-Metal Electrodes in Aprotic Organic-Solvents Containing Lithium-Salts. *J. Electroanal. Chem. Interfacial Electrochem.* **1991**, *297*, 225−244.
(249) Whittingham, S. Metal-Air Batteries: A Reality Check, *ECS Meeting Abstracts*; MA2012−02; The Electrochemical Society: Pennington, NJ, 2012; pp 1099.
(250) Radin, M. D.; Siegel, D. J. Charge Transport in Lithium Peroxide: Relevance for Rechargeable Metal-Air Batteries. *Energy Environ. Sci.* **2013**, *6*, 2370−2379.
(251) Black, R.; Lee, J. H.; Adams, B.; Mims, C. A.; Nazar, L. F. The Role of Catalysts and Peroxide Oxidation in Lithium-Oxygen Batteries. *Angew. Chem., Int. Ed.* **2013**, *52*, 392−396.
(252) Kavakli, C.; Meini, S.; Harzer, G.; Tsiouvaras, N.; Piana, M.; Siebel, A.; Garsuch, A.; Gasteiger, H. A.; Herranz, J. Nanosized Carbon-Supported Manganese Oxide Phases as Lithium-Oxygen Battery Cathode Catalysts. *ChemCatChem* **2013**, *5*, 3358−3373.
(253) Yilmaz, E.; Yogi, C.; Yamanaka, K.; Ohta, T.; Byon, H. R. Promoting formation of noncrystalline Li_2O_2 in the Li-O_2 battery with RuO_2 nanoparticles. *Nano Lett.* **2013**, *13*, 4679−4684.
(254) Li, C. M.; Fontaine, O.; Freunberger, S. A.; Johnson, L.; Grugeon, S.; Laruelle, S.; Bruce, P. G.; Armand, M. Aprotic Li-O-2 Battery: Influence of Complexing Agents on Oxygen Reduction in an Aprotic Solvent. *J. Phys. Chem. C* **2014**, *118*, 3393−3401.
(255) Kwak, W.-J.; Hirshberg, D.; Sharon, D.; Afri, M.; Frimer, A. A.; Jung, H.-G.; Aurbach, D.; Sun, Y.-K. Li−O_2 Cells with LiBr as an Electrolyte and a Redox Mediator. *Energy Environ. Sci.* **2016**, *9*, 2334−2345.
(256) Kwak, W.-J.; Hirshberg, D.; Sharon, D.; Shin, H.-J.; Afri, M.; Park, J.-B.; Garsuch, A.; Chesneau, F. F.; Frimer, A. A.; Aurbach, D.; et al. Understanding the Behavior of Li−Oxygen Cells Containing LiI. *J. Mater. Chem. A* **2015**, *3*, 8855−8864.
(257) Bergner, B. J.; Schurmann, A.; Peppler, K.; Garsuch, A.; Janek, J. TEMPO: A Mobile Catalyst for Rechargeable Li-O Batteries. *J. Am. Chem. Soc.* **2014**, *136*, 15054−15064.
(258) Chen, Y. H.; Freunberger, S. A.; Peng, Z. Q.; Fontaine, O.; Bruce, P. G. Charging a Li-O_2 Battery Using a Redox Mediator. *Nat. Chem.* **2013**, *5*, 489−494.
(259) Balaish, M.; Kraytsberg, A.; Ein-Eli, Y. A Critical Review on Lithium-Air Battery Electrolytes. *Phys. Chem. Chem. Phys.* **2014**, *16*, 2801−2822.
(260) Li, F. J.; Zhang, T.; Zhou, H. S. Challenges of Non-Aqueous Li-O_2 Batteries: Electrolytes, Catalysts, and Anodes. *Energy Environ. Sci.* **2013**, *6*, 1125−1141.

DOI: 10.1021/acs.chemrev.6b00504
Chem. Rev. 2017, 117, 7190−7239

(261) Freunberger, S. A.; Chen, Y. H.; Peng, Z. Q.; Griffin, J. M.; Hardwick, L. J.; Barde, F.; Novak, P.; Bruce, P. G. Reactions in the Rechargeable Lithium-O_2 Battery with Alkyl Carbonate Electrolytes. *J. Am. Chem. Soc.* **2011**, *133*, 8040−8047.
(262) Okamoto, Y.; Kubo, Y. Ab Initio Calculations for Decomposition Mechanism of $CH_3O(CH_2CH_2O)_NCH_3$ (N = 1−4) by the Attack of O_2^- Anion. *J. Phys. Chem. C* **2013**, *117*, 15940−15946.
(263) Freunberger, S. A.; Chen, Y. H.; Drewett, N. E.; Hardwick, L. J.; Barde, F.; Bruce, P. G. The Lithium-Oxygen Battery with Ether-Based Electrolytes. *Angew. Chem., Int. Ed.* **2011**, *50*, 8609−8613.
(264) Kwabi, D. G.; Batcho, T. P.; Amanchukwu, C. V.; Ortiz-Vitoriano, N.; Hammond, P.; Thompson, C. V.; Shao-Horn, Y. Chemical Instability of Dimethyl Sulfoxide in Lithium-Air Batteries. *J. Phys. Chem. Lett.* **2014**, *5*, 2850−2856.
(265) García, J. M.; Horn, H. W.; Rice, J. E. Dominant Decomposition Pathways for Ethereal Solvents in Li−O_2 Batteries. *J. Phys. Chem. Lett.* **2015**, *6*, 1795−1799.
(266) Bonnet-Mercier, N.; Wong, R. A.; Thomas, M. L.; Dutta, A.; Yamanaka, K.; Yogi, C.; Ohta, T.; Byon, H. R. A Structured Three-Dimensional Polymer Electrolyte with Enlarged Active Reaction Zone for Li-O_2 Batteries. *Sci. Rep.* **2014**, *4*, 7127.
(267) Gallagher, K. G.; Goebel, S.; Greszler, T.; Mathias, M.; Oelerich, W.; Eroglu, D.; Srinivasan, V. Quantifying the Promise of Lithium−Air Batteries for Electric Vehicles. *Energy Environ. Sci.* **2014**, *7*, 1555.
(268) Yoshida, T.; Kojima, K. Toyota MIRAI Fuel Cell Vehicle and Progress Toward a Future Hydrogen Society. *Electrochem. Soc. Interface* **2015**, *24*, 45−49.
(269) Hayyan, M.; Hashim, M. A.; AlNashef, I. M. Superoxide Ion: Generation and Chemical Implications. *Chem. Rev.* **2016**, *116*, 3029−3085.
(270) Buzzeo, M. C.; Klymenko, O. V.; Wadhawan, J. D.; Hardacre, C.; Seddon, K. R.; Compton, R. G. Voltammetry of Oxygen in the Room-Temperature Ionic Liquids 1-ethyl-3-methylimidazolium bis-((trifluoromethyl)sulfonyl)imide and hexyltriethylammonium bis-((trifluoromethyl)sulfonyl)imide: One-Electron Reduction to Form Superoxide. Steady-State and Transient Behavior in the Same Cyclic Voltammogram Resulting from Widely Different Diffusion Coefficients of Oxygen and Superoxide. *J. Phys. Chem. A* **2003**, *107*, 8872−8878.
(271) Neale, A. R.; Li, P.; Jacquemin, J.; Goodrich, P.; Ball, S. C.; Compton, R. G.; Hardacre, C. Effect of Cation Structure on the Oxygen Solubility and Diffusivity in a Range of Bis{(trifluoromethyl)-sulfonyl}imide Anion Based Ionic Liquids for Lithium-Air Battery Electrolytes. *Phys. Chem. Chem. Phys.* **2016**, *18*, 11251−11262.
(272) De Giorgio, F.; Soavi, F.; Mastragostino, M. Effect of Lithium Ions on Oxygen Reduction in Ionic Liquid-Based Electrolytes. *Electrochem. Commun.* **2011**, *13*, 1090−1093.
(273) Allen, C. J.; Mukerjee, S.; Plichta, E. J.; Hendrickson, M. A.; Abraham, K. M. Oxygen Electrode Rechargeability in an Ionic Liquid for the Li-Air Battery. *J. Phys. Chem. Lett.* **2011**, *2*, 2420−2424.
(274) Allen, C. J.; Hwang, J.; Kautz, R.; Mukerjee, S.; Plichta, E. J.; Hendrickson, M. A.; Abraham, K. M. Oxygen Reduction Reactions in Ionic Liquids and the Formulation of a General ORR Mechanism for Li−Air Batteries. *J. Phys. Chem. C* **2012**, *116*, 20755−20764.
(275) Bryantsev, V. S.; Giordani, V.; Walker, W.; Blanco, M.; Zecevic, S.; Sasaki, K.; Uddin, J.; Addison, D.; Chase, G. V. Predicting Solvent Stability in Aprotic Electrolyte Li-Air Batteries: Nucleophilic Substitution by the Superoxide Anion Radical ($O_2\bullet^-$). *J. Phys. Chem. A* **2011**, *115*, 12399−12409.
(276) Bryantsev, V. S.; Uddin, J.; Giordani, V.; Walker, W.; Addison, D.; Chase, G. V. The Identification of Stable Solvents for Nonaqueous Rechargeable Li-Air Batteries. *J. Electrochem. Soc.* **2013**, *160*, A160−A171.
(277) Bryantsev, V. S. Predicting the Stability of Aprotic Solvents in Li-Air Batteries: pK_a Calculations of Aliphatic C-H Acids in Dimethyl Sulfoxide. *Chem. Phys. Lett.* **2013**, *558*, 42−47.
(278) Katayama, Y.; Onodera, H.; Yamagata, M.; Miura, T. Electrochemical Reduction of Oxygen in Some Hydrophobic Room-Temperature Molten Salt Systems. *J. Electrochem. Soc.* **2004**, *151*, A59−A63.
(279) Islam, M. M.; Imase, T.; Okajima, T.; Takahashi, M.; Niikura, Y.; Kawashima, N.; Nakamura, Y.; Ohsaka, T. Stability of superoxide ion in imidazolium cation-based room-temperature ionic liquids. *J. Phys. Chem. A* **2009**, *113*, 912−916.
(280) Ernst, S.; Aldous, L.; Compton, R. G. The Electrochemical Reduction of Oxygen at Boron-Doped Diamond and Glassy Carbon Electrodes: A Comparative Study in a Room-Temperature Ionic Liquid. *J. Electroanal. Chem.* **2011**, *663*, 108−112.
(281) Frith, J. T.; Russell, A. E.; Garcia-Araez, N.; Owen, J. R. An in-situ Raman Study of the Oxygen Reduction Reaction in Ionic Liquids. *Electrochem. Commun.* **2014**, *46*, 33−35.
(282) AlNashef, I. M.; Hashim, M. A.; Mjalli, F. S.; Ali, M. Q. A.-h.; Hayyan, M. A Novel Method for the Synthesis of 2-Imidazolones. *Tetrahedron Lett.* **2010**, *51*, 1976−1978.
(283) Rodriguez, H.; Gurau, G.; Holbrey, J. D.; Rogers, R. D. Reaction of Elemental Chalcogens with Imidazolium Acetates to yield Imidazole-2-Chalcogenones: Direct Evidence for Ionic Liquids as Proto-carbenes. *Chem. Commun.* **2011**, *47*, 3222−3224.
(284) Gurau, G.; Rodriguez, H.; Kelley, S. P.; Janiczek, P.; Kalb, R. S.; Rogers, R. D. Demonstration of Chemisorption of Carbon Dioxide in 1,3-Dialkylimidazolium Acetate Ionic Liquids. *Angew. Chem., Int. Ed.* **2011**, *50*, 12024−12026.
(285) Cai, K. D.; Pu, W. H.; Gao, Y.; Hou, J. B.; Deng, C. S.; Wang, C.; Mao, Z. Q. Investigation of Ionic Liquid Composite Electrolyte for Lithium-Oxygen Battery. *Int. J. Hydrogen Energy* **2013**, *38*, 11023−11027.
(286) Zhang, T.; Zhou, H. S. From Li-O_2 to Li-Air Batteries: Carbon Nanotubes/Ionic Liquid Gels with a Tricontinuous Passage of Electrons, Ions, and Oxygen. *Angew. Chem., Int. Ed.* **2012**, *51*, 11062−11067.
(287) Kuboki, T.; Okuyama, T.; Ohsaki, T.; Takami, N. Lithium-Air Batteries Using Hydrophobic Room Temperature Ionic Liquid Electrolyte. *J. Power Sources* **2005**, *146*, 766−769.
(288) Takechi, K.; Higashi, S.; Mizuno, F.; Nishikoori, H.; Iba, H.; Shiga, T. Stability of Solvents against Superoxide Radical Species for the Electrolyte of Lithium-Air Battery. *ECS Electrochem. Lett.* **2012**, *1*, A27−A29.
(289) Mizuno, F.; Takechi, K.; Higashi, S.; Shiga, T.; Shiotsuki, T.; Takazawa, N.; Sakurabayashi, Y.; Okazaki, S.; Nitta, I.; Kodama, T.; et al. Cathode Reaction Mechanism of Non-Aqueous Li−O_2 Batteries with Highly Oxygen Radical Stable Electrolyte Solvent. *J. Power Sources* **2013**, *228*, 47−56.
(290) Higashi, S.; Kato, Y.; Takechi, K.; Nakamoto, H.; Mizuno, F.; Nishikoori, H.; Iba, H.; Asaoka, T. Evaluation and Analysis of Li-Air Battery using Ether-Functionalized Ionic Liquid. *J. Power Sources* **2013**, *240*, 14−17.
(291) Nakamoto, H.; Suzuki, Y.; Shiotsuki, T.; Mizuno, F.; Higashi, S.; Takechi, K.; Asaoka, T.; Nishikoori, H.; Iba, H. Ether-Functionalized Ionic Liquid Electrolytes for Lithium-Air Batteries. *J. Power Sources* **2013**, *243*, 19−23.
(292) Elia, G. A.; Hassoun, J.; Kwak, W. J.; Sun, Y. K.; Scrosati, B.; Mueller, F.; Bresser, D.; Passerini, S.; Oberhumer, P.; Tsiouvaras, N.; et al. An Advanced Lithium-Air Battery Exploiting an Ionic Liquid-Based Electrolyte. *Nano Lett.* **2014**, *14*, 6572−6577.
(293) Jung, K. N.; Lee, J. I.; Jung, J. H.; Shin, K. H.; Lee, J. W. A Quasi-Solid-State Rechargeable Lithium-Oxygen Battery Based on a Gel Polymer Electrolyte with an Ionic Liquid. *Chem. Commun.* **2014**, *50*, 5458−5461.
(294) Piana, M.; Wandt, J.; Meini, S.; Buchberger, I.; Tsiouvaras, N.; Gasteiger, H. A. Stability of a Pyrrolidinium-Based Ionic Liquid in Li-O_2 Cells. *J. Electrochem. Soc.* **2014**, *161*, A1992−A2001.
(295) Meini, S.; Solchenbach, S.; Piana, M.; Gasteiger, H. A. The Role of Electrolyte Solvent Stability and Electrolyte Impurities in the Electrooxidation of Li_2O_2 in Li-O_2 Batteries. *J. Electrochem. Soc.* **2014**, *161*, A1306−A1314.

DOI: 10.1021/acs.chemrev.6b00504
Chem. Rev. 2017, 117, 7190−7239

(296) Zhang, T.; Liao, K.; He, P.; Zhou, H. A Self-Defense Redox Mediator for Efficient Lithium−O_2 Batteries. *Energy Environ. Sci.* **2016**, *9*, 1024−1030.
(297) Das, S.; Højberg, J.; Knudsen, K. B.; Younesi, R.; Johansson, P.; Norby, P.; Vegge, T. Instability of Ionic Liquid-Based Electrolytes in Li−O_2 Batteries. *J. Phys. Chem. C* **2015**, *119*, 18084−18090.
(298) Ahmed, O. U.; Mjalli, F. S.; Al-Wahaibi, T.; Al-Wahaibi, Y.; AlNashef, I. M. Stability of Superoxide Ion in Phosphonium-Based Ionic Liquids. *Ind. Eng. Chem. Res.* **2015**, *54*, 2074−2080.
(299) Li, P.; Barnes, E. O.; Hardacre, C.; Compton, R. G. Microelectrode Voltammetry of Dioxygen Reduction in a Phosphonium Cation-Based Room-Temperature Ionic Liquid: Quantitative Studies. *J. Phys. Chem. C* **2015**, *119*, 2716−2726.
(300) Pozo-Gonzalo, C.; Howlett, P. C.; Hodgson, J. L.; Madsen, L. A.; MacFarlane, D. R.; Forsyth, M. Insights into the Reversible Oxygen Reduction Reaction in a Series of Phosphonium-Based Ionic Liquids. *Phys. Chem. Chem. Phys.* **2014**, *16*, 25062−25070.
(301) Hayyan, M.; Mjalli, F. S.; Hashim, M. A.; AlNashef, I. M.; Al-Zahrani, S. M.; Chooi, K. L. Long Term Stability of Superoxide Ion in Piperidinium, Pyrrolidinium and Phosphonium Cations-Based Ionic Liquids and its Utilization in the Destruction of Chlorobenzenes. *J. Electroanal. Chem.* **2012**, *664*, 26−32.
(302) Liu, T.; Leskes, M.; Yu, W.; Moore, A. J.; Zhou, L.; Bayley, P. M.; Kim, G.; Grey, C. P. Cycling Li-O_2 batteries via LiOH formation and decomposition. *Science* **2015**, *350*, 530−533.
(303) Liu, T.; Kim, G.; Carretero-Gonzalez, J.; Castillo-Martinez, E.; Bayley, P. M.; Liu, Z.; Grey, C. P. Response to Comment on "Cycling Li-O_2 batteries via LiOH formation and decomposition". *Science* **2016**, *352*, 667.
(304) Meini, S.; Piana, M.; Tsiouvaras, N.; Garsuch, A.; Gasteiger, H. A. The Effect of Water on the Discharge Capacity of a Non-Catalyzed Carbon Cathode for Li-O_2 Batteries. *Electrochem. Solid-State Lett.* **2012**, *15*, A45−A48.
(305) Cho, M. H.; Trottier, J.; Gagnon, C.; Hovington, P.; Clement, D.; Vijh, A.; Kim, C. S.; Guerfi, A.; Black, R.; Nazar, L.; et al. The Effects of Moisture Contamination in the Li-O_2 Battery. *J. Power Sources* **2014**, *268*, 565−574.
(306) Huang, S.; Cui, Z.; Zhao, N.; Sun, J.; Guo, X. Influence of Ambient Air on Cell Reactions of Li-air Batteries. *Electrochim. Acta* **2016**, *191*, 473−478.
(307) Xu, S.; Lau, S.; Archer, L. CO_2 and Ambient Air in Metal-Oxygen Batteries: Steps towards Reality. *Inorg. Chem. Front.* **2015**, *2*, 1070−1079.
(308) Pozo-Gonzalo, C.; Torriero, A. A. J.; Forsyth, M.; MacFarlane, D. R.; Howlett, P. C. Redox Chemistry of the Superoxide Ion in a Phosphonium-Based Ionic Liquid in the Presence of Water. *J. Phys. Chem. Lett.* **2013**, *4*, 1834−1837.
(309) Thomas, M. L.; Oda, Y.; Tatara, R.; Kwon, H.-M.; Ueno, K.; Dokko, K.; Watanabe, M. Suppression of Water Absorption by Molecular Design of Ionic Liquid Electrolyte for Li-Air Battery. *Adv. Energy Mater.* **2016**, 1601753.
(310) Han, S. M.; Kim, J. H.; Kim, D. W. Cycling Performances of Lithium-Air Cells Assembled with Mixed Electrolytes of Ionic Liquid and Diethylene Glycol Diethyl Ether. *J. Electrochem. Soc.* **2015**, *162*, A3103−A3109.
(311) Elia, G. A.; Bernhard, R.; Hassoun, J. A Lithium-Ion Oxygen Battery Using a Polyethylene Glyme Electrolyte Mixed with an Ionic Liquid. *RSC Adv.* **2015**, *5*, 21360−21365.
(312) Cecchetto, L.; Salomon, M.; Scrosati, B.; Croce, F. Study of a Li-Air Battery Having an Electrolyte Solution Formed by a Mixture of an Ether-Based Aprotic Solvent and an Ionic Liquid. *J. Power Sources* **2012**, *213*, 233−238.
(313) Tatara, R.; Tachikawa, N.; Kwon, H.-M.; Ueno, K.; Dokko, K.; Watanabe, M. Solvate Ionic Liquid, $[Li(triglyme)_1][NTf_2]$, as Electrolyte for Rechargeable Li-Air Battery: Discharge Depth and Reversibility. *Chem. Lett.* **2013**, *42*, 1053−1055.
(314) Adams, B. D.; Black, R.; Williams, Z.; Fernandes, R.; Cuisinier, M.; Berg, E. J.; Novak, P.; Murphy, G. K.; Nazar, L. F. Towards a Stable Organic Electrolyte for the Lithium Oxygen Battery. *Adv. Energy Mater.* **2015**, *5*, 1400867.
(315) Monaco, S.; Soavi, F.; Mastragostino, M. Role of Oxygen Mass Transport in Rechargeable Li/O_2 Batteries Operating with Ionic Liquids. *J. Phys. Chem. Lett.* **2013**, *4*, 1379−1382.
(316) Bresser, D.; Paillard, E.; Passerini, S. Ionic Liquid-based Electrolytes for Li Metal/Air Batteries: A Review of Materials and the New 'LABOHR' Flow Cell Concept. *J. Electrochem. Sci. Technol.* **2014**, *5*, 37−44.
(317) Grande, L.; Ochel, A.; Monaco, S.; Mastragostino, M.; Tonti, D.; Palomino, P.; Paillard, E.; Passerini, S. Li/Air Flow Battery Employing Ionic Liquid Electrolytes. *Energy Technology* **2016**, *4*, 85−89.
(318) Giordani, V.; Tozier, D.; Tan, H.; Burke, C. M.; Gallant, B. M.; Uddin, J.; Greer, J. R.; McCloskey, B. D.; Chase, G. V.; Addison, D. A Molten Salt Lithium-Oxygen Battery. *J. Am. Chem. Soc.* **2016**, *138*, 2656−2663.
(319) Yoo, K.; Dive, A. M.; Kazemiabnavi, S.; Banerjee, S.; Dutta, P. Effects of Operating Temperature on the Electrical Performance of a Li-air Battery operated with Ionic Liquid Electrolyte. *Electrochim. Acta* **2016**, *194*, 317−329.
(320) Roberts, M.; Younesi, R.; Richardson, W.; Liu, J.; Gustafsson, T.; Zhu, J. F.; Edstrom, K. Increased Cycling Efficiency of Lithium Anodes in Dimethyl Sulfoxide Electrolytes For Use in Li-O_2 Batteries. *ECS Electrochem. Lett.* **2014**, *3*, A62−A65.
(321) Younesi, R.; Hahlin, M.; Edstrom, K. Surface Characterization of the Carbon Cathode and the Lithium Anode of Li-O_2 Batteries Using $LiClO_4$ or LiBOB Salts. *ACS Appl. Mater. Interfaces* **2013**, *5*, 1333−1341.
(322) Younesi, R.; Hahlin, M.; Roberts, M.; Edström, K. The SEI Layer Formed on Lithium Metal in the Presence of Oxygen: A Seldom Considered Component in the development of the Li−O2 battery. *J. Power Sources* **2013**, *225*, 40−45.
(323) Togasaki, N.; Momma, T.; Osaka, T. Role of the Solid Electrolyte Interphase on a Li Metal Anode in a Dimethylsulfoxide-Based Electrolyte for a Lithium−Oxygen Battery. *J. Power Sources* **2015**, *294*, 588−592.
(324) Xue, K. H.; McTurk, E.; Johnson, L.; Bruce, P. G.; Franco, A. A. A Comprehensive Model for Non-Aqueous Lithium Air Batteries Involving Different Reaction Mechanisms. *J. Electrochem. Soc.* **2015**, *162*, A614−A621.
(325) Mauritz, K. A.; Moore, R. B. State of Understanding of Nafion. *Chem. Rev.* **2004**, *104*, 4535−4586.
(326) Asano, N.; Aoki, M.; Suzuki, S.; Miyatake, K.; Uchida, H.; Watanabe, M. Aliphatic/Aromatic Polyimide Ionomers as a Proton Conductive Membrane for Fuel Cell Applications. *J. Am. Chem. Soc.* **2006**, *128*, 1762−1769.
(327) Wang, F.; Hickner, M.; Kim, Y. S.; Zawodzinski, T. A.; McGrath, J. E. Direct Polymerization of Sulfonated Poly(arylene ether sulfone) Random (Statistical) Copolymers: Candidates for New Proton Exchange Membranes. *J. Membr. Sci.* **2002**, *197*, 231−242.
(328) Schuster, M.; Kreuer, K.-D.; Andersen, H. T.; Maier, J. Sulfonated Poly(phenylene sulfone) Polymers as Hydrolytically and Thermooxidatively Stable Proton Conducting Ionomers. *Macromolecules* **2007**, *40*, 598−607.
(329) Umezawa, K.; Oshima, T.; Yoshizawa-Fujita, M.; Takeoka, Y.; Rikukawa, M. Synthesis of Hydrophilic−Hydrophobic Block Copolymer Ionomers Based on Polyphenylenes. *ACS Macro Lett.* **2012**, *1*, 969−972.
(330) Wainright, J. S.; Wang, J.-T.; Weng, D.; Savinell, R. F.; Litt, M. Acid-Doped Polybenzimidazoles: A New Polymer Electrolyte. *J. Electrochem. Soc.* **1995**, *142*, L121.
(331) Yoshizawa, M.; Xu, W.; Angell, C. A. Ionic Liquids by Proton Transfer: Vapor Pressure, Conductivity, and the Relevance of ΔpK_a from Aqueous Solutions. *J. Am. Chem. Soc.* **2003**, *125*, 15411−15419.
(332) Nakamoto, H.; Watanabe, M. Brønsted Acid−Base Ionic Liquids for Fuel Cell Electrolytes. *Chem. Commun.* **2007**, *43*, 2539−2541.

DOI: 10.1021/acs.chemrev.6b00504
Chem. Rev. 2017, 117, 7190−7239

(333) Miran, M. S.; Kinoshita, H.; Yasuda, T.; Susan, M. A. B. H.; Watanabe, M. Physicochemical Properties Determined by ΔpKa for Protic Ionic Liquids based on an Organic Super-Strong Base with Various Brønsted Acids. *Phys. Chem. Chem. Phys.* **2012**, *14*, 5178−5186.
(334) Luo, H.; Baker, G. A.; Lee, J. S.; Pagni, R. M.; Dai, S. Ultrastable Superbase-Derived Protic Ionic Liquids. *J. Phys. Chem. B* **2009**, *113*, 4181−4183.
(335) Tsuzuki, S.; Shinoda, W.; Miran, M. S.; Kinoshita, H.; Yasuda, T.; Watanabe, M. Interactions in Ion Pairs of Protic Ionic Liquids: Comparison with Aprotic Ionic Liquids. *J. Chem. Phys.* **2013**, *139*, 174504.
(336) Yasuda, T.; Ogawa, A.; Kanno, M.; Mori, K.; Sakakibara, K.; Watanabe, M. Hydrophobic Protic Ionic Liquid for Nonhumidified Intermediate-temperature Fuel Cells. *Chem. Lett.* **2009**, *38*, 692−693.
(337) Anouti, M.; Caillon-Caravanier, M.; Dridi, Y.; Galiano, H.; Lemordant, D. Synthesis and Characterization of New Pyrrolidinium Based Protic Ionic Liquids. Good and Superionic Liquids. *J. Phys. Chem. B* **2008**, *112*, 13335−13343.
(338) Belieres, J.-P.; Angell, C. A. Protic Ionic Liquids: Preparation, Characterization, and Proton Free Energy Level Representation. *J. Phys. Chem. B* **2007**, *111*, 4926−4937.
(339) Luo, J.; Hu, J.; Saak, W.; Beckhaus, R.; Wittstock, G.; Vankelecom, I. F. J.; Agert, C.; Conrad, O. Protic Ionic Liquid and Ionic Melts Prepared from Methanesulfonic Acid and 1H-1,2,4-triazole as High Temperature PEMFC Electrolytes. *J. Mater. Chem.* **2011**, *21*, 10426−10436.
(340) Noda, A.; Susan, M. A. B. H.; Kudo, K.; Mitsushima, S.; Hayamizu, K.; Watanabe, M. Brønsted Acid−Base Ionic Liquids as Proton-Conducting Nonaqueous Electrolytes. *J. Phys. Chem. B* **2003**, *107*, 4024−4033.
(341) Tsunashima, K.; Fukushima, M.; Matsumiya, M. Physicochemical Properties of Trialkylphosphonium-Based Protic Ionic Liquids. *Electrochemistry* **2012**, *80*, 904−906.
(342) Rana, U. A.; Forsyth, M.; MacFarlane, D. R.; Pringle, J. M. Toward Protic Ionic Liquid and Organic Ionic Plastic Crystal Electrolytes for Fuel Cells. *Electrochim. Acta* **2012**, *84*, 213−222.
(343) Brigouleix, C.; Anouti, M.; Jacquemin, J.; Caillon-Caravanier, M.; Galiano, H.; Lemordant, D. Physicochemical Characterization of Morpholinium Cation Based Protic Ionic Liquids Used As Electrolytes. *J. Phys. Chem. B* **2010**, *114*, 1757−1766.
(344) Anouti, M.; Caillon-Caravanier, M.; Le Floch, C.; Lemordant, D. Alkylammonium-Based Protic Ionic Liquids. II. Ionic Transport and Heat-Transfer Properties: Fragility and Ionicity Rule. *J. Phys. Chem. B* **2008**, *112*, 9412−9416.
(345) Nakamoto, H.; Noda, A.; Hayamizu, K.; Hayashi, S.; Hamaguchi, H.; Watanabe, M. Proton-Conducting Properties of a Brønsted Acid−Base Ionic Liquid and Ionic Melts Consisting of Bis(trifluoromethanesulfonyl)imide and Benzimidazole for Fuel Cell Electrolytes. *J. Phys. Chem. C* **2007**, *111*, 1541−1548.
(346) Yasuda, T.; Kinoshita, H.; Miran, M. S.; Tsuzuki, S.; Watanabe, M. Comparative Study on Physicochemical Properties of Protic Ionic Liquids Based on Allylammonium and Propylammonium Cations. *J. Chem. Eng. Data* **2013**, *58*, 2724−2732.
(347) Susan, M. A. B. H.; Noda, A.; Mitsushima, S.; Watanabe, M. Brønsted Acid−Base Ionic Liquids and Their Use as New Materials for Anhydrous Proton Conductors. *Chem. Commun.* **2003**, *39*, 938.
(348) Miran, M. S.; Yasuda, T.; Susan, M. A. B. H.; Dokko, K.; Watanabe, M. Electrochemical Properties of Protic Ionic Liquids: Correlation Between Open Circuit Potential for H_2/O_2 cells Under Non-Humidified Conditions and ΔpKa. *RSC Adv.* **2013**, *3*, 4141.
(349) Miran, M. S.; Yasuda, T.; Susan, M. A. B. H.; Dokko, K.; Watanabe, M. Binary Protic Ionic Liquid Mixtures as a Proton Conductor: High Fuel Cell Reaction Activity and Facile Proton Transport. *J. Phys. Chem. C* **2014**, *118*, 27631−27639.
(350) Kanzaki, R.; Uchida, K.; Hara, S.; Umebayashi, Y.; Ishiguro, S.; Nomura, S. Acid−Base Property of Ethylammonium Nitrate Ionic Liquid Directly Obtained Using Ion-selective Field Effect Transistor Electrode. *Chem. Lett.* **2007**, *36*, 684−685.
(351) Michot, T.; Nishimoto, A.; Watanabe, M. Electrochemical Properties of Polymer Gel Electrolytes Based on Poly(vinylidene fluoride) Copolymer and Homopolymer. *Electrochim. Acta* **2000**, *45*, 1347−1360.
(352) Navarra, M. A.; Panero, S.; Scrosati, B. Novel, Ionic-Liquid-Based, Gel-Type Proton Membranes. *Electrochem. Solid-State Lett.* **2005**, *8*, A324−A327.
(353) Sekhon, S. S.; Krishnan, P.; Singh, B.; Yamada, K.; Kim, C. S. Proton Conducting Membrane Containing Room Temperature Ionic Liquid. *Electrochim. Acta* **2006**, *52*, 1639−1644.
(354) Gao, J.; Guo, Y.; Wu, B.; Qi, L.; Li, B.; Liu, J.; Wang, Z.; Liu, W.; Gu, J.; Zou, Z. Impact of Cation Selection on Proton Exchange Membrane Fuel Cell Performance with Trimethylethyl Amide, Ethylpyridinium and Ethylmethyl Imidazolium Ionic Liquid Carried by Poly(vinylidene fluoride) Membrane as Electrolyte. *J. Power Sources* **2014**, *251*, 432−438.
(355) Doyle, M.; Choi, S. K.; Proulx, G. High-Temperature Proton Conducting Membranes Based on Perfluorinated Ionomer Membrane-Ionic Liquid Composites. *J. Electrochem. Soc.* **2000**, *147*, 34.
(356) Sood, R.; Iojoiu, C.; Espuche, E.; Gouanvé, F.; Gebel, G.; Mendil-Jakani, H.; Lyonnard, S.; Jestin, J. Comparative Study of Proton Conducting Ionic Liquid Doped Nafion Membranes Elaborated by Swelling and Casting Methods: Processing Conditions, Morphology, and Functional Properties. *J. Phys. Chem. C* **2014**, *118*, 14157−14168.
(357) Di Noto, V.; Piga, M.; Giffin, G. A.; Lavina, S.; Smotkin, E. S.; Sanchez, J.-Y.; Iojoiu, C. Influence of Anions on Proton-Conducting Membranes Based on Neutralized Nafion 117, Triethylammonium Methanesulfonate, and Triethylammonium Perfluorobutanesulfonate. 1. Synthesis and Properties. *J. Phys. Chem. C* **2012**, *116*, 1361−1369.
(358) Di Noto, V.; Piga, M.; Giffin, G. A.; Lavina, S.; Smotkin, E. S.; Sanchez, J.-Y.; Iojoiu, C. Influence of Anions on Proton-Conducting Membranes Based on Neutralized Nafion 117, Triethylammonium Methanesulfonate, and Triethylammonium Perfluorobutanesulfonate. 2. Electrical Properties. *J. Phys. Chem. C* **2012**, *116*, 1370−1379.
(359) Sood, R.; Iojoiu, C.; Espuche, E.; Gouanvé, F.; Gebel, G.; Mendil-Jakani, H.; Lyonnard, S.; Jestin, J. Proton Conducting Ionic Liquid Doped Nafion Membranes: Nano-Structuration, Transport Properties and Water Sorption. *J. Phys. Chem. C* **2012**, *116*, 24413−24423.
(360) Iojoiu, C.; Hana, M.; Molmeret, Y.; Martinez, M.; Cointeaux, L.; El Kissi, N.; Teles, J.; Leprêtre, J. C.; Judeinstein, P.; Sanchez, J. Y. Ionic Liquids and Their Hosting by Polymers for HT-PEMFC Membranes. *Fuel Cells* **2010**, *10*, 778−789.
(361) Martinez, M.; Molmeret, Y.; Cointeaux, L.; Iojoiu, C.; Leprêtre, J.-C.; El Kissi, N.; Judeinstein, P.; Sanchez, J.-Y. Proton-Conducting Ionic Liquid-based Proton Exchange Membrane Fuel Cell Membranes: The Key Role of Ionomer−Ionic Liquid Interaction. *J. Power Sources* **2010**, *195*, 5829−5839.
(362) Iojoiu, C.; Martinez, M.; Hanna, M.; Molmeret, Y.; Cointeaux, L.; Leprêtre, J.-C.; Kissi, N. E.; Guindet, J.; Judeinstein, P.; Sanchez, J.-Y. PILs-Based Nafion Membranes: A Route to High-Temperature PEFMCs Dedicated to Electric and Hybrid Vehicles. *Polym. Adv. Technol.* **2008**, *19*, 1406−1414.
(363) Sun, D.; Zhou, J. Ionic Liquid Confined in Nafion: Toward Molecular-Level Understanding. *AIChE J.* **2013**, *59*, 2630−2639.
(364) Sunda, A. P. Ammonium-Based Protic Ionic Liquid Doped Nafion Membranes as Anhydrous Fuel Cell Electrolytes. *J. Mater. Chem. A* **2015**, *3*, 12905−12912.
(365) Kim, S. Y.; Kim, S.; Park, M. J. Enhanced Proton Transport in Nanostructured Polymer Electrolyte/Ionic Liquid Membranes Under Water-Free Conditions. *Nat. Commun.* **2010**, *1*, 1.
(366) Hoarfrost, M. L.; Tyagi, M. S.; Segalman, R. A.; Reimer, J. A. Effect of Confinement on Proton Transport Mechanisms in Block Copolymer/Ionic Liquid Membranes. *Macromolecules* **2012**, *45*, 3112−3120.
(367) Lee, S.-Y.; Yasuda, T.; Watanabe, M. Fabrication of Protic Ionic Liquid/Sulfonated Polyimide Composite Membranes for Non-Humidified Fuel Cells. *J. Power Sources* **2010**, *195*, 5909−5914.

DOI: 10.1021/acs.chemrev.6b00504
Chem. Rev. 2017, 117, 7190−7239

(368) Lee, S.-Y.; Ogawa, A.; Kanno, M.; Nakamoto, H.; Yasuda, T.; Watanabe, M. Nonhumidified Intermediate Temperature Fuel Cells Using Protic Ionic Liquids. *J. Am. Chem. Soc.* **2010**, *132*, 9764−9773.
(369) Yasuda, T.; Nakamura, S.-i.; Honda, Y.; Kinugawa, K.; Lee, S.-Y.; Watanabe, M. Effects of Polymer Structure on Properties of Sulfonated Polyimide/Protic Ionic Liquid Composite Membranes for Nonhumidified Fuel Cell Applications. *ACS Appl. Mater. Interfaces* **2012**, *4*, 1783−1790.
(370) Yasuda, T.; Watanabe, M. Protic Ionic Liquids: Fuel Cell Applications. *MRS Bull.* **2013**, *38*, 560−566.
(371) Mamlouk, M.; Ocon, P.; Scott, K. Preparation and Characterization of Polybenzimidzaole/Diethylamine Hydrogen Sulphate for Medium Temperature Proton Exchange Membrane Fuel Cells. *J. Power Sources* **2014**, *245*, 915−926.
(372) Ryoo, R.; Joo, S. H.; Kruk, M.; Jaroniec, M. Ordered Mesoporous Carbons. *Adv. Mater.* **2001**, *13*, 677−681.
(373) Liang, C. D.; Li, Z. J.; Dai, S. Mesoporous Carbon Materials: Synthesis and Modification. *Angew. Chem., Int. Ed.* **2008**, *47*, 3696−3717.
(374) Shao, Y. Y.; Sui, J. H.; Yin, G. P.; Gao, Y. Z. Nitrogen-Doped Carbon Nanostructures and Their Composites as Catalytic Materials for Proton Exchange Membrane Fuel Cell. *Appl. Catal., B* **2008**, *79*, 89−99.
(375) Ewels, C. P.; Glerup, M. Nitrogen Doping in Carbon Nanotubes. *J. Nanosci. Nanotechnol.* **2005**, *5*, 1345−1363.
(376) Wang, H. B.; Maiyalagan, T.; Wang, X. Review on Recent Progress in Nitrogen-Doped Graphene: Synthesis, Characterization, and Its Potential Applications. *ACS Catal.* **2012**, *2*, 781−794.
(377) Pachfule, P.; Dhavale, V. M.; Kandambeth, S.; Kurungot, S.; Banerjee, R. Porous-Organic-Framework-Templated Nitrogen-Rich Porous Carbon as a More Proficient Electrocatalyst than Pt/C for the Electrochemical Reduction of Oxygen. *Chem. - Eur. J.* **2013**, *19*, 974−980.
(378) Ma, T.-Y.; Liu, L.; Yuan, Z.-Y. Direct Synthesis of Ordered Mesoporous Carbons. *Chem. Soc. Rev.* **2013**, *42*, 3977−4003.
(379) Paraknowitsch, J. P.; Zhang, J.; Su, D.; Thomas, A.; Antonietti, M. Ionic Liquids as Precursors for Nitrogen-Doped Graphitic Carbon. *Adv. Mater.* **2010**, *22*, 87−92.
(380) Zhang, S. G.; Miran, M. S.; Ikoma, A.; Dokko, K.; Watanabe, M. Protic Ionic Liquids and Salts as Versatile Carbon Precursors. *J. Am. Chem. Soc.* **2014**, *136*, 1690−1693.
(381) Czerw, R.; Terrones, M.; Charlier, J. C.; Blase, X.; Foley, B.; Kamalakaran, R.; Grobert, N.; Terrones, H.; Tekleab, D.; Ajayan, P. M.; et al. Identification of Electron Donor States in N-Doped Carbon Nanotubes. *Nano Lett.* **2001**, *1*, 457−460.
(382) Yang, Q. H.; Xu, W. H.; Tomita, A.; Kyotani, T. Double Coaxial Structure and Dual Physicochemical Properties of Carbon Nanotubes Composed of Stacked Nitrogen-Doped and Undoped Multiwalls. *Chem. Mater.* **2005**, *17*, 2940−2945.
(383) Wiggins-Camacho, J. D.; Stevenson, K. J. Effect of Nitrogen Concentration on Capacitance, Density of States, Electronic Conductivity, and Morphology of N-Doped Carbon Nanotube Electrodes. *J. Phys. Chem. C* **2009**, *113*, 19082−19090.
(384) Zhang, S.; Dokko, K.; Watanabe, M. Direct Synthesis of Nitrogen-doped Carbon Materials from Protic Ionic Liquids and Protic Salts: Structural and Physicochemical Correlations between Precursor and Carbon. *Chem. Mater.* **2014**, *26*, 2915−2926.
(385) Sakaushi, K.; Antonietti, M. Carbon- and Nitrogen-Based Porous Solids: A Recently Emerging Class of Materials. *Bull. Chem. Soc. Jpn.* **2015**, *88*, 386−398.
(386) Palkovits, R.; Antonietti, M.; Kuhn, P.; Thomas, A.; Schuth, F. Solid Catalysts for the Selective Low-Temperature Oxidation of Methane to Methanol. *Angew. Chem., Int. Ed.* **2009**, *48*, 6909−6912.
(387) Zheng, Y.; Jiao, Y.; Jaroniec, M.; Jin, Y. G.; Qiao, S. Z. Nanostructured Metal-Free Electrochemical Catalysts for Highly Efficient Oxygen Reduction. *Small* **2012**, *8*, 3550−3566.
(388) Choi, C. H.; Park, S. H.; Woo, S. I. Phosphorus-Nitrogen Dual Doped Carbon as an Effective Catalyst for Oxygen Reduction Reaction in Acidic Media: Effects of the Amount of P-Doping on the Physical and Electrochemical Properties of Carbon. *J. Mater. Chem.* **2012**, *22*, 12107−12115.
(389) Gao, W.; Feng, X.; Zhang, T.; Huang, H.; Li, J.; Song, W. One-Step Pyrolytic Synthesis of Nitrogen and Sulfur Dual-Doped Porous Carbon with High Catalytic Activity and Good Accessibility to Small Biomolecules. *ACS Appl. Mater. Interfaces* **2014**, *6*, 19109−19117.
(390) Fuertes, A.; Ferrero, G.; Sevilla, M. One-Pot Synthesis of Microporous Carbons Highly Enriched in Nitrogen and Their Electrochemical Performance. *J. Mater. Chem. A* **2014**, *2*, 14439−14448.
(391) Zhang, S.; Dokko, K.; Watanabe, M. Carbon Materialization of Ionic Liquids: from Solvents to Materials. *Mater. Horiz.* **2015**, *2*, 168−197.
(392) Paraknowitsch, J. P.; Thomas, A. Functional Carbon Materials from Ionic Liquid Precursors. *Macromol. Chem. Phys.* **2012**, *213*, 1132−1145.
(393) Fellinger, T. P.; Thomas, A.; Yuan, J.; Antonietti, M. 25th Anniversary Article:"Cooking Carbon with Salt": Carbon Materials and Carbonaceous Frameworks from Ionic Liquids and Poly (ionic liquid) s. *Adv. Mater.* **2013**, *25*, 5838−5855.
(394) Xie, Z. L.; Su, D. S. Ionic Liquid Based Approaches to Carbon Materials Synthesis. *Eur. J. Inorg. Chem.* **2015**, *2015*, 1137−1147.
(395) Wooster, T. J.; Johanson, K. M.; Fraser, K. J.; MacFarlane, D. R.; Scott, J. L. Thermal Degradation of Cyano Containing Ionic Liquids. *Green Chem.* **2006**, *8*, 691−696.
(396) Lee, J. S.; Wang, X.; Luo, H.; Baker, G. A.; Dai, S. Facile Ionothermal Synthesis of Microporous and Mesoporous Carbons from Task Specific Ionic Liquids. *J. Am. Chem. Soc.* **2009**, *131*, 4596−4597.
(397) Lee, J. S.; Wang, X. Q.; Luo, H. M.; Dai, S. Fluidic Carbon Precursors for Formation of Functional Carbon under Ambient Pressure Based on Ionic Liquids. *Adv. Mater.* **2010**, *22*, 1004−1007.
(398) Zhu, X.; Hillesheim, P. C.; Mahurin, S. M.; Wang, C. M.; Tian, C. C.; Brown, S.; Luo, H. M.; Veith, G. M.; Han, K. S.; Hagaman, E. W.; et al. Efficient CO_2 Capture by Porous, Nitrogen-Doped Carbonaceous Adsorbents Derived from Task-Specific Ionic Liquids. *ChemSusChem* **2012**, *5*, 1912−1917.
(399) Fellinger, T.-P.; Su, D. S.; Engenhorst, M.; Gautam, D.; Schlögl, R.; Antonietti, M. Thermolytic Synthesis of Graphitic Boron Carbon Nitride from an Ionic Liquid Precursor: Mechanism, Structure Analysis and Electronic Properties. *J. Mater. Chem.* **2012**, *22*, 23996−24005.
(400) Paraknowitsch, J. P.; Wienert, B.; Zhang, Y.; Thomas, A. Intrinsically Sulfur-and Nitrogen-Co-doped Carbons from Thiazolium Salts. *Chem. - Eur. J.* **2012**, *18*, 15416−15423.
(401) Fahsi, K.; Dumail, X.; Dutremez, S. G.; van der Lee, A.; Vioux, A.; Viau, L. Diacetylenes with Ionic-Liquid-Like Substituents: Associating a Polymerizing Cation with a Polymerizing Anion in a Single Precursor for the Synthesis of N-Doped Carbon Materials. *Chem. - Eur. J.* **2016**, *22*, 1682−1695.
(402) Paraknowitsch, J. P.; Thomas, A.; Antonietti, M. A Detailed View on the Polycondensation of Ionic Liquid Monomers Towards Nitrogen Doped Carbon Materials. *J. Mater. Chem.* **2010**, *20*, 6746−6758.
(403) Yuan, J.; Antonietti, M. Poly(ionic liquid)s: Polymers Expanding Classical Property Profiles. *Polymer* **2011**, *52*, 1469−1482.
(404) Yuan, J.; Mecerreyes, D.; Antonietti, M. Poly(ionic liquid)s: An Update. *Prog. Polym. Sci.* **2013**, *38*, 1009−1036.
(405) Lu, J.; Yan, F.; Texter, J. Advanced Applications of Ionic Liquids in Polymer Science. *Prog. Polym. Sci.* **2009**, *34*, 431−448.
(406) Green, O.; Grubjesic, S.; Lee, S.; Firestone, M. A. The Design of Polymeric Ionic Liquids for the Preparation of Functional Materials. *Polym. Rev.* **2009**, *49*, 339−360.
(407) Yuan, J.; Márquez, A. G.; Reinacher, J.; Giordano, C.; Janek, J.; Antonietti, M. Nitrogen-Doped Carbon Fibers and Membranes by Carbonization of Electrospun Poly(ionic liquid)s. *Polym. Chem.* **2011**, *2*, 1654−1657.
(408) Zhao, Q.; Fellinger, T. P.; Antonietti, M.; Yuan, J. Nitrogen-Doped Carbon Capsules via Poly (ionic liquid)-Based Layer-by-Layer Assembly. *Macromol. Rapid Commun.* **2012**, *33*, 1149−1153.

DOI: 10.1021/acs.chemrev.6b00504
Chem. Rev. 2017, 117, 7190−7239

(409) Men, Y.; Siebenbürger, M.; Qiu, X.; Antonietti, M.; Yuan, J. Low Fractions of Ionic Liquid or Poly(ionic liquid) can Activate Polysaccharide Biomass into Shaped, Flexible and Fire-Retardant Porous Carbons. *J. Mater. Chem. A* **2013**, *1*, 11887−11893.
(410) Einert, M.; Wessel, C.; Badaczewski, F.; Leichtweiß, T.; Eufinger, C.; Janek, J.; Yuan, J.; Antonietti, M.; Smarsly, B. M. Nitrogen-Doped Carbon Electrodes: Influence of Microstructure and Nitrogen Configuration on the Electrical Conductivity of Carbonized Polyacrylonitrile and Poly (ionic liquid) Blends. *Macromol. Chem. Phys.* **2015**, *216*, 1930−1944.
(411) Li, J.; Zhu, W.; Ji, J. W.; Wang, P.; Lan, Y.; Gao, N.; Yin, X. P.; Wang, H.; Li, G. T. Pyrrole-Terminated Ionic Liquid Surfactant: One Molecule with Multiple Functions for Controlled Synthesis of Diverse Multispecies Co-Doped Porous Hollow Carbon Spheres. *ACS Appl. Mater. Interfaces* **2016**, *8*, 11008−11017.
(412) Yuan, J.; Giordano, C.; Antonietti, M. Ionic Liquid Monomers and Polymers as Precursors of Highly Conductive, Mesoporous, Graphitic Carbon Nanostructures. *Chem. Mater.* **2010**, *22*, 5003−5012.
(413) Wu, B.; Kuang, Y.; Zhang, Y.; Zhang, X.; Chen, J. Carbonization of Ionic Liquid Polymer-Functionalized Carbon Nanotubes for High Dispersion of PtRu Nanoparticles and Their Electrocatalytic Oxidation of Methanol. *J. Mater. Chem.* **2012**, *22*, 13085−13090.
(414) Balach, J.; Wu, H.; Polzer, F.; Kirmse, H.; Zhao, Q.; Wei, Z.; Yuan, J. Poly (Ionic Liquid)-Derived Nitrogen-Doped Hollow Carbon Spheres: Synthesis and Loading with Fe_2O_3 for High-Performance Lithium Ion Batteries. *RSC Adv.* **2013**, *3*, 7979−7986.
(415) Kuzmicz, D.; Coupillaud, P.; Men, Y.; Vignolle, J.; Vendraminetto, G.; Ambrogi, M.; Taton, D.; Yuan, J. Functional Mesoporous Poly(ionic liquid)-Based Copolymer Monoliths: From Synthesis to Catalysis and Microporous Carbon Production. *Polymer* **2014**, *55*, 3423−3430.
(416) Bo, X.; Bai, J.; Ju, J.; Guo, L. Highly Dispersed Pt Nanoparticles Supported on Poly(ionic liquids) Derived Hollow Carbon Spheres for Methanol Oxidation. *J. Power Sources* **2011**, *196*, 8360−8365.
(417) Antonietti, M.; Kuang, D.; Smarsly, B.; Zhou, Y. Ionic Liquids for the Convenient Synthesis of Functional Nanoparticles and Other Inorganic Nanostructures. *Angew. Chem., Int. Ed.* **2004**, *43*, 4988−4992.
(418) Abbott, A. P.; Capper, G.; Davies, D. L.; Rasheed, R. K.; Tambyrajah, V. Novel Solvent Properties of Choline Chloride/Urea Mixtures. *Chem. Commun.* **2003**, 70−71.
(419) Parnham, E. R.; Drylie, E. A.; Wheatley, P. S.; Slawin, A. M.; Morris, R. E. Ionothermal Materials Synthesis Using Unstable Deep-Eutectic Solvents as Template-Delivery Agents. *Angew. Chem.* **2006**, *118*, 5084−5088.
(420) Wagle, D. V.; Zhao, H.; Baker, G. A. Deep Eutectic Solvents: Sustainable Media for Nanoscale and Functional Materials. *Acc. Chem. Res.* **2014**, *47*, 2299−2308.
(421) Gutiérrez, M. a. C.; Rubio, F.; del Monte, F. Resorcinol-Formaldehyde Polycondensation in Deep Eutectic Solvents for the Preparation of Carbons and Carbon− Carbon Nanotube Composites. *Chem. Mater.* **2010**, *22*, 2711−2719.
(422) Carriazo, D.; Gutiérrez, M. a. C.; Ferrer, M. L.; del Monte, F. Resorcinol-Based Deep Eutectic Solvents as Both Carbonaceous Precursors and Templating Agents in the Synthesis of Hierarchical Porous Carbon Monoliths. *Chem. Mater.* **2010**, *22*, 6146−6152.
(423) Carriazo, D.; Gutiérrez, M. C.; Picó, F.; Rojo, J. M.; Fierro, J. L.; Ferrer, M. L.; del Monte, F. Phosphate-Functionalized Carbon Monoliths from Deep Eutectic Solvents and their Use as Monolithic Electrodes in Supercapacitors. *ChemSusChem* **2012**, *5*, 1405−1409.
(424) Patiño, J.; Gutiérrez, M. C.; Carriazo, D.; Ania, C. O.; Parra, J. B.; Ferrer, M. L.; del Monte, F. Deep Eutectic Assisted Synthesis of Carbon Adsorbents Highly Suitable for Low-Pressure Separation of CO_2−CH_4 Gas Mixtures. *Energy Environ. Sci.* **2012**, *5*, 8699−8707.
(425) Gutiérrez, M. C.; Carriazo, D.; Ania, C. O.; Parra, J. B.; Ferrer, M. L.; del Monte, F. Deep Eutectic Solvents as Both Precursors and Structure Directing Agents in the Synthesis of Nitrogen Doped Hierarchical Carbons Highly Suitable for CO_2 Capture. *Energy Environ. Sci.* **2011**, *4*, 3535−3544.
(426) Patiño, J.; Gutiérrez, M.; Carriazo, D.; Ania, C.; Fierro, J.; Ferrer, M.; del Monte, F. DES Assisted Synthesis of Hierarchical Nitrogen-Doped Carbon Molecular Sieves for Selective CO_2 Versus N_2 Adsorption. *J. Mater. Chem. A* **2014**, *2*, 8719−8729.
(427) Carriazo, D.; Gutiérrez, M. C.; Jiménez, R.; Ferrer, M. L.; del Monte, F. Deep-Eutectic-Assisted Synthesis of Bimodal Porous Carbon Monoliths with High Electrical Conductivities. *Particle & Particle Systems Characterization* **2013**, *30*, 316−320.
(428) Gutiérrez, M. C.; Carriazo, D.; Tamayo, A.; Jiménez, R.; Picó, F.; Rojo, J. M.; Ferrer, M. L.; del Monte, F. Deep-Eutectic-Solvent-Assisted Synthesis of Hierarchical Carbon Electrodes Exhibiting Capacitance Retention at High Current Densities. *Chem. - Eur. J.* **2011**, *17*, 10533−10537.
(429) López-Salas, N.; Gutiérrez, M. C.; Ania, C. O.; Fierro, J. L. G.; Ferrer, M. L.; del Monte, F. Efficient Nitrogen-Doping and Structural Control of Hierarchical Carbons using Unconventional Precursors in the Form of Deep Eutectic Solvents. *J. Mater. Chem. A* **2014**, *2*, 17387−17399.
(430) Zhang, S. G.; Ikoma, A.; Ueno, K.; Chen, Z. J.; Dokko, K.; Watanabe, M. Protic-Salt-Derived Nitrogen/Sulfur-Codoped Mesoporous Carbon for the Oxygen Reduction Reaction and Supercapacitors. *ChemSusChem* **2015**, *8*, 1608−1617.
(431) Zhang, S. G.; Li, Z.; Ueno, K.; Tatara, R.; Dokko, K.; Watanabe, M. One-Step, Template-Free Synthesis of Highly Porous Nitrogen/Sulfur-Codoped Carbons from a Single Protic Salt and Their Application to CO_2 Capture. *J. Mater. Chem. A* **2015**, *3*, 17849−17857.
(432) Zhang, S. G.; Kwon, H. M.; Li, Z.; Ikoma, A.; Dokko, K.; Watanabe, M. Nitrogen-Doped Inverse Opal Carbons Derived from an Ionic Liquid Precursor for the Oxygen Reduction Reaction. *ChemElectroChem* **2015**, *2*, 1080−1085.
(433) Zhang, S. G.; Mandai, T.; Ueno, K.; Dokko, K.; Watanabe, M. Hydrogen-Bonding Supramolecular Protic Salt as an "All-In-One" Precursor for Nitrogen-Doped Mesoporous Carbons for CO_2 Adsorption. *Nano Energy* **2015**, *13*, 376−386.
(434) Wang, X. Q.; Dai, S. Ionic Liquids as Versatile Precursors for Functionalized Porous Carbon and Carbon-Oxide Composite Materials by Confined Carbonization. *Angew. Chem., Int. Ed.* **2010**, *49*, 6664−6668.
(435) Fulvio, P. F.; Hillesheim, P. C.; Bauer, J. C.; Mahurin, S. M.; Dai, S. Magadiite Templated High Surface Area Graphene-Type Carbons from Metal-Halide Based Ionic Liquids. *J. Mater. Chem. A* **2013**, *1*, 59−62.
(436) Chen, S.; Lim, H. E.; Miyata, Y.; Kitaura, R.; Bando, Y.; Golberg, D.; Shinohara, H. Transformation of Ionic Liquid into Carbon Nanotubes in Confined Nanospace. *Chem. Commun.* **2011**, *47*, 10368−10370.
(437) Ding, Y. X.; Sun, X. Y.; Zhang, L. Y.; Mao, S. J.; Xie, Z. L.; Liu, Z. W.; Su, D. S. Entrapping an Ionic Liquid with Nanocarbon: The Formation of a Tailorable and Functional Surface. *Angew. Chem., Int. Ed.* **2015**, *54*, 231−235.
(438) Yi, Y. S.; Lu, Z. G.; Ni, M.; Li, L.; Leung, M. K. H. Facile Synthesis of Nitrogen and Sulfur Codoped Carbon from Ionic Liquid as Metal-Free Catalyst for Oxygen Reduction Reaction. *ACS Appl. Mater. Interfaces* **2015**, *7*, 7214−7221.
(439) Zhang, J.; Xu, D.; Qian, W.; Zhu, J.; Yan, F. Host−Guest Inclusion Complexes Derived Heteroatom-Doped Porous Carbon Materials. *Carbon* **2016**, *105*, 183−190.
(440) Sa, Y. J.; Park, C.; Jeong, H. Y.; Park, S. H.; Lee, Z.; Kim, K. T.; Park, G. G.; Joo, S. H. Carbon Nanotubes/Heteroatom-Doped Carbon Core-Sheath Nanostructures as Highly Active, Metal-Free Oxygen Reduction Electrocatalysts for Alkaline Fuel Cells. *Angew. Chem., Int. Ed.* **2014**, *53*, 4102−4106.
(441) Yu, C.; Fang, H.; Liu, Z.; Hu, H.; Meng, X.; Qiu, J. Chemically Grafting Graphene Oxide to B, N Co-Doped Graphene via Ionic Liquid and Their Superior Performance for Triiodide Reduction. *Nano Energy* **2016**, *25*, 184−192.

DOI: 10.1021/acs.chemrev.6b00504
Chem. Rev. 2017, 117, 7190−7239

(442) Wilson, B. E.; He, S. Y.; Buffington, K.; Rudisill, S.; Smyrl, W. H.; Stein, A. Utilizing Ionic Liquids for Controlled N-Doping in Hard-Templated, Mesoporous Carbon Electrodes for High-Performance Electrochemical Double-Layer Capacitors. *J. Power Sources* **2015**, *298*, 193−202.
(443) Zhu, J. Y.; Xu, D.; Qian, W. J.; Zhang, J. Y.; Yan, F. Heteroatom-Containing Porous Carbons Derived from Ionic Liquid-Doped Alkali Organic Salts for Supercapacitors. *Small* **2016**, *12*, 1935−1944.
(444) Zhu, C. Z.; Zhai, J. F.; Dong, S. J. Ionic Liquid-Induced Three-Dimensional Macroassembly of Graphene and its Applications in Electrochemical Energy Storage. *Nanoscale* **2014**, *6*, 10077−10083.
(445) Zhao, L.; Hu, Y. S.; Li, H.; Wang, Z. X.; Chen, L. Q. Porous $Li_4Ti_5O_{12}$ Coated with N-Doped Carbon from Ionic Liquids for Li-Ion Batteries. *Adv. Mater.* **2011**, *23*, 1385−1388.
(446) Ding, Z.; Zhao, L.; Suo, L.; Jiao, Y.; Meng, S.; Hu, Y.-S.; Wang, Z.; Chen, L. Towards Understanding the Effects of Carbon and Nitrogen-Doped Carbon Coating on the Electrochemical Performance of $Li_4Ti_5O_{12}$ in Lithium Ion Batteries: a Combined Experimental and Theoretical Study. *Phys. Chem. Chem. Phys.* **2011**, *13*, 15127−15133.
(447) Cao, J.; Chu, Y.; Tan, X. Pt/XC-72 Catalysts Coated with Nitrogen-Doped Carbon (Pt/XC-72@ C−N) for Methanol Electro-Oxidation. *Mater. Chem. Phys.* **2014**, *144*, 17−24.
(448) Tuaev, X.; Paraknowitsch, J. P.; Illgen, R.; Thomas, A.; Strasser, P. Nitrogen-Doped Coatings on Carbon Nanotubes and Their Stabilizing Effect on Pt Nanoparticles. *Phys. Chem. Chem. Phys.* **2012**, *14*, 6444−6447.
(449) Jin, Z. Y.; Lu, A. H.; Xu, Y. Y.; Zhang, J. T.; Li, W. C. Ionic Liquid-Assisted Synthesis of Microporous Carbon Nanosheets for Use in High Rate and Long Cycle Life Supercapacitors. *Adv. Mater.* **2014**, *26*, 3700−3705.
(450) Yan, Y.; Yin, Y.-X.; Xin, S.; Guo, Y.-G.; Wan, L.-J. Ionothermal Synthesis of Sulfur-Doped Porous Carbons Hybridized with Graphene as Superior Anode Materials for Lithium-Ion Batteries. *Chem. Commun.* **2012**, *48*, 10663−10665.
(451) Zhou, M.; Li, X.; Cui, J.; Liu, T.; Cai, T.; Zhang, H.; Guan, S. Synthesis and Capacitive Performances of Graphene/N-Doping Porous Carbon Composite with High Nitrogen Content and Two-Dimensional Nanoarchitecture. *Int. J. Electrochem. Sci.* **2012**, *7*, 9984−9996.
(452) Liu, J.-Y.; Chang, H.-Y.; Truong, Q.-D.; Ling, Y.-C. Synthesis of Nitrogen-Doped Graphene by Pyrolysis of Ionic-Liquid-Functionalized Graphene. *J. Mater. Chem. C* **2013**, *1*, 1713−1716.
(453) Guo, D.-C.; Mi, J.; Hao, G.-P.; Dong, W.; Xiong, G.; Li, W.-C.; Lu, A.-H. Ionic Liquid $C_{16}mimBF_4$ Assisted Synthesis of Poly(benzoxazine-co-resol)-Based Hierarchically Porous Carbons with Superior Performance in Supercapacitors. *Energy Environ. Sci.* **2013**, *6*, 652−659.
(454) Fuchs, I.; Fechler, N.; Antonietti, M.; Mastai, Y. Enantioselective Nanoporous Carbon Based on Chiral Ionic Liquids. *Angew. Chem., Int. Ed.* **2016**, *55*, 408−412.
(455) Yang, W.; Fellinger, T. P.; Antonietti, M. Efficient Metal-Free Oxygen Reduction in Alkaline Medium on High-Surface-Area Mesoporous Nitrogen-Doped Carbons Made from Ionic Liquids and Nucleobases. *J. Am. Chem. Soc.* **2011**, *133*, 206−209.
(456) Gong, K. P.; Du, F.; Xia, Z. H.; Durstock, M.; Dai, L. M. Nitrogen-Doped Carbon Nanotube Arrays with High Electrocatalytic Activity for Oxygen Reduction. *Science* **2009**, *323*, 760−764.
(457) Meng, Y.; Gu, D.; Zhang, F.; Shi, Y.; Yang, H.; Li, Z.; Yu, C.; Tu, B.; Zhao, D. Ordered Mesoporous Polymers and Homologous Carbon Frameworks: Amphiphilic Surfactant Templating and Direct Transformation. *Angew. Chem.* **2005**, *117*, 7215−7221.
(458) Zhang, S.; Tsuzuki, S.; Ueno, K.; Dokko, K.; Watanabe, M. Upper Limit of Nitrogen Content in Carbon Materials. *Angew. Chem., Int. Ed.* **2015**, *54*, 1302−1306.
(459) Fulvio, P. F.; Lee, J. S.; Mayes, R. T.; Wang, X.; Mahurin, S. M.; Dai, S. Boron and Nitrogen-Rich Carbons from Ionic Liquid Precursors with Tailorable Surface Properties. *Phys. Chem. Chem. Phys.* **2011**, *13*, 13486−13491.
(460) He, F.; Chen, X.; Shen, Y.; Li, Y.; Liu, A.; Liu, S.; Mori, T.; Zhang, Y. Ionic Liquid-Derived Fe−N/C Catalysts for Highly Efficient Oxygen Reduction Reaction without any Supports,Ttemplates, or Multi-Step Pyrolysis. *J. Mater. Chem. A* **2016**, *4*, 6630−6638.
(461) Li, Z. L.; Li, G. L.; Jiang, L. H.; Li, J. L.; Sun, G. Q.; Xia, C. G.; Li, F. W. Ionic Liquids as Precursors for Efficient Mesoporous Iron-Nitrogen-Doped Oxygen Reduction Electrocatalysts. *Angew. Chem., Int. Ed.* **2015**, *54*, 1494−1498.
(462) Kim, T. W.; Park, I. S.; Ryoo, R. A Synthetic Route to Ordered Mesoporous Carbon Materials with Graphitic Pore Walls. *Angew. Chem., Int. Ed.* **2003**, *42*, 4375−4379.
(463) Kim, C. H.; Lee, D. K.; Pinnavaia, T. J. Graphitic Mesostructured Carbon Prepared from Aromatic Precursors. *Langmuir* **2004**, *20*, 5157−5159.
(464) Iyer, V. S.; Vollhardt, K. P. C.; Wilhelm, R. Near-Quantitative Solid-State Synthesis of Carbon Nanotubes from Homogeneous Diphenylethynecobalt and -nickel Complexes. *Angew. Chem., Int. Ed.* **2003**, *42*, 4379−4383.
(465) Xia, Y. D.; Mokaya, R. Synthesis of Ordered Mesoporous Carbon and Nitrogen-Doped Carbon Materials with Graphitic Pore Walls via a Simple Chemical Vapor Deposition Method. *Adv. Mater.* **2004**, *16*, 1553−1558.
(466) Kyotani, M.; Matsushita, S.; Nagai, T.; Matsui, Y.; Shimomura, M.; Kaito, A.; Akagi, K. Helical Carbon and Graphitic Films Prepared from Iodine-Doped Helical Polyacetylene Film using Morphology-Retaining Carbonization. *J. Am. Chem. Soc.* **2008**, *130*, 10880−10881.
(467) Ding, W.; Wei, Z.; Chen, S.; Qi, X.; Yang, T.; Hu, J.; Wang, D.; Wan, L.-J.; Alvi, S. F.; Li, L. Space-Confinement-Induced Synthesis of Pyridinic- and Pyrrolic-Nitrogen-Doped Graphene for the Catalysis of Oxygen Reduction. *Angew. Chem., Int. Ed.* **2013**, *52*, 11755−11759.
(468) Dillon, A. C.; Gennett, T.; Jones, K. M.; Alleman, J. L.; Parilla, P. A.; Heben, M. J. A Simple and Complete Purification of Single-Walled Carbon Nanotube Materials. *Adv. Mater.* **1999**, *11*, 1354−1358.
(469) Kruk, M.; Jaroniec, M.; Ryoo, R.; Joo, S. H. Characterization of Ordered Mesoporous Carbons Synthesized using MCM-48 Silicas as Templates. *J. Phys. Chem. B* **2000**, *104*, 7960−7968.
(470) Carvalho, A. C. M.; dos Santos, M. C. Nitrogen-Substituted Nanotubes and Nanojunctions: Conformation and Electronic Properties. *J. Appl. Phys.* **2006**, *100*, 08430510.1063/1.2357646.
(471) Fulvio, P. F.; Hillesheim, P. C.; Oyola, Y.; Mahurin, S. M.; Veith, G. M.; Dai, S. A New Family of Fluidic Precursors for the Self-Templated Synthesis of Hierarchical Nanoporous Carbons. *Chem. Commun.* **2013**, *49*, 7289−7291.
(472) Zhao, Q.; Fellinger, T.-P.; Antonietti, M.; Yuan, J. A Novel Polymeric Precursor for Micro/Mesoporous Nitrogen-Doped Carbons. *J. Mater. Chem. A* **2013**, *1*, 5113−5120.
(473) Lim, K. H.; Kim, H. Nitrogen-Doped Carbon Catalysts Derived from Ionic Liquids in the Presence of Transition Metals for the Oxygen Reduction Reaction. *Appl. Catal., B* **2014**, *158−159*, 355−360.
(474) Ma, Z.; Yu, J.; Dai, S. Preparation of Inorganic Materials using Ionic Liquids. *Adv. Mater.* **2010**, *22*, 261−285.
(475) Fellinger, T. P.; Hasche, F.; Strasser, P.; Antonietti, M. Mesoporous Nitrogen-Doped Carbon for the Electrocatalytic Synthesis of Hydrogen Peroxide. *J. Am. Chem. Soc.* **2012**, *134*, 4072−4075.
(476) Fechler, N.; Fellinger, T. P.; Antonietti, M. Salt Templating": a Simple and Sustainable Pathway Toward Highly Porous Functional Carbons from Ionic Liquids. *Adv. Mater.* **2013**, *25*, 75−79.
(477) Mascotto, S.; Kuzmicz, D.; Wallacher, D.; Siebenbürger, M.; Clemens, D.; Risse, S.; Yuan, J.; Antonietti, M.; Ballauff, M. Poly(ionic liquid)-Derived Nanoporous Carbon Analyzed by Combination of Gas Physisorption and Small-Angle Neutron Scattering. *Carbon* **2015**, *82*, 425−435.
(478) Fechler, N.; Tiruye, G. A.; MARCILLA, R.; Antonietti, M. Vanadium Nitride@ N-Doped Carbon Nanocomposites: Tuning of Pore Structure and Particle Size Through Salt Templating and its Influence on Supercapacitance in Ionic Liquid Media. *RSC Adv.* **2014**, *4*, 26981−26989.

DOI: 10.1021/acs.chemrev.6b00504
Chem. Rev. 2017, 117, 7190−7239

(479) Wan, M. M.; Sun, X. D.; Li, Y. Y.; Zhou, J.; Wang, Y.; Zhu, J. H. Facilely Fabricating Multifunctional N-Enriched Carbon. *ACS Appl. Mater. Interfaces* **2016**, *8*, 1252−1263.
(480) Aijaz, A.; Akita, T.; Yang, H.; Xu, Q. From Ionic-Liquid@ Metal−Organic Framework Composites to Heteroatom-Decorated Large-Surface Area Carbons: Superior CO_2 and H_2 Uptake. *Chem. Commun.* **2014**, *50*, 6498−6501.
(481) Karimi, B.; Behzadnia, H.; Rafiee, M.; Vali, H. Electrochemical Performance of a Novel Ionic Liquid Derived Mesoporous Carbon. *Chem. Commun.* **2012**, *48*, 2776−2778.
(482) Karimi, B.; Behzadnia, H.; Bostina, M.; Vali, H. A Nano-Fibrillated Mesoporous Carbon as an Effective Support for Palladium Nanoparticles in the Aerobic Oxidation of Alcohols "on Pure Water. *Chem. - Eur. J.* **2012**, *18*, 8634−8640.
(483) Kazemi, S. H.; Karimi, B.; Fashi, A.; Behzadnia, H.; Vali, H. High-Performance Supercapacitors Based on an Ionic Liquid-Derived Nanofibrillated Mesoporous Carbon. *J. Solid State Electrochem.* **2014**, *18*, 2419−2424.
(484) Karimi, B.; Behzadnia, H.; Vali, H. Palladium on Ionic Liquid Derived Nanofibrillated Mesoporous Carbon: A Recyclable Catalyst for the Ullmann Homocoupling Reactions of Aryl Halides in Water. *ChemCatChem* **2014**, *6*, 745−748.
(485) Qiu, B.; Pan, C.; Qian, W.; Peng, Y.; Qiu, L.; Yan, F. Nitrogen-Doped Mesoporous Carbons Originated from Ionic Liquids as Electrode Materials for Supercapacitors. *J. Mater. Chem. A* **2013**, *1*, 6373−6378.
(486) Xu, X.; Li, Y.; Gong, Y. T.; Zhang, P. F.; Li, H. R.; Wang, Y. Synthesis of Palladium Nanoparticles Supported on Mesoporous N-Doped Carbon and Their Catalytic Ability for Biofuel Upgrade. *J. Am. Chem. Soc.* **2012**, *134*, 16987−16990.
(487) Hasché, F.; Fellinger, T. P.; Oezaslan, M.; Paraknowitsch, J. P.; Antonietti, M.; Strasser, P. Mesoporous Nitrogen Doped Carbon Supported Platinum PEM Fuel Cell Electrocatalyst made from Ionic Liquids. *ChemCatChem* **2012**, *4*, 479−483.
(488) Zhang, P.; Yuan, J.; Li, H.; Liu, X.; Xu, X.; Antonietti, M.; Wang, Y. Mesoporous Nitrogen-Doped Carbon for Copper-Mediated Ullmann-Type C−O/−N/−S Cross-Coupling Reactions. *RSC Adv.* **2013**, *3*, 1890−1895.
(489) Zhang, Z.; Veith, G. M.; Brown, G. M.; Fulvio, P. F.; Hillesheim, P. C.; Dai, S.; Overbury, S. H. Ionic Liquid Derived Carbons as Highly Efficient Oxygen Reduction Catalysts: First Elucidation of Pore Size Distribution Dependent Kinetics. *Chem. Commun.* **2014**, *50*, 1469−1471.
(490) Cui, Z.; Wang, S.; Zhang, Y.; Cao, M. A Simple and Green Pathway Toward Nitrogen and Sulfur Dual Doped Hierarchically Porous Carbons from Ionic Liquids for Oxygen Reduction. *J. Power Sources* **2014**, *259*, 138−144.
(491) Wu, H.; Shi, L.; Lei, J.; Liu, D.; Qu, D.; Xie, Z.; Du, X.; Yang, P.; Hu, X.; Li, J.; et al. Nitrogen and Sulfur Co-Doped Carbon with Three-Dimensional Ordered Macroporosity: An Efficient Metal-Free Oxygen Reduction Catalyst Derived from Ionic Liquid. *J. Power Sources* **2016**, *323*, 90−96.
(492) Zheng, F.; Mu, G.; Zhang, Z.; Shen, Y.; Zhao, M.; Pang, G. Nitrogen-Doped Hollow Macroporous Carbon Spheres with High Electrocatalytic Activity for Oxygen Reduction. *Mater. Lett.* **2012**, *68*, 453−456.
(493) Han, C.; Wang, J.; Gong, Y.; Xu, X.; Li, H.; Wang, Y. Nitrogen-Doped Hollow Carbon Hemispheres as Efficient Metal-Free Electrocatalysts for Oxygen Reduction Reaction in Alkaline Medium. *J. Mater. Chem. A* **2014**, *2*, 605−609.
(494) Yang, W.; Yue, X.; Liu, X.; Zhai, J.; Jia, J. IL-Derived N, S Co-Doped Ordered Mesoporous Carbon for High-Performance Oxygen Reduction. *Nanoscale* **2015**, *7*, 11956−11961.
(495) Soll, S.; Fellinger, T. P.; Wang, X.; Zhao, Q.; Antonietti, M.; Yuan, J. Water Dispersible, Highly Graphitic and Nitrogen-Doped Carbon Nanobubbles. *Small* **2013**, *9*, 4135−4141.
(496) Ranjbar Sahraie, N.; Paraknowitsch, J. P.; Gobel, C.; Thomas, A.; Strasser, P. Noble-Metal-Free Electrocatalysts with Enhanced ORR Performance by Task-Specific Functionalization of Carbon using Ionic Liquid Precursor Systems. *J. Am. Chem. Soc.* **2014**, *136*, 14486−14497.
(497) Ma, R.; Xia, B. Y.; Zhou, Y.; Li, P.; Chen, Y.; Liu, Q.; Wang, J. Ionic Liquid-Assisted Synthesis of Dual-Doped Graphene as Efficient Electrocatalysts for Oxygen Reduction. *Carbon* **2016**, *102*, 58−65.
(498) Elumeeva, K.; Antonietti, M.; Fechler, N.; Fellinger, T. Metal-free Ionic Liquid-derived Electrocatalyst for High-Performance Oxygen Reduction in Acidic and Alkaline Electrolytes. *Mater. Horiz.* **2014**, *1*, 588−594.
(499) Liu, S. H.; Chen, S. C. Well-Dispersed FeN_4 Decorated Mesoporous Carbons for Efficient Oxygen Reduction in Acid Media. *Carbon* **2016**, *105*, 282−290.
(500) Chen, S.; Duan, J.; Zheng, Y.; Chen, X.; Du, X. W.; Jaroniec, M.; Qiao, S.-Z. Ionic Liquid-Assisted Synthesis of N/S-Double Doped Graphene Microwires for Oxygen Evolution and Zn−Air Batteries. *Energy Storage Materials* **2015**, *1*, 17−24.
(501) Sakaushi, K.; Fellinger, T. P.; Antonietti, M. Bifunctional Metal-Free Catalysis of Mesoporous Noble Carbons for Oxygen Reduction and Evolution Reactions. *ChemSusChem* **2015**, *8*, 1156−1160.
(502) Zhu, J. X.; Sakaushi, K.; Clavel, G.; Shalom, M.; Antonietti, M.; Fellinger, T. P. A General Salt-Templating Method To Fabricate Vertically Aligned Graphitic Carbon Nanosheets and Their Metal Carbide Hybrids for Superior Lithium Ion Batteries and Water Splitting. *J. Am. Chem. Soc.* **2015**, *137*, 5480−5485.
(503) Li, L.; Chu, Y. Y.; Cao, J.; Dai, Z.; Zhao, S. H.; Tan, X. Y. Preparation of Pt/XC-72@C-N Electrocatalysts by the in-situ Carbonization of Ionic Liquid for Methanol Oxidation. *Int. J. Hydrogen Energy* **2015**, *40*, 3900−3908.
(504) Pan, C.; Qiu, L.; Peng, Y.; Yan, F. Facile Synthesis of Nitrogen-Doped Carbon−Pt Nanoparticle Hybrids via Carbonization of Poly([Bvim][Br]-co-acrylonitrile) for Electrocatalytic Oxidation of Methanol. *J. Mater. Chem.* **2012**, *22*, 13578−13584.
(505) Peng, Y.; Wu, X.; Qiu, L.; Liu, C.; Wang, S.; Yan, F. Synthesis of Carbon−PtAu Nanoparticle Hybrids Originating from Triethoxysilane-Derivatized Ionic Liquids for Methanol Electrooxidation and the Catalytic Reduction of 4-nitrophenol. *J. Mater. Chem. A* **2013**, *1*, 9257−9263.
(506) Zhang, X.; Böckenfeld, N.; Berkemeier, F.; Balducci, A. Ionic-Liquid-Assisted Synthesis of Nanostructured and Carbon-Coated $Li_3V_2(PO_4)_3$ for High-Power Electrochemical Storage Devices. *ChemSusChem* **2014**, *7*, 1710−1718.
(507) Yang, L.; Guo, G.; Sun, H.; Shen, X.; Hu, J.; Dong, A.; Yang, D. Ionic Liquid as the C and N Sources to Prepare Yolk-shell Fe_3O_4@ N-doped Carbon Nanoparticles and its High Performance in Lithium-ion Battery. *Electrochim. Acta* **2016**, *190*, 797−803.
(508) Yoon, S.; Liao, C.; Sun, X.-G.; Bridges, C. A.; Unocic, R. R.; Nanda, J.; Dai, S.; Paranthaman, M. P. Conductive Surface Modification of $LiFePO_4$ with Nitrogen-Doped Carbon Layers for Lithium-Ion Batteries. *J. Mater. Chem.* **2012**, *22*, 4611−4614.
(509) Zhang, X. F.; Kuhnel, R. S.; Hu, H. T.; Eder, D.; Balducci, A. Going Nano with Protic Ionic Liquids-the Synthesis of Carbon Coated $Li_3V_2(PO_4)_3$ Nanoparticles Encapsulated in a Carbon Matrix for High Power Lithium-Ion Batteries. *Nano Energy* **2015**, *12*, 207−214.
(510) Cheng, Y. H.; Chen, Z.; Wu, H. B.; Zhu, M. F.; Lu, Y. F. Ionic Liquid-Assisted Synthesis of TiO2-Carbon Hybrid Nanostructures for Lithium-Ion Batteries. *Adv. Funct. Mater.* **2016**, *26*, 1338−1346.
(511) Reitz, C.; Breitung, B.; Schneider, A.; Wang, D.; von der Lehr, M.; Leichtweiss, T.; Janek, J. r.; Hahn, H.; Brezesinski, T. Hierarchical Carbon with High Nitrogen Doping Level: A Versatile Anode and Cathode Host Material for Long-Life Lithium-Ion and Lithium−Sulfur Batteries. *ACS Appl. Mater. Interfaces* **2016**, *8*, 10274−10282.
(512) Suo, L. M.; Zhu, Y. J.; Han, F. D.; Gao, T.; Luo, C.; Fan, X. L.; Hu, Y. S.; Wang, C. S. Carbon Cage Encapsulating Nano-Cluster Li_2S by Ionic Liquid Polymerization and Pyrolysis for High Performance Li-S Batteries. *Nano Energy* **2015**, *13*, 467−473.
(513) Schneider, A.; Weidmann, C.; Suchomski, C.; Sommer, H.; Janek, J.; Brezesinski, T. Ionic Liquid-Derived Nitrogen-Enriched Carbon/Sulfur Composite Cathodes with Hierarchical Microstructure-

DOI: 10.1021/acs.chemrev.6b00504
Chem. Rev. 2017, 117, 7190−7239

A Step Toward Durable High-Energy and High-Performance Lithium-Sulfur Batteries. *Chem. Mater.* **2015**, *27*, 1674−1683.
(514) Ni, W. P.; Liu, S. M.; Fei, Y. Q.; He, Y. D.; Ma, X. Y.; Lu, L. J.; Deng, Y. Q. CoO@Co and N-Doped Mesoporous Carbon Composites Derived from Ionic Liquids as Cathode Catalysts for Rechargeable Lithium-Oxygen Batteries. *J. Mater. Chem. A* **2016**, *4*, 7746−7753.
(515) Song, H.; Li, N.; Cui, H.; Wang, C. Enhanced Storage Capability and Kinetic Processes by Pores-and Hetero-atoms-Riched Carbon Nanobubbles for Lithium-Ion and Sodium-Ion Batteries Anodes. *Nano Energy* **2014**, *4*, 81−87.
(516) Kaskhedikar, N. A.; Maier, J. Lithium Storage in Carbon Nanostructures. *Adv. Mater.* **2009**, *21*, 2664−2680.
(517) Ma, Y.; Zhang, C.; Ji, G.; Lee, J. Y. Nitrogen-Doped Carbon-Encapsulation of Fe_3O_4 for Increased Reversibility in Li+ Storage by the Conversion Reaction. *J. Mater. Chem.* **2012**, *22*, 7845−7850.
(518) Ryu, M.-H.; Jung, K.-N.; Shin, K.-H.; Han, K.-S.; Yoon, S. High Performance N-Doped Mesoporous Carbon Decorated TiO2 Nano-fibers as Anode Materials for Lithium-Ion Batteries. *J. Phys. Chem. C* **2013**, *117*, 8092−8098.
(519) Winter, M.; Brodd, R. J. What are Batteries, Fuel cells, and Supercapacitors? *Chem. Rev.* **2004**, *104*, 4245−4269.
(520) Zhao, L.; Fan, L. Z.; Zhou, M. Q.; Guan, H.; Qiao, S.; Antonietti, M.; Titirici, M. M. Nitrogen-Containing Hydrothermal Carbons with Superior Performance in Supercapacitors. *Adv. Mater.* **2010**, *22*, 5202−5206.
(521) Hulicova-Jurcakova, D.; Kodama, M.; Shiraishi, S.; Hatori, H.; Zhu, Z. H.; Lu, G. Q. Nitrogen-Enriched Nonporous Carbon Electrodes with Extraordinary Supercapacitance. *Adv. Funct. Mater.* **2009**, *19*, 1800−1809.
(522) Yang, P.; Huang, N.; Leng, Y. X.; Yao, Z. Q.; Zhou, H. F.; Maitz, M.; Leng, Y.; Chu, P. K. Wettability and Biocompatibility of Nitrogen-Doped Hydrogenated Amorphous Carbon Films: Effect of Nitrogen. *Nucl. Instrum. Methods Phys. Res., Sect. B* **2006**, *242*, 22−25.
(523) Ostrowski, J. H. J.; Eaves, J. D. The Tunable Hydrophobic Effect on Electrically Doped Graphene. *J. Phys. Chem. B* **2014**, *118*, 530−536.
(524) Sui, Z. Y.; Meng, Y. N.; Xiao, P. W.; Zhao, Z. Q.; Wei, Z. X.; Han, B. H. Nitrogen-Doped Graphene Aerogels as Efficient Supercapacitor Electrodes and Gas Adsorbents. *ACS Appl. Mater. Interfaces* **2015**, *7*, 1431−1438.
(525) Kim, M. H.; Yun, S.; Park, H. S.; Han, J. T.; Kim, K. B.; Roh, K. C. Retransformed Graphitic Activated Carbon from Ionic Liquid-Derived Carbon Containing Nitrogen. *J. Mater. Chem. A* **2015**, *3*, 2564−2567.

DOI: 10.1021/acs.chemrev.6b00504
Chem. Rev. 2017, 117, 7190−7239